8-2015

Mathematical studies of the glucose-insulin regulatory system models.

Minghu Wang
University of Louisville

MATHEMATICAL STUDIES OF THE GLUCOSE-INSULIN REGULATORY SYSTEM MODELS

By

Minghu Wang
B.S., Sichuan University, 2008,
M.A., University of Louisville, 2011

A Dissertation
Submitted to the Faculty of the
College of Arts and Sciences of the University of Louisville
in Partial Fulfillment of the Requirements
for the Degree of

Doctor of Philosophy in Applied and Industrial Mathematics

Department of Mathematics
University of Louisville
Louisville, Kentucky

August 2015

MATHEMATICAL STUDIES OF THE GLUCOSE-INSULIN REGULATORY SYSTEM MODELS

By

Minghu Wang
B.S., Sichuan University, 2008,
M.A., University of Louisville, 2011

A Dissertation Approved On

Date: May 22, 2015

by the following Dissertation Committee:

Dissertation Director: Jiaxu Li

Bingtuan Li

Changbing Hu

Ryan Gill

Ted Kalbfleisch

ACKNOWLEDGEMENTS

The author thanks Dr. Jiaxu Li for his immeasurable effort to advise me in this doctoral research and valuable comments for revision of this dissertation. The author also thanks Dr. Bingtuan Li, Dr. Ryan Gill, Dr. Changbing Hu and Dr. Ted Kalbfleisch for their continuous support being committee members and thought-provoking comments. The author acknowledges the DOE grant: DE-EM0000197 for the support of this research.

ABSTRACT

MATHEMATICAL STUDIES OF THE GLUCOSE-INSULIN REGULATORY SYSTEM MODELS

Minghu Wang

May 22, 2015

Three dynamic models are proposed to study the mechanism of glucose-insulin regulatory system and the possible causes of diabetes mellitus. The progression of diabetes comes along with the apoptosis of pancreatic beta-cells. A dynamical system model is formulated based on physiology and studied by geometric singular perturbation theory. The analytical studies reveal rich analytical features, such as persistence of solutions, Hopf bifurcation and backward bifurcation, while numerical studies successfully fit available longitudinal T2DM data of Pima Indian tribe. These studies together not only validate our model, but also point out key intrinsic factors leading to the development of T2DM. We found that the intermittent rests of beta-cells in insulin secretion are essential for the cells to survive through the observation of the existence of a limit cycle. A delay differential equation model for IVGTT is also studied thoroughly to determine the range of time delay and the globally asymptotic stability by Liapunov function. The third kinetic model aims to investigate the scaling effect of local insulin in islet on proliferation and apoptosis of beta-cells. It is revealed that the local concentration of monomeric insulin within the islet is in the biologist defined picomolar 'sweet spot' range of insulin doses, which activate the insulin receptors and have the most potent effects on beta-cells *in vitro*.

TABLE OF CONTENTS

LIST OF TABLES

LIST OF FIGURES

CHAPTER I

INTRODUCTION

1 Diabetes statistics

During recent decades, diabetes mellitus has become an epidemic disease in the sense of life style [56]. It shows a rapidly growing trend for the past years. In 2002, 20.8 million, or 7% of population in US are diabetics with health expenses at $170 billion [1]. In 2011, the American diabetic population became 25.8 million, or 8.5% of the population in US. This number rapidly grew to approximately 30 million in the most recent year [1]. Diabetes is the 7^{th} leading cause of death in US. As of 2014, an estimated 387 million people worldwide suffer from diabetes [98]. Therefore, diabetes has obtained the attention of researchers from different disciplines.

Diabetes mellitus, commonly referred to as diabetes, is a group of metabolic diseases in which there are high blood sugar levels over a prolonged period [98]. Diabetes is a disease with considerable complications including but not limited to retinopathy, nephropathy(kidney damage), peripheral neuropathy (nerve damage) and blindness [16]. It is due to either the body not producing enough insulin or the inability of cells properly using insulin to metabolize glucose [8]. There are three main types of diabetes: type 1, type 2, and gestational diabetes [98]. Type 1 diabetes mellitus (T1DM) results from body's failure to produce enough insulin. It was also referred to as 'insulin-dependent diabetes mellitus'. Type 2 diabetes mellitus (T2DM) begins with insulin resistance, a condition in which the cells fail to respond to insulin efficiently. A lack of insulin secretion may also follow as the disease progresses. It was often referred to as 'non insulin-dependent diabetes mellitus'. Gestational diabetes

occurs when pregnant women without a previous diabetic history develop a high blood glucose level [98]. Out of the American diabetic population, nearly 95% are T2DM [1]. The problem is even greater for the minority and ethnic populations. For example, the extreme incidence rates occuring among American Indians are noteworthy [1].

The diagnosis of diabetes relates to the sketch of the so-called metabolic portrait, including the insulin sensitivity and glucose effectiveness of the subject. Several glucose tolerance tests have been developed and applied in clinics and experiments to determine whether an individual subject has already been diabetic or has the potential to develop certain type of diabetes. These tests include the Intravenous Glucose Tolerance Test(IVGTT) and the Oral Glucose Tolerance Test(OGTT) [7],[30].

Transplantation of the pancreas or the islets of Langerhans in the pancreas, would be the only real cure for diabetes, at least for T1DM [21]. Unfortunately, due to the immunological issues and the expense of transplantation, this approach is usually not practical. Further, approaches for beta-cell neogenesis and cell differentiation from stem cells are still under research ([9], [21]). For these reasons, the daily insulin subcutaneous injection is still the most widely used therapy of diabetes. This task is fulfilled by the insulin analogues, such as Lispro, Aspart, Glargine and so on, with the purpose of simply supplying the need of insulin in the body exogenously. These insulin analogues are able to mimic the physiological insulin secretion occuring in normal subjects.

2 Sketch of the objectives

General objectives of the studies in this area are to better understand how the glucose-insulin regulatory system works, how the mechanism functions, and how to determine the pathways of the dysfunctions of the system. To this end, we make the effort to investigate the causes for the progression of diabetes, detect the onset of diabetes(IVGTT, OGTT, etc) [8], and attempt to understand the insulin scaling

effect. We hope these relevant studies can provide sufficient information to eventually help develop reasonable, effective, efficient and economic clinical treatment (insulin analogues, insulin pump, artificial pancreas) in the near future.

Insulin is secreted from beta cells, the only cell which produces insulin. Loss of beta-cells will lead to diabetes over time. Therefore, the control of pancreatic beta-cell function and survival is essential for maintaining glucose homeostasis and preventing diabetes. It has been hypothesized that overworking leads beta-cells to die. The goal of this dissertation is to study these understandings of beta-cells in a mathematical context.

There are several popular approaches to conduct the analysis in regard to the physiology. One of them is done as follows: first formulate or choose a well-developed kinetic model based on the background of the objectives; then estimate the model parameters with experimental data or adopt them from the literature; the model and parameter values are used in numeric simulations in order to obtain physiological information, for instance, insulin sensitivity and glucose effectiveness and further, to make certain explanations and predictions. We utilize such an approach throughout the dissertation, aiming to seek helpful advises in clinical practices in future treatment of diabetes.

3 Background of glucose-insulin endocrine regulatory system

It is known that the human body maintains glucose homeostasis within a narrow range (70-109 mg/dl) [57]. In the glucose-insulin regulatory system, elevated glucose level triggers secretion of insulin from the beta-cells in the pancreas. Insulin augments the glucose utilization by muscle cells and adipose cells, which helps the glucose concentration return to normal level. The secretion of insulin stops gradually as the glucose level declines. For a normal subject, the basal plasma insulin level is in the range of 5-10 μU/ml after an overnight fast [2]. Under continuous enteral nutrition, however, this range can be as wide as 10-40 μU/ml [84]. It could also rises

to as large as 30-150 μU/ml during meal consumption while the glucose level is high [2]. The insulin secretion pathways consist of complex processes in molecular level, involving typical electric and chemical events. They are summarized in Chapter 3, section 2.

It is also worth-mentioning that the insulin secretion in the glucose-insulin endocrine metabolic system in healthy subjects occurs mainly in an oscillatory manner over a range of 50-150 min, and is usually referred to as ultradian oscillations ([89],[92],[84]). It is best observed after meal ingestion, oral glucose intake, intravenous glucose infusion and continuous enteral nutrition. This phenominon will be discussed in more details in Chapter 2.

Evidence also suggests that there is another type of oscillation in addition to the above mentioned ultradian oscillation. Numerous *in vivo* and *in vitro* studies have revealed that the secretion of insulin also undergoes a rapid oscillation occuring with a different time scale of 5-15 min compared to the ultradian oscillation [79]. This rapid oscillations are superimposed on the slower ultradian oscillations according to [89]. The mechanism underlying both types of oscillations is still under research. The rapid oscillations may arise from an intra-pancreatic pacemaker mechanism which causes a coordination of insulin periodic secretory bursting from beta-cells contained in the millions islets of Langerhans ([89],[92]). At the basal level, these bursts are believed to be the dominant mechanism of insulin release.

Although the precise mechanism remains unclear, the ultradian oscillations are assumed to be the result of an instability in the glucose-insulin endocrine metabolic regulatory system ([89],[92],[84],[62]). In addition to various types of glucose input mentioned above, the continuous glucose utilization of muscles, the brain and nerves, and other tissues complete the regulatory system feedback loop ([89],[92]). The hypothesis that the ultradian oscillation results from instability in the regulatory system has been the subject of a number of researches, ([89],[43],[92],[22],[6]) among which several mathematical models are proposed to describe the glucose-insulin feedback

loop ([89],[92]). However, rigorous mathematical proofs are still needed to show the feedback system is the mechanism of the ultradian oscillation of insulin secretion. We will be addressing this issue in the model analysis part in Chapter 2.

4 Existing studies of the glucose-insulin regulatory system

As we mentioned above, a number of studies on the regulatory system have been conducted in the last few decades. Pioneering work to model such system and the ultradian secretory oscillations can be traced back to Bolie (1961), in which a linearized system in terms of differential equations was analyzed. In a paper by Topp et al.[93], the authors proposed a model incorporating beta-cell mass as a variable, to study the long-term effect of the regulatory system on the beta-cells. In the same year, Sturis et al.[92] also published a paper studying the glucose-insulin feedback system and the observed ultradian oscillatory behavior. Li, Kuang and Mason generalized the modeling of such feedback system by proposing a system of delay differential equations with two time delays, in a study in 2006 [57].

5 Contents organization

This dissertation is organized as follows. After introduction of the general information of diabetes and the related physiological background in Chapter 1, Introduction, we propose a dynamic model to study the glucose-insulin regulatory system and beta-cell mass change over a long time frame in Chapter 2. The model formulation will be thoroughly explained and examined. Then the mathematical properties of such model will be carefully studied, such as the equilibrium points, their local stability and the conditions of the existence of Hopf bifurcation. Next we are going to carry out some numerical simulations with estimated parameters from the literature. These simulations are done to verify the preceding mathematical findings and to explore some new features possessed by the model. The results of these simulations are to be translated to physiological explanations of diabetic observations. Our effort

to make such attempts will contribute to useful discussion of the likely treatment of diabetic patients.

Chapter 3 introduces an IVGTT model in which delay effect is studied with emphasis. The length of the delay time has been carefully studied. Further the delay-dependent conditions of the global stability of the equilibrium point is obtained by utilizing the Liapunov function. Numeric simulations are also conducted after the analytical part and are followed by a discussion.

Chapter 4 focuses on discussing a microscopic view of the complex regulatory system. The context of the study is a single islet of Langerhans in the pancreas. The *in vivo* glucose and insulin concentrations in an islet are modeled by a system of ordinary differential equations. The *in vivo* concentrations in such tiny micro-organs are currently impossible to measure by existing techniques. Therefore our mathematical analysis proves to be essential in understanding the dynamics in this small scale. Experimental data also plays important role in estimating parameter values in the numeric simulations thereafter.

CHAPTER II

MATHEMATICAL STUDIES OF THE ANTI-APOPTOTIC EFFECTS ON PANCREATIC BETA-CELLS

In this chapter, applying the Mass Conservation Law, we propose a system of ordinary differential equations to model the glucose-insulin regulatory system and beta-cell mass. Then we conduct a thorough mathematical analysis followed by numeric simulations. Several core theorems are established in order to understand the key characteristics of the model dynamics. The results obtained from the study would be used to either explain the existing observations in diabetic patients, or to aim in predicting potential diabetes.

1 Model formulation

The model is formulated by applying the Mass Conservation Law, similar to the approach of [93]

Rate of Change = Input - Output.

The two major factors in the regulatory system to be modeled are glucose and insulin. Let $G(t)$ denote the plasma glucose concentration at time $t \geq 0$. In order to describe the complex mechanism of the regulatory system, we consider the insulin in two compartments. One is plasma insulin and the other is interstitial insulin, which are denoted by $I_p(t)$ and $I_i(t)$, respectively. The transport of insulin between them is assumed to be a passive diffusion process driven by the difference in insulin, with

transfer rate E [78]. Then we obtain the following word equation

dG(t)/dt = glucose production - glucose utilization,

$\mathrm{dI}_p(t)/dt$ = insulin secretion - compartments exchange - insulin clearance,

$\mathrm{dI}_i(t)/dt$ = compartments exchange - insulin clearance.

Further to access the complex mechanism of such regulatory system, we are also interested in the rate of change for beta-cell mass, which is denoted by $\beta(t)$.

$\mathrm{d}\beta(t)/dt$ = formation - loss.

Next we discuss the physiology for each term in the above word equations and determine their mathematical expressions.

Glucose production: There are two main sources of glucose production. Glucose is released from dietary carbohydrates, subsequently being absorbed into the blood. Meal ingestion, oral glucose and continuous enteral nutrition infusion are the most common ways of glucose infusion ([89],[92]). We assume that the average glucose infusion rate is a constant, denoted by $G_{in} \geq 0$. The liver is the other source of glucose production. When the blood glucose level drops, beta-cells stop releasing insulin, but alpha-cells, also located in the Langerhans islets in the pancreas, start to release another hormone, glucagon. Glucagon leads the liver to dispense glucose through certain metabolic pathways. This part of glucose production is denoted as $f_5(I)$ controlled by insulin concentration. It is assumed to satisfy that $f_5(0) > 0$ and $f_5' < 0$ for $x > 0$. When the insulin level is three-fold above its basal level, glucose production by the liver can be quickly halted. Therefore we also assume the functions $f_5(x)$ and $|f_5'(x)|$ are bounded above for $x > 0$, and $f_5(x)$ rapidly decreases to zero as x increases (refer to Fig. 1 for the shape of function f_5).

Glucose utilization: Glucose utilization also consists of two parts, namely, insulin-independent utilization and insulin-dependent utilization. The main insulin-

independent glucose consumers are brain and nerve cells. The utilization of this type is denoted by $f_2(G)$ indicating its dependency on the glucose level alone. Further, we assume that $f_2(x) > 0$ is in the sigmoidal shape with $f_2(0) = 0$, and $f_2'(x)$ is bounded for $x > 0$. The insulin-dependent glucose uptake is mostly due to muscle, fat cells and other tissues. These cells consume the glucose and convert it into energy for the body. We denote the insulin-dependent glucose utilization by $f_3(G)f_4(I_p)$. Moreover, we may reasonably assume that $f_3(0) = 0$, $0 < f_3(x) \leq k_3 x$, and $f_3'(x) > 0$ for $x > 0$, where k_3 is a constant. Similarly, $f_4(0) > 0$, $f_4(x) > 0$ and $f_4'(x) > 0$ are bounded above for $x > 0$. Again we require that $f_4(x)$ has a sigmoidal shape according to [89] (refer to Fig. 1 for the shape of functions f_3 and f_4).

Insulin production: Insulin can only be produced through beta-cell secretion, mainly in response to elevated blood glucose level. Although other secretagogues such as free fatty acid and most amino acids can still stimulate the insulin secretion, glucose is the most critical stimulus for insulin release [2]. A series of complex electric processes occur inside of each islet upon glucose stimulus. Here $f_1(G)$ is used to stand for insulin production stimulated by glucose concentration G. Likewise, we assume $f_1(G)$ is bounded, of sigmoidal shape, $f_1(0) > 0$, $f_1(x) > 0$, and $f_1'(x) > 0$ for $x > 0$.(refer to Fig. 1 for the shape of function f_1)

Insulin degradation and clearance: Insulin is cleared by all insulin sensitive tissues. The primary sites of portal insulin degradation and peripheral insulin clearance are the liver and kidney, respectively. Insulin not cleared by these two organs is ultimately removed by other tissues, for instance, muscle and adipose cells. Insulin degradation is a regulated process involving insulin binding to its receptor, internalization, and degradation as in other tissues. The function of insulin degradation and clearance is to remove and inactivate circulating insulin, in order to control insulin action [19]. Here insulin degradation is assumed to be exponential, with time con-

stant t_p for insulin in plasma and t_i for insulin in the intercellular space.

Beta-cell proliferation: The proliferation of beta-cells is not surprisingly assumed to be proportional to beta-cell mass itself. Furthermore, recent studies proposed the 'Sweet Spot' hypothesis tempting to explain the complex non-linear concentration-response profile of autocrine insulin signaling [39]. These studies speculated that modestly increased local insulin might drive the compensatory beta-cell hyperplasia that normally occurs before type 2 diabetes. Once local insulin increases past a certain level, it would cease to protect beta-cells or stimulate their growth. Beta-cell mass is expected to decrease as a result, marking the transition to type 2 diabetes. To model such phenomena, we assume that the proliferation rate $p(I_p) = \frac{p_0 I_p}{r_0 + I_p^2}$, where $\frac{I_p}{r_0 + I_p^2}$ reflects insulin signaling. This factor increases as insulin level increases to a certain point, after which it starts to decrease.

Beta-cell apoptosis: In vitro beta-cell apoptosis has been shown to vary non-linearly with glucose ([34],[20]). Increasing the glucose concentration from 0 to approximately 11 mM in the medium surrounding cultured beta-cells reduced the rate of beta-cell death. However above 11 mM glucose level, beta-cell death is either remained low or increased, due to the possible glucose toxicity. Thus we model such behavior with a simple second-degree polynomial $a(I_p, G) = \frac{a_0 I_p}{r_0 + I_p^2}(1 - r_a G + r_b G^2)$ [93], still taking into account the insulin signaling factor, where a_0 is the apoptosis rate at zero glucose and r_a, r_b are constants.

The rate of change of glucose concentration is determined by the glucose infusion rate, insulin independent glucose uptake, insulin dependent glucose uptake, and hepatic glucogen store transformation. The rate of change of plasma insulin concentration is determined by the beta-cell secretion, exchange with interstitial compartment [78] and its degradation over time. Interstitial insulin comes from plasma, so

its rate of change is the difference between the exchange with plasma insulin and its degradation. The rate of change of beta-cell mass is a combining effect of proliferation and apoptosis, but could be much slower than that of glucose and insulin.

We use the following state variables.

G - plasma glucose concentration

I_p - plasma insulin concentration

I_i - interstitial insulin concentration

x_1, x_2, x_3 - auxilliary variables that mimic a delay of duration τ in the release of glucose from hepatic glycogen stores

β - beta cell mass

By [77], the pancreatic insulin production stimulated by the glucose concentration is specified by the function

$$f_1(G) = \frac{R_m}{1 + exp((C_1 - G/V_g)/a_1)}.$$

Insulin-independent glucose utilization is described by the following funtion, which is estimated in [97]

$$f_2(G) = U_b(1 - exp(-G/(C_2V_g))).$$

Insulin-dependent glucose utilization depends on both insulin and glucose concentrations. The glucose-dependent term is assumed to be

$$f_3(G) = \frac{G}{C_3V_g},$$

and the insulin-dependent term is determined ([80],[97]) by

$$f_4(I_i) = U_0 + \frac{U_m - U_0}{1 + exp(-\beta ln(I_i/C_4(1/V_i + 1/Et_i)))}.$$

The hepatic glucose production by the influence of insulin, according to [80], is well specified by the function

$$f_5(x_3) = \frac{R_g}{1 + exp(\alpha(x_3/V_p - C_5))}.$$

Figure 1. Sigmoidal functions used in the model

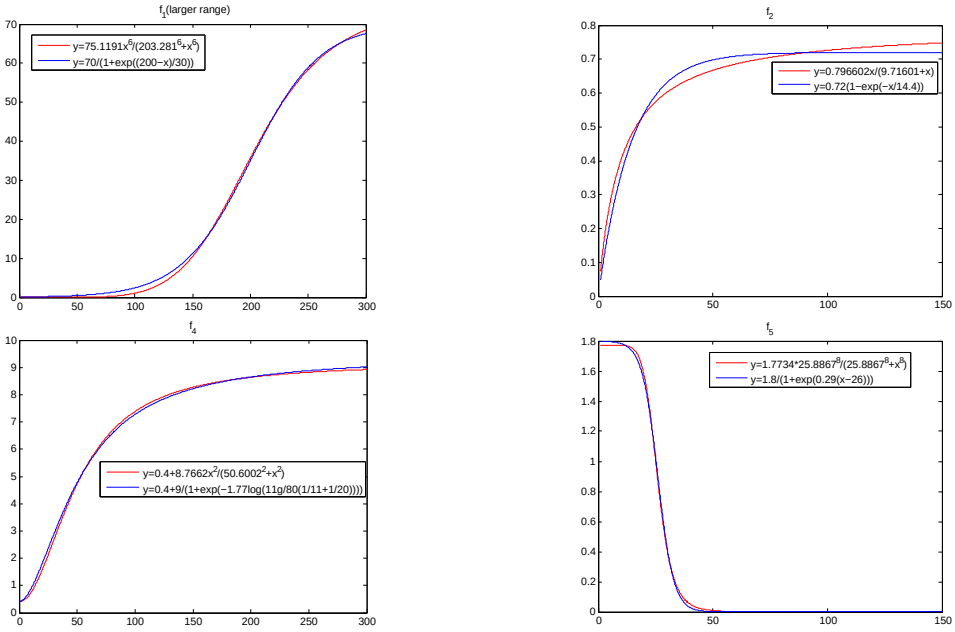

The shapes of the functions, instead of their specific forms, are more essential in analysis. Therefore, we further fitted these functions with sigmoidal type functions, just for the sake of relative simplicity in mathematical manipulation.

The functions f_j, $j = 1, 2, 3, 4, 5$, are fitted by functions in exponential forms. The least quare method is used to determine the parameters of the sigmoidal functions. The following figures presented show that the sigmoidal functions fit the functions in exponential forms quite well. The new functions capture the key characteristics of the functions used in [89].

The chain trick is applied to mimic the delay effect in the release of glucose hepatic glycogen store. Eventually, the model is formulated as follow:

$$\begin{cases} G' = G_{in} - f_2(G) - f_3(G)f_4(I_i) + f_5(x_3) \\ I_p' = \beta f_1(G) - E(I_p - I_i) - \frac{I_p}{t_p} \\ I_i' = E(I_p - I_i) - \frac{I_i}{t_i} \\ x_1' = \frac{3}{t_d}(I_p - x_1) \\ x_2' = \frac{3}{t_d}(x_1 - x_2) \\ x_3' = \frac{3}{t_d}(x_2 - x_3) \\ \beta' = \epsilon(p(I_p) - a(G, I_i))\beta \end{cases}, \tag{1}$$

where

$$\begin{aligned} f_1(G) &= \frac{r_1 G^{n_1}}{k_1^{n_1} + G^{n_1}}, \\ f_2(G) &= \frac{r_2 G}{k_2 + G}, \\ f_3(G) &= c_1 G, \\ f_4(I_i) &= \frac{r_3 I_i^{n_2}}{k_3^{n_2} + I_i^{n_2}} + c_2, \\ f_5(x_3) &= \frac{r_4 k_4^{n_3}}{k_4^{n_3} + x_3^{n_3}}, \\ p(I_p) &= \frac{p_0 I_p}{r_0 + I_p^2}, \\ a(G, I_p) &= \frac{a_0 I_p}{r_0 + I_p^2}(1 - r_a G + r_b G^2). \end{aligned}$$

With ϵ in the equation involving β being sufficiently small, system (1) is considered to be a fast-slow dynamical system.

2 Model Analysis

The model has two time scales: the fast scale in which glucose and insulin dynamics are easily observable with beta-cell mass nearly unchanged, and the slow scale in which beta-cell mass develops over a long period with relatively stable glucose

and insulin levels.

More specifically, by fast system, we refer to the glucose-insulin regulatory system in which the glucose and insulin level dynamics are studied, using minutes as the time scale. The plasma concentrations by minutes are mainly taken into consideration. At meantime beta-cell mass only changes slightly in minutes time scale. By slow system, we mean the one in which the beta-cell mass dynamic noticably takes place, using days, months or even years as the time scale. Although glucose and insulin levels change quickly in this time scale, they can be treated as stable values, in days. The amount of beta-cell mass by days is the main variable to be studied.

By the general fast-slow system setting, we write the original model in simplified form.

$$\begin{cases} \frac{dY}{dt} = F(Y, \beta) \\ \frac{d\beta}{dt} = \epsilon g(Y, \beta) \end{cases}, \tag{2}$$

where $Y = (G, I_p, I_i, x_1, x_2, x_3)^T$ are considered the fast variables and β the slow variable.

To analyze such fast-slow system, we refer to Fenichel's theory [28],

Theorem II.1 ***(Fenichel)*** *Suppose $\mathcal{M}_0 \subset \{Y \mid F(Y, \beta) = 0\}$ is compact, possibly with boundary, and normally hyperbolic, that is, the eigenvalues λ of the Jacobian $\frac{\partial F}{\partial Y}(Y, \beta, 0)|_{M_0}$ all satisfy $Re(\lambda) \neq 0$. Suppose F and G are smooth. Then for $\epsilon > 0$ and sufficiently small, there exists a manifold M_ϵ, $O(\epsilon)$ close and diffeomorphic to $\mathcal{M}_0$, that is locally invariant under the flow of the full problem (1).*

This theorem gives us an approach to understand the dynamics of the full system by knowing the dynamics on its critical manifold, which is usually of lower dimension.

The critical manifold of model (1) is given by

$$\mathcal{M}_0 = \{Y \mid F(Y, \beta) = 0\}. \tag{3}$$

The dynamics on this manifold can give us a good approximation of the dynamics of full system by Fenichel's first theorem. Thus the next step is to do analyses on critical manifold $\mathcal{M}_0$.

Now we consider the fast sub-system

$$\begin{cases} G' = G_{in} - f_2(G) - f_3(G)f_4(I_i) + f_5(x_3) \\ I_p' = \beta f_1(G) - E(I_p - I_i) - \frac{I_p}{t_p} \\ I_i' = E(I_p - I_i) - \frac{I_i}{t_i} \\ x_1' = \frac{3}{t_d}(I_p - x_1) \\ x_2' = \frac{3}{t_d}(x_1 - x_2) \\ x_3' = \frac{3}{t_d}(x_2 - x_3) \end{cases}, \tag{4}$$

where we view β as a parameter of the fast sub-system.

Theorem II.2 *System (4) has a unique equilibium point*

$$E^*_\beta = (G^*(\beta), I^*_p(\beta), cI^*_p(\beta), I^*_p(\beta), I^*_p(\beta), I^*_p(\beta))$$

for each $\beta \geq 0$.

Proof. We set the right-hand side of all equations of system(4) to zero. The resulting system of equations to be solved is

$$\begin{cases} G_{in} - f_2(G) - f_3(G)f_4(I_i) + f_5(x_3) = 0 \\ \beta f_1(G) - E(I_p - I_i) - \frac{I_p}{t_p} = 0 \\ E(I_p - I_i) - \frac{I_i}{t_i} = 0 \\ \frac{3}{t_d}(I_p - x_1) = 0 \\ \frac{3}{t_d}(x_1 - x_2) = 0 \\ \frac{3}{t_d}(x_2 - x_3) = 0 \end{cases}. \tag{5}$$

By the last three equations, we have $I_p = x_1 = x_2 = x_3$. The third equation results in

$$\begin{aligned} EI_p &- EI_i - \frac{I_i}{t_i} = 0, \\ EI_p &= EI_i + \frac{I_i}{t_i}, \\ I_p &= I_i + \frac{I_i}{Et_i}, \\ I_p &= (1 + \frac{1}{Et_i})I_i, \\ I_i &= (1 + \frac{1}{Et_i})^{-1} I_p. \end{aligned}$$

If we denote $c = (1+\frac{1}{Et_i})^{-1}$, then $I_p = cI_i$. Substituting it into the first two equations, we have

$$\begin{cases} G_{in} - f_2(G) - f_3(G) f_4(cI_p) + f_5(I_p) = 0 \\ \beta f_1(G) - E(I_p - cI_p) - \frac{I_p}{t_p} = 0 \end{cases}. \tag{6}$$

The second equation gives

$$\begin{aligned} \beta f_1(G) &- E(1-c)I_p - \frac{I_p}{t_p} = 0, \\ \beta f_1(G) &- \Big(E(1-c) + \frac{1}{t_p}\Big) I_p = 0, \\ \beta f_1(G) &= \Big(E(1-c) + \frac{1}{t_p}\Big) I_p, \\ I_p &= \beta f_1(G) \Big(E(1-c) + \frac{1}{t_p}\Big)^{-1}, \\ &= \beta f_1(G) \Big(E(1 - \frac{1}{1+\frac{1}{Et_i}}) + \frac{1}{t_p}\Big)^{-1}, \\ &= \beta f_1(G) \Big(E\Big(\frac{\frac{1}{Et_i}}{1+\frac{1}{Et_i}}\Big) + \frac{1}{t_p}\Big)^{-1}, \\ &= \beta f_1(G) \Big(E\Big(\frac{1}{1+Et_i}\Big) + \frac{1}{t_p}\Big)^{-1}, \end{aligned}$$

$$
\begin{aligned}
&= \beta f_1(G)\Big(\frac{E}{1+Et_i}+\frac{1}{t_p}\Big)^{-1},\\
&= \beta f_1(G)\Big(\frac{1}{E^{-1}+t_i}+\frac{1}{t_p}\Big)^{-1}.
\end{aligned}
$$

Again if we denote $c' = (\frac{1}{E^{-1}+t_i}) + \frac{1}{t_p})^{-1}$, then $I_p = c'\beta f_1(G)$. Next we substitute it into the first equation of (6) to get

$\mathrm{G}_{in} - f_2(G) - f_3(G)f_4(cc'\beta f_1(G)) + f_5(c'\beta f_1(G)) = 0$. Rearrange it to get

$$G_{in} + f_5(c'\beta f_1(G)) = f_2(G) + f_3(G)f_4(cc'\beta f_1(G)). \tag{7}$$

Notice that the functions f_1, f_2, f_3, f_4 are increasing with respect to G on $(0,\infty)$, while function f_5 is decreasing. Thus it follows that the left side of equation (7) is decreasing on $(0,\infty)$ with lower bound G_{in}, and the right side is increasing on $(0,\infty)$ with no upper bound. Therefore, equation (7) has a unique solution G^* on $(0,\infty)$.

Further, we are able to find the solution of system (5) as

$$(G^*, c'\beta f_1(G^*), cc'\beta f_1(G^*), c'\beta f_1(G^*), c'\beta f_1(G^*), c'\beta f_1(G^*)). \tag{8}$$

Note again we view β as a varying parameter in the fast sub-system. Hence we refer to the unique solution as

$$E^*_\beta = (G^*(\beta), I^*_p(\beta), cI^*_p(\beta), I^*_p(\beta), I^*_p(\beta), I^*_p(\beta)) \tag{9}$$

for each $\beta \geq 0$, which is the unique equilibrium point of the fast sub-system (4). The proof is complete.

Moreover, we can find the equilibria of the whole system (1) by solving

$$\epsilon(p(I_p) - a(G, I_p))\beta = 0 \tag{10}$$

restricted on the critical manifold $\mathcal{M}_0$.

Since $p(I_p) = \frac{p_0 I_p}{r_0 + I_p^2}$, and $a(G, I_p) = \frac{a_0 I_p}{r_0 + I_p^2}(1 - r_a G + r_b G^2)$, Eq. (10) can be simplified as follows.

$$\begin{aligned}
\epsilon(p(I_p) - a(G, I_p))\beta &= \epsilon\Big(\frac{p_0 I_p}{r_0 + I_p^2} - \frac{a_0 I_p}{r_0 + I_p^2}(1 - r_a G + r_b G^2)\Big)\beta \\
&= \epsilon\frac{I_p}{r_0 + I_p^2}\Big(p_0 - a_0(1 - r_a G + r_b G^2\Big)\beta = 0.
\end{aligned}$$

Since $\epsilon > 0$ and $\frac{I_p}{r_0 + I_p^2} > 0$, Eq. (10) is equivalent to

$$(p_0 - a_0(1 - r_a G + r_b G^2))\beta = 0.$$

Then $\beta = 0$ or $(p_0 - a_0(1 - r_a G + r_b G^2)) = 0$. The latter equation can be rewritten as

$$-r_b G^2 + r_a G + (p_0/a_0 - 1) = 0. \tag{11}$$

The following theorem is the result.

Theorem II.3 *Let* $\Delta = r_a^2 + 4r_b(p_0/a_0 - 1)$.

(1) if $\Delta < 0$*, the complete model (1) has only one trivial equilibrium point.*

(2) if $\Delta = 0$*, the complete model (1) has two equilibrium points, one of which is trivial.*

(3) if $\Delta > 0$*, the complete model (1) has three equilibrium points, one of which is trivial.*

Proof. This is the direct result from the property of quadratic equations. The trivial equilibrium point is found by letting $\beta = 0$ and substituting it into the unique solution (8) or (9), with one more coordinate for β. This results in

$$\begin{aligned}
E(0) &= (G^*(0), 0 \cdot c' f_1(G^*), 0 \cdot cc' f_1(G^*), 0 \cdot c' f_1(G^*), 0 \cdot c' f_1(G^*), 0 \cdot c' f_1(G^*), 0), \\
&= (G^*(0), 0, 0, 0, 0, 0, 0), \\
E_0 &= (G_0^*, 0, 0, 0, 0, 0, 0),
\end{aligned}$$

where G_0^* is the solution of equation (7) when $\beta = 0$, i.e.

$$\begin{aligned} G_{in} + f_5(0) &= f_2(G) + f_3(G)f_4(0), \\ G_{in} + r_4 &= f_2(G) + c_2 f_3(G). \end{aligned}$$

When the quadratic equation (11) has two positive zeros G_1^* and G_2^*, where

$$G_{1,2}^* = \frac{r_a \pm \Delta^{1/2}}{2r_b}. \tag{12}$$

By (8) or (9) we end up with three equilibrium points of the complete model.

$$\begin{aligned} E_0 &= (G_0^*, 0, 0, 0, 0, 0, 0), \\ E_1 &= (G_1^*, I_{p1}^*, cI_{p1}^*, I_{p1}^*, I_{p1}^*, I_{p1}^*, \beta_1^*), \\ E_2 &= (G_2^*, I_{p2}^*, cI_{p2}^*, I_{p2}^*, I_{p2}^*, I_{p2}^*, \beta_2^*). \end{aligned}$$

The proof is complete.

Remark. This theorem has some physiological implications. Let us express the conditions in another way. Starting from $\Delta < 0$, we make some transformations

$$\begin{aligned} \Delta &= r_a^2 + 4r_b(p_0/a_0 - 1) < 0, \\ & 4r_b(p_0/a_0 - 1) < -r_a^2, \\ & p_0/a_0 - 1 < -\frac{r_a^2}{4r_b}, \\ & p_0/a_0 < 1 - \frac{r_a^2}{4r_b}. \end{aligned}$$

In the model, p_0 is the proliferation parameter and a_0 the apoptosis parameter. Hence we consider the ratio value $w = p_0/a_0$ as the 'relative strength of beta-cell functionality'. The above condition becomes $w < 1 - \frac{r_a^2}{4r_b}$. In physiological context, if

the relative strength of beta-cell functionality is too weak, the body will develop the pathological state, which in our model is the trivial equilibrium point. However, if the relative strength of beta-cell functionality is strong, with $w > 1 - \frac{r_a^2}{4r_b}$, the body could have healthy states, which in the model are represented by the interior equilibrium points.

Suppose we consider the more common situation that three equilibrium points exist. Plotting them on a three-dimensional phase space consisting of glucose, insulin and beta-cell axis, we have the following Fig. 2. The green curve demonstrates the shape of the critical manifold, along which the three equilibrium points locate. The red dot represents the trivial equilibrium point E_0, and the blue and purple dots represent the other two the interior equilibrium points E_1 and E_2, standing for the pathological state and the healthy states, respectively.

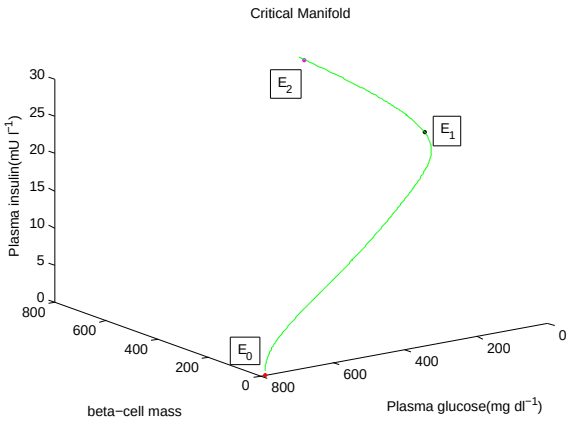

Figure 2. Critical manifold M_0 and equilibia of whole system

1 Local stability of the equilibria

The next step is to examine the stability of these equilibria of the fast subsystem (4) corresponding to varying β.

Carry out the linearization process and we have the Jacobian of system (4)

$$J|_{E^*_\beta} = \left[\frac{\partial F_i}{\partial Y_j}\right]_{ij}|_{E^*_\beta} = \begin{bmatrix} -q_{11} & 0 & -q_{13} & 0 & 0 & -q_{16} \\ q_{21} & -q_{22} & E & 0 & 0 & 0 \\ 0 & E & -q_{33} & 0 & 0 & 0 \\ 0 & \frac{3}{t_d} & 0 & -\frac{3}{t_d} & 0 & 0 \\ 0 & 0 & 0 & \frac{3}{t_d} & -\frac{3}{t_d} & 0 \\ 0 & 0 & 0 & 0 & \frac{3}{t_d} & -\frac{3}{t_d} \end{bmatrix} \tag{13}$$

The following details show the calculation of this matrix.

$$\begin{aligned} & \frac{\partial F_1}{\partial Y_1} = \frac{\partial F_1}{\partial G} \\ = & \frac{\partial}{\partial G}[G_{in} - f_2(G) - f_3(G)f_4(I_i) + f_5(x_3)] \\ = & -\frac{\partial}{\partial G} f_2(G) - f_4(I_i)\frac{\partial}{\partial G} f_3(G) \\ = & -\frac{\partial}{\partial G}\frac{r_2 G}{k_2 + G} - f_4(I_i)\frac{\partial}{\partial G}(c_1 G) \\ = & -r_2\frac{\partial}{\partial G}(1 - \frac{k_2}{k_2 + G}) - c_1 f_4(I_i) \\ = & r_2 k_2 \frac{\partial}{\partial G}(k_2 + G)^{-1} - c_1 f_4(I_i) \\ = & -r_2 k_2 (k_2 + G)^{-2} - c_1 f_4(I_i) \\ = & -\frac{r_2 k_2}{(k_2 + G)^2} - c_1(\frac{r_3 I_i^{n_2}}{k_3^{n_2} + I_i^{n_2}} + c_2) \end{aligned}$$

$$\frac{\partial F_1}{\partial Y_2} = \frac{\partial F_1}{\partial I_p} = \frac{\partial}{\partial I_p}[G_{in} - f_2(G) - f_3(G)f_4(I_i) + f_5(x_3)] = 0.$$

$$\begin{aligned} & \frac{\partial F_1}{\partial Y_3} = \frac{\partial F_1}{\partial I_i} \\ = & \frac{\partial}{\partial I_i}[G_{in} - f_2(G) - f_3(G)f_4(I_i) + f_5(x_3)] \end{aligned}$$

$$
\begin{aligned}
&= -f_3(G)\frac{\partial}{\partial I_i}f_4(I_i)\\
&= -f_3(G)\frac{\partial}{\partial I_i}(\frac{r_3 I_i^{n_2}}{k_3^{n_2}+I_i^{n_2}}+c_2)\\
&= -r_3 f_3(G)\frac{\partial}{\partial I_i}\frac{I_i^{n_2}}{k_3^{n_2}+I_i^{n_2}}\\
&= -r_3 f_3(G)\frac{\partial}{\partial I_i}(1-\frac{k_3^{n_2}}{k_3^{n_2}+I_i^{n_2}})\\
&= r_3 f_3(G)k_3^{n_2}\frac{\partial}{\partial I_i}(k_3^{n_2}+I_i^{n_2})^{-1}\\
&= -r_3 f_3(G)k_3^{n_2}(k_3^{n_2}+I_i^{n_2})^{-2}(n_2 I_i^{n_2-1})\\
&= -c_1 r_3 n_2 k_3^{n_2}\frac{G I_i^{n_2-1}}{(k_3^{n_2}+I_i^{n_2})^2}.
\end{aligned}
$$

$$
\frac{\partial F_1}{\partial Y_4}=\frac{\partial F_1}{\partial x_1}=\frac{\partial}{\partial x_1}[G_{in}-f_2(G)-f_3(G)f_4(I_i)+f_5(x_3)]=0.
$$

$$
\frac{\partial F_1}{\partial Y_5}=\frac{\partial F_1}{\partial x_2}=\frac{\partial}{\partial x_2}[G_{in}-f_2(G)-f_3(G)f_4(I_i)+f_5(x_3)]=0.
$$

$$
\begin{aligned}
\frac{\partial F_1}{\partial Y_6} &= \frac{\partial F_1}{\partial x_3}=\frac{\partial}{\partial x_3}[G_{in}-f_2(G)-f_3(G)f_4(I_i)+f_5(x_3)]\\
&= \frac{\partial}{\partial x_3}f_5(x_3)=\frac{\partial}{\partial x_3}\frac{r_4 k_4^{n_3}}{k_4^{n_3}+x_3^{n_3}}\\
&= r_4 k_4^{n_3}\frac{\partial}{\partial x_3}(k_4^{n_3}+x_3^{n_3})^{-1}\\
&= -r_4 k_4^{n_3}(k_4^{n_3}+x_3^{n_3})^{-2}(n_3 x_3^{n_3-1})\\
&= -r_4 n_3 k_4^{n_3}\frac{x_3^{n_3-1}}{(k_4^{n_3}+x_3^{n_3})^2}.
\end{aligned}
$$

$$
\begin{aligned}
\frac{\partial F_2}{\partial Y_1} &= \frac{\partial F_2}{\partial G}=\frac{\partial}{\partial G}[\beta f_1(G)-E_p(I_p-I_i)-\frac{I_p}{t_p}]\\
&= \beta\frac{\partial}{\partial G}f_1(G)=\beta\frac{\partial}{\partial G}\frac{r_1 G^{n_1}}{k_1^{n_1}+G^{n_1}}\\
&= \beta\frac{\partial}{\partial G}r_1(1-\frac{k_1^{n_1}}{k_1^{n_1}+G^{n_1}})
\end{aligned}
$$

$$
\begin{aligned}
&= -\beta r_1 \frac{\partial}{\partial G} \frac{k_1^{n_1}}{k_1^{n_1} + G^{n_1}} \\
&= -\beta r_1 k_1^{n_1} \frac{\partial}{\partial G} (k_1^{n_1} + G^{n_1})^{-1} \\
&= \beta r_1 k_1^{n_1} (k_1^{n_1} + G^{n_1})^{-2} (n_1 G^{n_1 - 1}) \\
&= \beta r_1 n_1 k_1^{n_1}
\end{aligned}
$$

$$
\begin{aligned}
\frac{\partial F_2}{\partial Y_2} &= \frac{\partial F_2}{\partial I_p} = \frac{\partial}{\partial I_p} [\beta f_1(G) - E(I_p - I_i) - \frac{I_p}{t_p}] \\
&= -E - \frac{1}{t_p}.
\end{aligned}
$$

$$
\frac{\partial F_2}{\partial Y_3} = \frac{\partial F_2}{\partial I_i} = \frac{\partial}{\partial I_i} [\beta f_1(G) - E(I_p - I_i) - \frac{I_p}{t_p}] = E.
$$

$$
\frac{\partial F_2}{\partial Y_4} = \frac{\partial F_2}{\partial x_1} = \frac{\partial}{\partial x_1} [\beta f_1(G) - E(I_p - I_i) - \frac{I_p}{t_p}] = 0.
$$

$$
\frac{\partial F_2}{\partial Y_5} = \frac{\partial F_2}{\partial x_2} = \frac{\partial}{\partial x_2} [\beta f_1(G) - E(I_p - I_i) - \frac{I_p}{t_p}] = 0.
$$

$$
\frac{\partial F_2}{\partial Y_6} = \frac{\partial F_2}{\partial x_3} = \frac{\partial}{\partial x_3} [\beta f_1(G) - E(I_p - I_i) - \frac{I_p}{t_p}] = 0.
$$

$$
\frac{\partial F_3}{\partial Y_1} = \frac{\partial F_3}{\partial G} = \frac{\partial}{\partial G} [E(I_p - I_i) - \frac{I_i}{t_i}] = 0.
$$

$$
\frac{\partial F_3}{\partial Y_2} = \frac{\partial F_3}{\partial I_p} = \frac{\partial}{\partial G} [E(I_p - I_i) - \frac{I_i}{t_i}] = E.
$$

$$
\begin{aligned}
\frac{\partial F_3}{\partial Y_3} &= \frac{\partial F_3}{\partial I_i} = \frac{\partial}{\partial I_i} [E(I_p - I_i) - \frac{I_i}{t_i}] \\
&= -E - \frac{1}{t_i}.
\end{aligned}
$$

$$\frac{\partial F_3}{\partial Y_4} = \frac{\partial F_3}{\partial x_1} = \frac{\partial}{\partial x_1}[E(I_p - I_i) - \frac{I_i}{t_i}] = 0.$$

$$\frac{\partial F_3}{\partial Y_5} = \frac{\partial F_3}{\partial x_2} = \frac{\partial}{\partial x_2}[E(I_p - I_i) - \frac{I_i}{t_i}] = 0.$$

$$\frac{\partial F_3}{\partial Y_6} = \frac{\partial F_3}{\partial x_3} = \frac{\partial}{\partial x_3}[E(I_p - I_i) - \frac{I_i}{t_i}] = 0.$$

$$\frac{\partial F_4}{\partial Y_1} = \frac{\partial F_4}{\partial G} = \frac{\partial}{\partial G}[\frac{3}{t_d}(I_p - x_1)] = 0.$$

$$\frac{\partial F_4}{\partial Y_2} = \frac{\partial F_4}{\partial I_p} = \frac{\partial}{\partial I_p}[\frac{3}{t_d}(I_p - x_1)] = \frac{3}{t_d}.$$

$$\frac{\partial F_4}{\partial Y_3} = \frac{\partial F_4}{\partial I_i} = \frac{\partial}{\partial I_i}[\frac{3}{t_d}(I_p - x_1)] = 0.$$

$$\frac{\partial F_4}{\partial Y_4} = \frac{\partial F_4}{\partial x_1} = \frac{\partial}{\partial x_1}[\frac{3}{t_d}(I_p - x_1)] = -\frac{3}{t_d}.$$

$$\frac{\partial F_4}{\partial Y_5} = \frac{\partial F_4}{\partial x_2} = \frac{\partial}{\partial x_2}[\frac{3}{t_d}(I_p - x_1)] = 0.$$

$$\frac{\partial F_4}{\partial Y_6} = \frac{\partial F_4}{\partial x_3} = \frac{\partial}{\partial x_3}[\frac{3}{t_d}(I_p - x_1)] = 0.$$

$$\frac{\partial F_5}{\partial Y_1} = \frac{\partial F_5}{\partial G} = \frac{\partial}{\partial G}[\frac{3}{t_d}(x_1 - x_2)] = 0.$$

$$\frac{\partial F_5}{\partial Y_2} = \frac{\partial F_5}{\partial I_p} = \frac{\partial}{\partial I_p}[\frac{3}{t_d}(x_1 - x_2)] = 0.$$

$$\frac{\partial F_5}{\partial Y_3} = \frac{\partial F_5}{\partial I_i} = \frac{\partial}{\partial I_i}[\frac{3}{t_d}(x_1 - x_2)] = 0.$$

$$\frac{\partial F_5}{\partial Y_4} = \frac{\partial F_5}{\partial x_1} = \frac{\partial}{\partial x_1}[\frac{3}{t_d}(x_1 - x_2)] = \frac{3}{t_d}.$$

$$\frac{\partial F_5}{\partial Y_5} = \frac{\partial F_5}{\partial x_2} = \frac{\partial}{\partial x_2}[\frac{3}{t_d}(x_1 - x_2)] = -\frac{3}{t_d}.$$

$$\frac{\partial F_5}{\partial Y_6} = \frac{\partial F_5}{\partial x_3} = \frac{\partial}{\partial x_3}[\frac{3}{t_d}(x_1 - x_2)] = 0.$$

$$\frac{\partial F_6}{\partial Y_1} = \frac{\partial F_6}{\partial G} = \frac{\partial}{\partial G}[\frac{3}{t_d}(x_2 - x_3)] = 0.$$

$$\frac{\partial F_6}{\partial Y_2} = \frac{\partial F_6}{\partial I_p} = \frac{\partial}{\partial I_p}[\frac{3}{t_d}(x_2 - x_3)] = 0.$$

$$\frac{\partial F_6}{\partial Y_3} = \frac{\partial F_6}{\partial I_i} = \frac{\partial}{\partial I_i}[\frac{3}{t_d}(x_2 - x_3)] = 0.$$

$$\frac{\partial F_6}{\partial Y_4} = \frac{\partial F_6}{\partial x_1} = \frac{\partial}{\partial x_1}[\frac{3}{t_d}(x_2 - x_3)] = 0.$$

$$\frac{\partial F_6}{\partial Y_5} = \frac{\partial F_6}{\partial x_2} = \frac{\partial}{\partial x_2}[\frac{3}{t_d}(x_2 - x_3)] = \frac{3}{t_d}.$$

$$\frac{\partial F_6}{\partial Y_6} = \frac{\partial F_6}{\partial x_3} = \frac{\partial}{\partial x_3}[\frac{3}{t_d}(x_2 - x_3)] = -\frac{3}{t_d}.$$

Therefore, in the Jacobian matrix (13),

$$\begin{aligned}
q_{11} &= \frac{r_2 k_2}{(k_2+G)^2} + c_1\left(\frac{r_3 I_i^{n_2}}{k_3^{n_2}+I_i^{n_2}} + c_2\right),\\
q_{13} &= c_1 r_3 n_2 k_3^{n_2} G \frac{I_i^{n_2-1}}{(k_3^{n_2}+I_i^{n_2})^2},\\
q_{16} &= r_4 n_3 k_4^{n_3} \frac{x_3^{n_3-1}}{(k_4^{n_3}+x_3^{n_3})^2},\\
q_{21} &= \beta r_1 n_1 k_1^{n_1} \frac{G^{n_1-1}}{(k_1^{n_1}+G^{n_1})^2},\\
q_{22} &= E + \frac{1}{t_p},\\
q_{33} &= E + \frac{1}{t_i}.
\end{aligned}$$

By Jacobian of the sub-system (4), we obtain its characteristic equation

$$\Delta(\lambda) = \lambda^6 + a_1\lambda^5 + a_2\lambda^4 + a_3\lambda^3 + a_4\lambda^2 + a_5\lambda + a_6 = 0, \tag{15}$$

where a_j, $j = 1, 2, \ldots, 6$ are expressions of all the given parameters.

The calculation details are presented as follows.

$$det(\lambda I - J)|_{E^*_\beta} = \begin{vmatrix} \lambda & 0 & 0 & 0 & 0 & 0\\ 0 & \lambda & 0 & 0 & 0 & 0\\ 0 & 0 & \lambda & 0 & 0 & 0\\ 0 & 0 & 0 & \lambda & 0 & 0\\ 0 & 0 & 0 & 0 & \lambda & 0\\ 0 & 0 & 0 & 0 & 0 & \lambda \end{vmatrix} - \begin{vmatrix} -q_{11} & 0 & -q_{13} & 0 & 0 & -q_{16}\\ q_{21} & -q_{22} & E & 0 & 0 & 0\\ 0 & E & -q_{33} & 0 & 0 & 0\\ 0 & \frac{3}{t_d} & 0 & -\frac{3}{t_d} & 0 & 0\\ 0 & 0 & 0 & \frac{3}{t_d} & -\frac{3}{t_d} & 0\\ 0 & 0 & 0 & 0 & \frac{3}{t_d} & -\frac{3}{t_d} \end{vmatrix}$$

$$
= \begin{vmatrix}
\lambda + q_{11} & 0 & q_{13} & 0 & 0 & q_{16} \\
-q_{21} & \lambda + q_{22} & -E & 0 & 0 & 0 \\
0 & -E & \lambda + q_{33} & 0 & 0 & 0 \\
0 & -\frac{3}{t_d} & 0 & \lambda + \frac{3}{t_d} & 0 & 0 \\
0 & 0 & 0 & -\frac{3}{t_d} & \lambda + \frac{3}{t_d} & 0 \\
0 & 0 & 0 & 0 & -\frac{3}{t_d} & \lambda + \frac{3}{t_d}
\end{vmatrix}
$$

$$
= (\text{-}1)^{1+6} q_{16} \begin{vmatrix}
-q_{21} & \lambda + q_{22} & -E & 0 & 0 \\
0 & -E & \lambda + q_{33} & 0 & 0 \\
0 & -\frac{3}{t_d} & 0 & \lambda + \frac{3}{t_d} & 0 \\
0 & 0 & 0 & -\frac{3}{t_d} & \lambda + \frac{3}{t_d} \\
0 & 0 & 0 & 0 & -\frac{3}{t_d}
\end{vmatrix}
$$

$$
+(\text{-}1)^{6+6}(\lambda + \tfrac{3}{t_d}) \begin{vmatrix}
\lambda + q_{11} & 0 & q_{13} & 0 & 0 \\
-q_{21} & \lambda + q_{22} & -E & 0 & 0 \\
0 & -E & \lambda + q_{33} & 0 & 0 \\
0 & -\frac{3}{t_d} & 0 & \lambda + \frac{3}{t_d} & 0 \\
0 & 0 & 0 & -\frac{3}{t_d} & \lambda + \frac{3}{t_d}
\end{vmatrix}
$$

$$
=\text{-}q_{16}(-1) \begin{vmatrix}
-q_{21} & -E & \lambda + q_{22} & 0 & 0 \\
0 & \lambda + q_{33} & -E & 0 & 0 \\
0 & 0 & -\frac{3}{t_d} & \lambda + \frac{3}{t_d} & 0 \\
0 & 0 & 0 & -\frac{3}{t_d} & \lambda + \frac{3}{t_d} \\
0 & 0 & 0 & 0 & -\frac{3}{t_d}
\end{vmatrix}
$$

$$
+(\lambda + \tfrac{3}{t_d})(-1)^{5+5}(\lambda + \tfrac{3}{t_d}) \begin{vmatrix}
\lambda + q_{11} & 0 & q_{13} & 0 \\
-q_{21} & \lambda + q_{22} & -E & 0 \\
0 & -E & \lambda + q_{33} & 0 \\
0 & -\frac{3}{t_d} & 0 & \lambda + \frac{3}{t_d}
\end{vmatrix}
$$

$$
=q_{16}(-q_{21}(\lambda + q_{33})(-\tfrac{3}{t_d})(-\tfrac{3}{t_d})(-\tfrac{3}{t_d}))
$$

$$+(\lambda+\tfrac{3}{t_d})^2(-1)^{4+4}(\lambda+\tfrac{3}{t_d})\begin{vmatrix}\lambda+q_{11} & 0 & q_{13}\\ -q_{21} & \lambda+q_{22} & -E\\ 0 & -E & \lambda+q_{33}\end{vmatrix}$$

$$=\mathrm{q}_{16}q_{21}(\tfrac{3}{t_d})^3(\lambda+q_{33})$$

$$+(\lambda+\tfrac{3}{t_d})^3\Big((-1)^{1+1}(\lambda+q_{11})\begin{vmatrix}\lambda+q_{22} & -E\\ -E & \lambda+q_{33}\end{vmatrix}+(-1)^{2+1}(-q_{21})\begin{vmatrix}0 & q_{13}\\ -E & \lambda+q_{33}\end{vmatrix}\Big)$$

$$=\mathrm{q}_{16}q_{21}(\tfrac{3}{t_d})^3(\lambda+q_{33})+(\lambda+\tfrac{3}{t_d})^3\Big((\lambda+q_{11})[(\lambda+q_{22})(\lambda+q_{33})-(-E)^2]+q_{21}[0\cdot(\lambda+q_{33})-(-E)q_{13}]\Big)$$

$$=\mathrm{q}_{16}q_{21}(\tfrac{3}{t_d})^3(\lambda+q_{33})+(\lambda+\tfrac{3}{t_d})^3\Big((\lambda+q_{11})[(\lambda+q_{22})(\lambda+q_{33})-E^2]+Eq_{21}q_{13}\Big)$$

$$=(\lambda+\tfrac{3}{t_d})^3(\lambda+q_{11})(\lambda+q_{22})(\lambda+q_{33})-E^2(\lambda+\tfrac{3}{t_d})^3(\lambda+q_{11})+Eq_{21}q_{13}(\lambda+\tfrac{3}{t_d})^3+q_{16}q_{21}(\tfrac{3}{t_d})^3(\lambda+q_{33}).$$

Then we are able to check the coefficient for every λ^j, $j=1,\ldots,6$.

For λ^5, $(\lambda+\frac{3}{t_d})^3(\lambda+q_{11})(\lambda+q_{22})(\lambda+q_{33})$ contains the term in such order. $(\lambda+\frac{3}{t_d})^3$ has $\lambda^3+3\Big(\frac{3}{t_d}\Big)\lambda^2$, which can contribute to the coefficient of λ^5, while $(\lambda+q_{11})(\lambda+q_{22})(\lambda+q_{33})$ has $\lambda^3+(q_{11}+q_{22}+q_{33})\lambda^2$ to contribute. Thus we have the coefficient

$$a_1=(q_{11}+q_{22}+q_{33})+3\Big(\frac{3}{t_d}\Big).$$

For λ^4, $(\lambda+\frac{3}{t_d})^3[(\lambda+q_{11})(\lambda+q_{22})(\lambda+q_{33})]$ and $-E^2(\lambda+\frac{3}{t_d})^3(\lambda+q_{11})$ contain the term in such order. The latter one can only contribute $-E^2$. For the former one, we check the $\lambda^3\lambda$, $\lambda^2\lambda^2$ and $\lambda\lambda^3$ formations, to get $(q_{11}q_{22}+q_{22}q_{33}+q_{11}q_{33})$, $3\Big(\frac{3}{t_d}\Big)(q_{11}+q_{22}+q_{33})$ and $3\Big(\frac{3}{t_d}\Big)^2$ respectively. Thus we have the coefficient

$$\begin{aligned}a_2 &= (q_{11}q_{22}+q_{22}q_{33}+q_{11}q_{33}-E^2)\\ &\quad +3\Big(\frac{3}{t_d}\Big)(q_{11}+q_{22}+q_{33})+3\Big(\frac{3}{t_d}\Big)^2.\end{aligned}$$

For λ^3, $(\lambda+\frac{3}{t_d})^3[(\lambda+q_{11})(\lambda+q_{22})(\lambda+q_{33})]$, $-E^2(\lambda+\frac{3}{t_d})^3(\lambda+q_{11})$ and $Eq_{21}q_{13}(\lambda+\frac{3}{t_d})^3$ contain the term in such order. For the first one, we check the $\lambda^3\lambda^0$, $\lambda^2\lambda$, $\lambda\lambda^2$ and $\lambda^0\lambda^3$ formations, to get $q_{11}q_{22}q_{33}$, $3\Big(\frac{3}{t_d}\Big)(q_{11}q_{22}+q_{22}q_{33}+q_{11}q_{33})$, $3\Big(\frac{3}{t_d}\Big)^2(q_{11}+q_{22}+q_{33})$ and $\Big(\frac{3}{t_d}\Big)^3$ respectively. For the second one, we check only the $\lambda^3\lambda^0$ and $\lambda^2\lambda$ formations, to get $-E^2q_{11}$ and $-3E^2\Big(\frac{3}{t_d}\Big)$. The third one contributes only $Eq_{21}q_{13}$. Thus we have the coefficient

$$\begin{aligned} a_3 &= (q_{11}q_{22}q_{33} - q_{11}E^2 + q_{13}q_{21}E) \\ &\quad +3\Big(\frac{3}{t_d}\Big)(q_{11}q_{22} + q_{22}q_{33} + q_{11}q_{33} - E^2) \\ &\quad +3\Big(\frac{3}{t_d}\Big)^2(q_{11} + q_{22} + q_{33}) + \Big(\frac{3}{t_d}\Big)^3. \end{aligned}$$

For λ^2, $(\lambda+\frac{3}{t_d})^3[(\lambda+q_{11})(\lambda+q_{22})(\lambda+q_{33})]$, $-E^2(\lambda+\frac{3}{t_d})^3(\lambda+q_{11})$ and $Eq_{21}q_{13}(\lambda+\frac{3}{t_d})^3$ contain the term in such order. For the first one, we check the $\lambda^2\lambda^0$, $\lambda\lambda$ and $\lambda^0\lambda^2$ formations, to get $3\Big(\frac{3}{t_d}\Big)q_{11}q_{22}q_{33}$, $3\Big(\frac{3}{t_d}\Big)^2(q_{11}q_{22}+q_{22}q_{33}+q_{11}q_{33})$, and $\Big(\frac{3}{t_d}\Big)^3(q_{11}+q_{22}+q_{33})$ respectively. For the second one, we check only the $\lambda^2\lambda^0$ and $\lambda\lambda$ formations, to get $-3E^2\Big(\frac{3}{t_d}\Big)q_{11}$ and $-3E^2\Big(\frac{3}{t_d}\Big)^2$. The third one contributes only $3Eq_{21}q_{13}\Big(\frac{3}{t_d}\Big)$. Thus we have the coefficient

$$\begin{aligned} a_4 &= 3\Big(\frac{3}{t_d}\Big)(q_{11}q_{22}q_{33} - q_{11}E^2 + q_{13}q_{21}E) \\ &\quad +3\Big(\frac{3}{t_d}\Big)^2(q_{11}q_{22} + q_{22}q_{33} + q_{11}q_{33} - E^2) \\ &\quad +\Big(\frac{3}{t_d}\Big)^3(q_{11} + q_{22} + q_{33}). \end{aligned}$$

For λ, all terms can contribute to it. Except for the last one, we check $\lambda\lambda^0$ and $\lambda^0\lambda$ formations.$(\lambda+\frac{3}{t_d})^3[(\lambda+q_{11})(\lambda+q_{22})(\lambda+q_{33})]$ results in $3\Big(\frac{3}{t_d}\Big)^2q_{11}q_{22}q_{33} + \Big(\frac{3}{t_d}\Big)^3(q_{11}q_{22}+q_{22}q_{33}+q_{11}q_{33})$. $-E^2(\lambda+\frac{3}{t_d})^3(\lambda+q_{11})$ gives $-E^2[3\Big(\frac{3}{t_d}\Big)^2q_{11}+\Big(\frac{3}{t_d}\Big)^3]$. And $Eq_{21}q_{13}(\lambda+\frac{3}{t_d})^3$ ends up with $Eq_{21}q_{13}\cdot 3\Big(\frac{3}{t_d}\Big)^2$. $q_{16}q_{21}(\frac{3}{t_d})^3(\lambda+q_{33})$ contains $q_{16}q_{21}(\frac{3}{t_d})^3$. Thus, we have the coefficient

$$
\begin{aligned}
a_5 &= 3\Big(\frac{3}{t_d}\Big)^2(q_{11}q_{22}q_{33} - q_{11}E^2 + q_{13}q_{21}E) \\
&\quad +\Big(\frac{3}{t_d}\Big)^3(q_{11}q_{22} + q_{22}q_{33} + q_{11}q_{33} + q_{16}q_{21} - E^2).
\end{aligned}
$$

For the constant term, we need only to find sum of the constants from each individual expression, which turns out to be

$$
a_6 = \Big(\frac{3}{t_d}\Big)^3(q_{11}q_{22}q_{33} + q_{16}q_{21}q_{33} - q_{11}E^2 + q_{13}q_{21}E).
$$

To sum up, we obtained

$$
a_1 = (q_{11} + q_{22} + q_{33}) + 3\Big(\frac{3}{t_d}\Big),
$$

$$
\begin{aligned}
a_2 &= (q_{11}q_{22} + q_{22}q_{33} + q_{11}q_{33} - E^2) \\
&\quad +3\Big(\frac{3}{t_d}\Big)(q_{11} + q_{22} + q_{33}) + 3\Big(\frac{3}{t_d}\Big)^2,
\end{aligned}
$$

$$
\begin{aligned}
a_3 &= (q_{11}q_{22}q_{33} - q_{11}E^2 + q_{13}q_{21}E) \\
&\quad +3\Big(\frac{3}{t_d}\Big)(q_{11}q_{22} + q_{22}q_{33} + q_{11}q_{33} - E^2) \\
&\quad +3\Big(\frac{3}{t_d}\Big)^2(q_{11} + q_{22} + q_{33}) + \Big(\frac{3}{t_d}\Big)^3
\end{aligned}
$$

$$
\begin{aligned}
a_4 &= 3\Big(\frac{3}{t_d}\Big)(q_{11}q_{22}q_{33} - q_{11}E^2 + q_{13}q_{21}E) \\
&\quad +3\Big(\frac{3}{t_d}\Big)^2(q_{11}q_{22} + q_{22}q_{33} + q_{11}q_{33} - E^2) \\
&\quad +\Big(\frac{3}{t_d}\Big)^3(q_{11} + q_{22} + q_{33}),
\end{aligned}
$$

$$
\begin{aligned}
a_5 &= 3\Big(\frac{3}{t_d}\Big)^2(q_{11}q_{22}q_{33} - q_{11}E^2 + q_{13}q_{21}E) \\
&\quad +\Big(\frac{3}{t_d}\Big)^3(q_{11}q_{22} + q_{22}q_{33} + q_{11}q_{33} + q_{16}q_{21} - E^2),
\end{aligned}
$$

$$a_6 = \Big(\frac{3}{t_d}\Big)^3(q_{11}q_{22}q_{33} + q_{16}q_{21}q_{33} - q_{11}E^2 + q_{13}q_{21}E).$$

Note: q_{ij}'s and a_i's are constant numbers evaluated at E^*_β. And the following property shows that all of them are nonnegative.

Property II.1 *For parameter expressions q_{ij} and a_i, $i = 1, \ldots, 6$,*

(i). $q_{ij} \geq 0$ for all (i, j); (ii). $a_i \geq 0$ for $i = 1, \ldots, 6$.

Proof. (i). Since all the parameters in the model are positive, by the definition of above q_{ij}'s, it is obvious that $q_{ij} \geq 0$ when evaluated at E^*_β. The equal sign holds for some q_{ij} at E^*_0.

(ii). To obtain $a_i \geq 0$, it is helpful to notice that

$$\begin{aligned} q_{22}q_{33} - E^2 &= \Big(E + \frac{1}{t_p}\Big)\Big(E + \frac{1}{t_i}\Big) \\ &= E^2 + \Big(\frac{1}{t_p} + \frac{1}{t_i}\Big)E + \frac{1}{t_p t_i} - E^2 \\ &= \Big(\frac{1}{t_p} + \frac{1}{t_i}\Big)E + \frac{1}{t_p t_i} > 0 \end{aligned}$$

And it is easy to observe that for every negative term in the expression of a_i, $i = 1, \ldots, 6$, it can be rearranged and factored out $(q_{22}q_{33} - E^2)$, which is positive. Thus we have $a_i \geq 0$ for $i = 1, \ldots, 6$.

Theorem II.4 *The fast sub-system (4) always has a locally stable trivial equilibrium point E'_0.*

Proof. For the fast sub-system, at $E'_0 = (G^*_0, 0, 0, 0, 0, 0)$, $q_{13} = q_{16} = q_{21} = 0$, thus

$$\begin{aligned} \Delta(\lambda)|_{E'_0} &= \Big(\lambda + \frac{3}{t_d}\Big)^3(\lambda + q_{11})[(\lambda + q_{22})(\lambda + q_{33}) - E_p E_i] \\ &= (\lambda + q_{11})[\lambda^2 + (q_{22} + q_{33})\lambda + (q_{22}q_{33} - E_p E_i)]\Big(\lambda + \frac{3}{t_d}\Big)^3. \end{aligned}$$

For the second factor in the characteristics Eq. (15), notice that

$$\begin{aligned}\delta &= (q_{22}+q_{33})^2 - 4(q_{22}q_{33}-E^2)\\ &= q_{22}^2+q_{33}^2+2q_{22}q_{33}-4q_{22}q_{33}+4E^2\\ &= q_{22}^2+q_{33}^2-2q_{22}q_{33}+4E^2\\ &= (q_{22}-q_{33})^2+4E^2\\ &> 0.\end{aligned}$$

Therefore this factor has two negative zeros. Hence, the characteristics Eq. (15) has total six negative zeros, which are given by

$$\begin{aligned}&\lambda_1 = -q_{11},\\ &\lambda_{2,3} = \frac{-(q_{22}+q_{33}) \pm \sqrt{(q_{22}-q_{33})^2+4E_pE_i}}{2},\\ &\lambda_{4,5,6} = -\frac{3}{t_d}.\end{aligned}$$

This implies that the trivial equilibrium point E_0' is locally stable for the fast sub-system.

Remark. This result indicates that if a subject's physical condition is 'near' the pathological state, i.e. the beta-cell mass is too small, then the situation is irreversible and the subject will eventually develop T1DM with no insulin produced.

2 Conditions of local stability

Next, the local stability of equilibria of the fast sub-system is determined by the varying β according to the following theorems.

We apply the Ruth-Hurwitz criterion to the characteristics Eq. (15).

Lemma II.1 ***(Routh-Hurwitz Criteria)*** *Given the polynomial,*

$$P(\lambda) = \lambda^n + a_1\lambda^{n-1} + \cdots + a_{n-1}\lambda + a_n,$$

where the coefficients a_i are real constants, $i = 1, \ldots, n$, define the n Hurwitz matrices using the coefficients a_i of the characteristic polynomial:

$$H_1 = (a_1),$$

$$H_2 = \begin{pmatrix} a_1 & 1 \\ a_3 & a_2 \end{pmatrix},$$

$$H_3 = \begin{pmatrix} a_1 & 1 & 0 \\ a_3 & a_2 & a_1 \\ a_5 & a_4 & a_3 \end{pmatrix},$$

$$\vdots$$

and

$$H_n = \begin{pmatrix} a_1 & 1 & 0 & 0 & \cdots & 0 \\ a_3 & a_2 & a_1 & 1 & \cdots & 0 \\ a_5 & a_4 & a_3 & a_2 & \cdots & 0 \\ \vdots & \vdots & \vdots & \vdots & \cdots & \vdots \\ 0 & 0 & 0 & 0 & \cdots & a_n \end{pmatrix}$$ *where $a_j = 0$ if $j > n$. All of the roots of the polynomial $P(\lambda)$ are negative or have negative real part iff the determinants of all Hurwitz matrices are positive:*

$$\det H_j > 0,\ j = 1, 2, \ldots, n.$$

For system (4), the determinants of Hurwitz matrices of its characteristic polynomial are given by

$$\det H_1 = |a_1| = a_1,$$

$$\det H_2 = \begin{vmatrix} a_1 & 1 \\ a_3 & a_2 \end{vmatrix} = a_1 a_2 - a_3,$$

$$\begin{aligned} \det H_3 &= \begin{vmatrix} a_1 & 1 & 0 \\ a_3 & a_2 & a_1 \\ a_5 & a_4 & a_3 \end{vmatrix} \\ &= a_3 |H_2| - a_1 \begin{vmatrix} a_1 & 1 \\ a_5 & a_4 \end{vmatrix} \end{aligned}$$

$$
\begin{aligned}
&= a_3|H_2| - a_1(a_1a_4 - a_5) \\
&= a_3|H_2| - a_1^2a_4 + a_1a_5,
\end{aligned}
$$

(expand by the last column)

$$
\begin{aligned}
\det H_4 &= \begin{vmatrix} a_1 & 1 & 0 & 0 \\ a_3 & a_2 & a_1 & 1 \\ a_5 & a_4 & a_3 & a_2 \\ 0 & a_6 & a_5 & a_4 \end{vmatrix} \\
&= a_4|H_3| - a_2 \begin{vmatrix} a_1 & 1 & 0 \\ a_3 & a_2 & a_1 \\ 0 & a_6 & a_5 \end{vmatrix} + \begin{vmatrix} a_1 & 1 & 0 \\ a_5 & a_4 & a_3 \\ 0 & a_6 & a_5 \end{vmatrix} \\
&= a_4|H_3| - a_2(a_5|H_2| - a_1^2a_6) + [a_5(a_1a_4 - a_5) - a_1a_3a_6] \\
&= a_4|H_3| - a_2a_5|H_2| + a_1^2a_2a_6 + a_1a_4a_5 - a_1a_3a_6 - a_5^2,
\end{aligned}
$$

(expand by the last column and then expand by the last column for the minor determinant)

$$
\begin{aligned}
\det H_5 &= \begin{vmatrix} a_1 & 1 & 0 & 0 & 0 \\ a_3 & a_2 & a_1 & 1 & 0 \\ a_5 & a_4 & a_3 & a_2 & a_1 \\ 0 & a_6 & a_5 & a_4 & a_3 \\ 0 & 0 & 0 & a_6 & a_5 \end{vmatrix} \\
&= a_5|H_4| - a_3 \begin{vmatrix} a_1 & 1 & 0 & 0 \\ a_3 & a_2 & a_1 & 1 \\ a_5 & a_4 & a_3 & a_2 \\ 0 & 0 & 0 & a_6 \end{vmatrix} + a_1 \begin{vmatrix} a_1 & 1 & 0 & 0 \\ a_3 & a_2 & a_1 & 1 \\ 0 & a_6 & a_5 & a_4 \\ 0 & 0 & 0 & a_6 \end{vmatrix}
\end{aligned}
$$

$$
\begin{aligned}
&= a_5|H_4| - a_3a_6|H_3| + a_1a_6 \begin{vmatrix} a_1 & 1 & 0 \\ a_3 & a_2 & a_1 \\ 0 & a_6 & a_5 \end{vmatrix} \\
&= a_5|H_4| - a_3a_6|H_3| + a_1a_6(a_5|H_2| - a_1^2a_6) \\
&= a_5|H_4| - a_3a_6|H_3| + a_1a_5a_6|H_2| - a_1^3a_6^2,
\end{aligned}
$$

(expand by the last column and then expand by the last row for the minor determinant)

$$
\det H_6 = \begin{vmatrix} a_1 & 1 & 0 & 0 & 0 & 0 \\ a_3 & a_2 & a_1 & 1 & 0 & 0 \\ a_5 & a_4 & a_3 & a_2 & a_1 & 1 \\ 0 & a_6 & a_5 & a_4 & a_3 & a_2 \\ 0 & 0 & 0 & a_6 & a_5 & a_4 \\ 0 & 0 & 0 & 0 & 0 & a_6 \end{vmatrix} = a_6|H_5|.
$$

(expand by the last row)

Therefore, the theorem follows.

Theorem II.5 *The equilibrium point E_β of system (4) is locally stable iff the following conditions are met.*

$$
\begin{aligned}
|H_1| &= a_1 > 0, \\
|H_2| &= a_1a_2 - a_3 > 0, \\
|H_3| &= a_3|H_2| - a_1^2a_4 + a_1a_5 > 0, \\
|H_4| &= a_4|H_3| - a_2a_5|H_2| + a_1^2a_2a_6 + a_1a_4a_5 \\
&\quad -a_1a_3a_6 - a_5^2 > 0, \\
|H_5| &= a_5|H_4| - a_3a_6|H_3| + a_1a_5a_6|H_2| - a_1^3a_6^2 > 0.
\end{aligned}
$$

Proof. This theorem is a direct result from Routh-Hurwitz Criteria. H_i's are Hurwitz

matrices after simplification. Particularly, noticing that $a_6 > 0$ and $|H_6| = a_6|H_5|$, we can eliminate the last inequality, for that $|H_5| > 0$ is equivalent to $|H_6| > 0$.

Remark. The theorem gives us the condition, or alternatively a threshold value of beta-cell mass when the body's glucose/insulin levels and the beta-cell mass tend to reach a steady state. This threshold value is determined by other physiological parameters. Depending on the starting condition of the parameters, it can approach either the pathological steady state or the healthy steady state. Namely, the starting beta-cell mass needs to exceed the threshold value to prevent the body from developing the diabetes.

3 Backward bifurcation

Let us take the relative strength of beta-cell functionality parameter w as a bifurcation parameter. We are interested in the possible backward bifurcation. Then examine the w-G bifurcation diagram, based on Eq. (12).

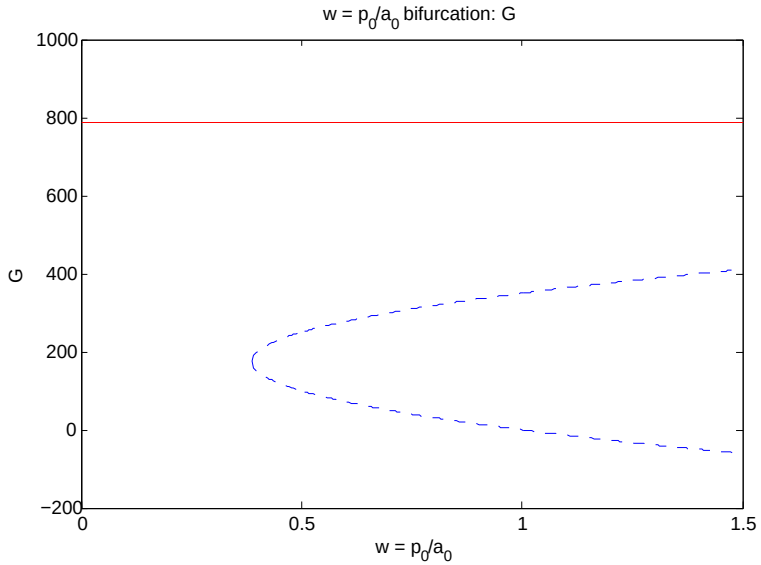

Figure 3. w bifurcation diagram against glucose

By Eq. (12), the lower branch of the bifurcation diagram 3 has the expression

$$G = \frac{r_a - \sqrt{r_a^2 - 4r_b(1-w)}}{2r_b}. \tag{16}$$

So we have

$$\begin{aligned}
\frac{\partial G}{\partial w} &= \frac{-\frac{1}{2}(r_a^2 - 4r_b(1-w))^{-\frac{1}{2}} \frac{\partial}{\partial w}(r_a^2 - 4r_b(1-w))}{2r_b} \\
&= \frac{-\frac{1}{2}(r_a^2 - 4r_b(1-w))^{-\frac{1}{2}} \cdot 4r_b}{2r_b} \\
&= -(r_a^2 - 4r_b(1-w))^{-\frac{1}{2}} < 0.
\end{aligned}$$

The negative partial derivative shows that the lower branch represents a backward bifurcation. That is, the glucose equilibrium concentration decreases as the relative strength of beta-cell functionality increases. This result can be interpreted as 'the higher beta-cell functionality, the lower equilibrium glucose level'.

4 Hopf Bifurcation Analysis

Next we examine the case when the insulin secretion experiences the intermittent rest. This behavior of the secretory regulation is hypothesized to help beta-cells sustain.

The ultradian oscillation of glucose and insulin concentrations has been observed in many studies. Model (1) should also possess similar features. We are mostly curious about whether a limit cycle exists in the dynamic of our model. Thus in this section, we try to find out the conditions under which the Hopf bifurcation exists. We start by examining the sufficient conditions of the existence of Hopf bifurcation. The following lemma helps us achieve this goal.

Lemma II.2 ***(Hopf)*** *Suppose that the C^4-system (4) with $Y \in R^6$ and $\mu \in R$ has a critical point Y_0 for some parameter $\mu = \mu_0$ and that $J = DF(Y_0, \mu_0)$ has a simple pair of pure imaginary eigenvalues and no other eigenvalues with zero real*

part. Furthermore, suppose

$$\frac{d}{d\mu}[Re\lambda(\mu)]_{\mu=\mu_0} \neq 0.$$

Then the Hopf bifurcation occurs at $\mu = \mu_0$.

By the characteristic Eq. (15), if it has a simple pair of pure imaginary eigenvalues $\lambda = \pm\omega i(\omega > 0)$ at $\mu = \mu_0$, then

$$\begin{aligned}
&\omega^6 i^6 + a_1\omega^5 i^5 + a_2\omega^4 i^4 + a_3\omega^3 i^3 + a_4\omega^2 i^2 + a_5\omega i + a_6 = 0,\\
&-\omega^6 + a_1\omega^5 i + a_2\omega^4 - a_3\omega^3 i - a_4\omega^2 + a_5\omega i + a_6 = 0,\\
&(-\omega^6 + a_2\omega^4 - a_4\omega^2 + a_6) + (a_1\omega^5 - a_3\omega^3 + a_5\omega)i = 0.
\end{aligned}$$

Thus the following holds

$$\begin{cases} -\omega^6 + a_2\omega^4 - a_4\omega^2 + a_6 = 0, \\ a_1\omega^5 - a_3\omega^3 + a_5\omega = 0. \end{cases} \tag{17}$$

Since $\omega > 0$, by the second equation of (17) we have that

$$a_1\omega^4 - a_3\omega^2 + a_5 = 0. \tag{18}$$

Therefore, the pair of pure imaginary eigenvalues can be found as

$$\omega^2 = \frac{a_3 \pm \sqrt{a_3^2 - 4a_1a_5}}{2a_1}. \tag{19}$$

Then substituting it into the first equation of (17) results in

$$\begin{aligned}
-\Big(\frac{a_3 \pm \sqrt{a_3^2 - 4a_1a_5}}{2a_1}\Big)^3 \quad &+ \quad a_2\Big(\frac{a_3 \pm \sqrt{a_3^2 - 4a_1a_5}}{2a_1}\Big)^2 \\
&- \quad a_4\Big(\frac{a_3 \pm \sqrt{a_3^2 - 4a_1a_5}}{2a_1}\Big) + a_6 = 0.
\end{aligned}$$

Next we compute $\frac{d\lambda}{d\mu}$ for some parameter μ. Again, by characteristic Eq. (15), it follows that

$$\begin{aligned}
&(6\lambda^5 + 5a_1\lambda^4 + 4a_2\lambda^3 + 3a_3\lambda^2 + 2a_4\lambda + a_5)\frac{d\lambda}{d\mu} \\
&+(\frac{da_1}{d\mu}\lambda^5 + \frac{da_2}{d\mu}\lambda^4 + \frac{da_3}{d\mu}\lambda^3 + \frac{da_4}{d\mu}\lambda^2 + \frac{da_5}{d\mu}\lambda + \frac{da_6}{d\mu}) = 0.
\end{aligned}$$

Notice $\lambda = \pm\omega i$ at $\mu = \mu_0$,

$$
\begin{aligned}
&(6\omega^5 i^5 + 5a_1\omega^4 i^4 + 4a_2\omega^3 i^3 + 3a_3\omega^2 i^2 + 2a_4\omega i + a_5)\frac{d\lambda}{d\mu} \\
&+(\frac{da_1}{d\mu}\omega^5 i^5 + \frac{da_2}{d\mu}\omega^4 i^4 + \frac{da_3}{d\mu}\omega^3 i^3 + \frac{da_4}{d\mu}\omega^2 i^2 + \frac{da_5}{d\mu}\omega i + \frac{da_6}{d\mu}) = 0, \\
&(6\omega^5 i + 5a_1\omega^4 - 4a_2\omega^3 i - 3a_3\omega^2 + 2a_4\omega i + a_5)\frac{d\lambda}{d\mu} \\
&+(\frac{da_1}{d\mu}\omega^5 i + \frac{da_2}{d\mu}\omega^4 - \frac{da_3}{d\mu}\omega^3 i - \frac{da_4}{d\mu}\omega^2 + \frac{da_5}{d\mu}\omega i + \frac{da_6}{d\mu}) = 0, \\
&[(6\omega^5 - 4a_2\omega^3 + 2a_4\omega)i + (5a_1\omega^4 - 3a_3\omega^2 + a_5)]\frac{d\lambda}{d\mu} \\
&+[(\frac{da_1}{d\mu}\omega^5 - \frac{da_3}{d\mu}\omega^3 + \frac{da_5}{d\mu}\omega)i + (\frac{da_2}{d\mu}\omega^4 - \frac{da_4}{d\mu}\omega^2 + \frac{da_6}{d\mu})] = 0, \\
&[(6\omega^5 - 4a_2\omega^3 + 2a_4\omega)i + (5a_1\omega^4 - 3a_3\omega^2 + a_5)]\frac{d\lambda}{d\mu} = \\
&-[(\frac{da_1}{d\mu}\omega^5 - \frac{da_3}{d\mu}\omega^3 + \frac{da_5}{d\mu}\omega)i + (\frac{da_2}{d\mu}\omega^4 - \frac{da_4}{d\mu}\omega^2 + \frac{da_6}{d\mu})], \\
&\frac{d\lambda}{d\mu} = -[(\frac{da_1}{d\mu}\omega^5 - \frac{da_3}{d\mu}\omega^3 + \frac{da_5}{d\mu}\omega)i + (\frac{da_2}{d\mu}\omega^4 - \frac{da_4}{d\mu}\omega^2 + \frac{da_6}{d\mu})]/ \\
&[(6\omega^5 - 4a_2\omega^3 + 2a_4\omega)i + (5a_1\omega^4 - 3a_3\omega^2 + a_5)].
\end{aligned}
$$

Therefore, we have

$$
\begin{aligned}
&sign\{\tfrac{d}{d\mu}[Re\lambda(\mu)]\} = sign\{Re(\tfrac{d\lambda}{d\mu})\} \\
&= -sign\tfrac{(\frac{da_2}{d\mu}\omega^4 - \frac{da_4}{d\mu}\omega^2 + \frac{da_6}{d\mu})(5a_1\omega^4 - 3a_3\omega^2 + a_5) + (\frac{da_1}{d\mu}\omega^5 - \frac{da_3}{d\mu}\omega^3 + \frac{da_5}{d\mu}\omega)(6\omega^5 - 4a_2\omega^3 + 2a_4\omega)}{(5a_1\omega^4 - 3a_3\omega^2 + a_5)^2 + (6\omega^5 - 4a_2\omega^3 + 2a_4\omega)^2} \\
&= -sign[(\tfrac{da_2}{d\mu}\omega^4 - \tfrac{da_4}{d\mu}\omega^2 + \tfrac{da_6}{d\mu})(5a_1\omega^4 - 3a_3\omega^2 + a_5) \\
&+(\tfrac{da_1}{d\mu}\omega^5 - \tfrac{da_3}{d\mu}\omega^3 + \tfrac{da_5}{d\mu}\omega)(6\omega^5 - 4a_2\omega^3 + 2a_4\omega)] \\
&= -sign[(\tfrac{da_2}{d\mu}\omega^4 - \tfrac{da_4}{d\mu}\omega^2 + \tfrac{da_6}{d\mu})(4a_1\omega^4 - 2a_3\omega^2) \\
&+(\tfrac{da_1}{d\mu}\omega^4 - \tfrac{da_3}{d\mu}\omega^2 + \tfrac{da_5}{d\mu})(6\omega^4 - 4a_2\omega^2 + 2a_4)\omega^2] \\
&= -sign[(\tfrac{da_2}{d\mu}\omega^4 - \tfrac{da_4}{d\mu}\omega^2 + \tfrac{da_6}{d\mu})(2a_1\omega^2 - a_3) \\
&+(\tfrac{da_1}{d\mu}\omega^4 - \tfrac{da_3}{d\mu}\omega^2 + \tfrac{da_5}{d\mu})(3\omega^4 - 2a_2\omega^2 + a_4)].
\end{aligned}
$$

By Eq. (19) it follows that

$$sign\Big\{\frac{d}{d\mu}[Re\lambda(\mu)]_{\mu=\mu_0}\Big\}$$

$$= -sign[(\frac{da_2}{d\mu}\Big(\frac{a_3 \pm \sqrt{a_3^2 - 4a_1a_5}}{2a_1}\Big)^2 - \frac{da_4}{d\mu}\Big(\frac{a_3 \pm \sqrt{a_3^2 - 4a_1a_5}}{2a_1}\Big) + \frac{da_6}{d\mu})$$
$$(2a_1\Big(\frac{a_3 \pm \sqrt{a_3^2 - 4a_1a_5}}{2a_1}\Big) - a_3)$$
$$+(\frac{da_1}{d\mu}\Big(\frac{a_3 \pm \sqrt{a_3^2 - 4a_1a_5}}{2a_1}\Big)^2 - \frac{da_3}{d\mu}\Big(\frac{a_3 \pm \sqrt{a_3^2 - 4a_1a_5}}{2a_1} + \frac{da_5}{d\mu}\Big)$$
$$(3\Big(\frac{a_3 \pm \sqrt{a_3^2 - 4a_1a_5}}{2a_1}\Big)^2 - 2a_2\Big(\frac{a_3 \pm \sqrt{a_3^2 - 4a_1a_5}}{2a_1}\Big) + a_4)].$$

By the above analysis, we can now state the following result.

Theorem II.6 *Suppose that parameter β varies while other parameters fix and system (4) with $Y \in R^6$ and $\beta \in R$ has a critical point Y_0 for parameter $\beta = \beta^*$. If the parameters of the system satisfy*

$$-(\frac{a_3 \pm \sqrt{a_3^2 - 4a_1a_5}}{2a_1})^3 + a_2(\frac{a_3 \pm \sqrt{a_3^2 - 4a_1a_5}}{2a_1})^2$$
$$-a_4(\frac{a_3 \pm \sqrt{a_3^2 - 4a_1a_5}}{2a_1}) + a_6 = 0,$$

then system (4) has a simple pair of pure imaginary eigenvalues given by

$$\lambda = \pm\omega i = \pm(\frac{a_3 + \sqrt{a_3^2 - 4a_1a_5}}{2a_1})^{\frac{1}{2}},$$

or

$$\lambda = \pm\omega i = \pm(\frac{a_3 - \sqrt{a_3^2 - 4a_1a_5}}{2a_1})^{\frac{1}{2}}.$$

Furthermore, if

$$\frac{d}{d\beta}[Re\lambda(\beta)]_{\beta=\beta^*} =$$
$$\Big(\frac{da_2}{d\beta}(\frac{a_3 \pm \sqrt{a_3^2 - 4a_1a_5}}{2a_1})^2 - \frac{da_4}{d\beta}\frac{a_3 \pm \sqrt{a_3^2 - 4a_1a_5}}{2a_1} + \frac{da_6}{d\beta}\Big)$$
$$(2a_1(\frac{a_3 \pm \sqrt{a_3^2 - 4a_1a_5}}{2a_1}) - a_3)$$
$$+\Big(\frac{da_1}{d\beta}(\frac{a_3 \pm \sqrt{a_3^2 - 4a_1a_5}}{2a_1})^2 - \frac{da_3}{d\beta}\frac{a_3 \pm \sqrt{a_3^2 - 4a_1a_5}}{2a_1} + \frac{da_5}{d\beta}\Big)$$

$$(3(\frac{a_3 \pm \sqrt{a_3^2 - 4a_1a_5}}{2a_1})^2 - 2a_2(\frac{a_3 \pm \sqrt{a_3^2 - 4a_1a_5}}{2a_1}) + a_4) \neq 0,$$

the system (4) undergoes a Hopf bifurcation at $\beta = \beta^*$, for some $\beta^* > 0$.

Next, we look for simpler and particular conditions that ensure the existence of a Hopf bifurcation. Denote that

$$h(\beta) := -(\frac{a_3 + \sqrt{a_3^2 - 4a_1a_5}}{2a_1})^3 + a_2(\frac{a_3 + \sqrt{a_3^2 - 4a_1a_5}}{2a_1})^2$$
$$-a_4(\frac{a_3 + \sqrt{a_3^2 - 4a_1a_5}}{2a_1}) + a_6 = 0,$$

and attempt to show

$$h(0) > 0;\ h(\infty) < 0.$$

Property II.2

$$a_1a_2|_{\beta=0} > a_3|_{\beta=0}.$$

Proof. To be concise, all the expressions $|_{\beta=0}$ in this proof are implicit. We show this property by proving $a_1a_2 - a_3 > 0$, which is obtained by comparing the terms of a_1a_2 and a_3. By expressions of q_{ij}'s, $q_{21} = 0$. We create following notation to simplify this discussion.

Let

$$\begin{aligned} T_d &= \frac{3}{t_d}, \\ e_1 &= q_{11} + q_{22} + q_{33}, \\ e_2 &= q_{11}q_{22} + q_{22}q_{33} + q_{11}q_{33} - E_pE_i, \\ e_3 &= q_{11}q_{22}q_{33} - q_{11}E_pE_i + q_{13}q_{21}E_i. \end{aligned} \tag{20}$$

Thus we have

$$a_1 = e_1 + 3T_d,$$

$$\begin{aligned} a_2 &= e_2 + 3T_d e_1 + 3T_d^2, \\ a_3 &= e_3 + 3T_d e_2 + 3T_d^2 e_1 + T_d^3. \end{aligned}$$

Then it follows that

$$\begin{aligned} & a_1 a_2 - a_3 = (e_1 + 3T_d)(e_2 + 3T_d e_1 + 3T_d^2) - (e_3 + 3T_d e_2 + 3T_d^2 e_1 + T_d^3), \\ = \;& e_1 e_2 + 3T_d e_1^2 + 3T_d^2 e_1 + 3T_d e_2 + 3T_d^2 e_1 + 9T_d^3 - e_3 - 3T_d e_2 - 3T_d^2 e_1 - T_d^3, \\ = \;& e_1 e_2 + 3T_d e_1^2 + 3T_d^2 e_1 + 8T_d^3 - e_3. \end{aligned}$$

Now we examine the expressions of e_1, e_2 and e_3. We can show that $e_1 e_2 - e_3 > 0$.

Therefore $a_1 a_2 - a_3 > 0$.

Lemma II.3 *If* $a_4|_{\beta=0} < \frac{a_3^2 - 4a_1 a_5}{a_1^2}|_{\beta=0} < (a_2^2 - 4a_4)|_{\beta=0}$, *then* $h(0) > 0$.

Proof. Similar to above treatment, the expressions $|_{\beta=0}$ are implicit. Taking a square root, we may rewrite the condition as $\sqrt{a_4} < \frac{\sqrt{a_3^2 - 4a_1 a_5}}{a_1} < \sqrt{a_2^2 - 4a_4}$. We are going to show

$$\begin{aligned} h(0) = & -\Big(\frac{a_3 + \sqrt{a_3^2 - 4a_1 a_5}}{2a_1}\Big)^3 + a_2\Big(\frac{a_3 + \sqrt{a_3^2 - 4a_1 a_5}}{2a_1}\Big)^2 \\ & -a_4\Big(\frac{a_3 + \sqrt{a_3^2 - 4a_1 a_5}}{2a_1}\Big) + a_6 > 0. \end{aligned}$$

We have

$$\begin{aligned} h(0) = & -\Big(\frac{a_3 + \sqrt{a_3^2 - 4a_1 a_5}}{2a_1}\Big)^3 + a_2\Big(\frac{a_3 + \sqrt{a_3^2 - 4a_1 a_5}}{2a_1}\Big)^2 \\ & -a_4\Big(\frac{a_3 + \sqrt{a_3^2 - 4a_1 a_5}}{2a_1}\Big) + a_6 \end{aligned}$$

$$
\begin{aligned}
&> -\Big(\frac{a_3+\sqrt{a_3^2-4a_1a_5}}{2a_1}\Big)^3 + a_2\Big(\frac{a_3+\sqrt{a_3^2-4a_1a_5}}{2a_1}\Big)^2 \\
&\quad -a_4\Big(\frac{a_3+\sqrt{a_3^2-4a_1a_5}}{2a_1}\Big) \\
&= -\Big(\frac{a_3+\sqrt{a_3^2-4a_1a_5}}{2a_1}\Big)[\Big(\frac{a_3+\sqrt{a_3^2-4a_1a_5}}{2a_1}\Big)^2 - a_2\Big(\frac{a_3+\sqrt{a_3^2-4a_1a_5}}{2a_1}\Big) + a_4].
\end{aligned}
$$

Thus it suffices to show that

$$
h(0) = -\Big(\frac{a_3+\sqrt{a_3^2-4a_1a_5}}{2a_1}\Big)[\Big(\frac{a_3+\sqrt{a_3^2-4a_1a_5}}{2a_1}\Big)^2 - a_2\Big(\frac{a_3+\sqrt{a_3^2-4a_1a_5}}{2a_1}\Big) + a_4] > 0.
$$

or equivalently,

$$
\Big(\frac{a_3+\sqrt{a_3^2-4a_1a_5}}{2a_1}\Big)^2 - a_2\Big(\frac{a_3+\sqrt{a_3^2-4a_1a_5}}{2a_1}\Big) + a_4 < 0. \tag{21}
$$

The left side of (21) is of quadratic form. To prove the above inequality, it is equivalent to prove $\frac{a_3+\sqrt{a_3^2-4a_1a_5}}{2a_1}$ falls between the two roots of $x^2 - a_2x + a_4 = 0$, i.e.

$$
\frac{a_2-\sqrt{a_2^2-4a_4}}{2} < \frac{a_3+\sqrt{a_3^2-4a_1a_5}}{2a_1} < \frac{a_2+\sqrt{a_2^2-4a_4}}{2}. \tag{22}
$$

First we consider the right-hand side inequality. By property (II.2), $\frac{a_3}{a_1} < a_2$. Together with the condition $\frac{\sqrt{a_3^2-4a_1a_5}}{a_1} < \sqrt{a_2^2-4a_4}$,

$$
\begin{aligned}
\frac{a_3+\sqrt{a_3^2-4a_1a_5}}{2a_1} &= \frac{a_3}{2a_1} + \frac{\sqrt{a_3^2-4a_1a_5}}{2a_1} \\
&< \frac{a_2}{2} + \frac{\sqrt{a_2^2-4a_4}}{2} \\
&= \frac{a_2+\sqrt{a_2^2-4a_4}}{2}.
\end{aligned}
$$

Then we consider the left-hand side inequality. By the condition $\sqrt{a_4} < \frac{\sqrt{a_3^2-4a_1a_5}}{a_1}$, $a_4 < \frac{a_3^2-4a_1a_5}{a_1^2}$. Then

$$
\begin{aligned}
\frac{a_2-\sqrt{a_2^2-4a_4}}{2} &= \frac{(a_2-\sqrt{a_2^2-4a_4})(a_2+\sqrt{a_2^2-4a_4})}{2(a_2+\sqrt{a_2^2-4a_4})} \\
&= \frac{a_2^2-(a_2^2-4a_4)}{2(a_2+\sqrt{a_2^2-4a_4})} = \frac{4a_4}{2(a_2+\sqrt{a_2^2-4a_4})} \\
&= \frac{2a_4}{a_2+\sqrt{a_2^2-4a_4}} < \frac{2a_4}{\frac{a_3+\sqrt{a_3^2-4a_1a_5}}{a_1}} \\
&< \frac{2a_4}{\frac{2\sqrt{a_3^2-4a_1a_5}}{a_1}} \\
&< \frac{2\frac{a_3^2-4a_1a_5}{a_1^2}}{\frac{2\sqrt{a_3^2-4a_1a_5}}{a_1}} \\
&= \frac{\sqrt{a_3^2-4a_1a_5}}{a_1} \\
&< \frac{a_3+\sqrt{a_3^2-4a_1a_5}}{2a_1}.
\end{aligned}
$$

The proof is done.

Lemma II.4 *If $\Delta = r_a^2 + 4r_b(p_0/a_0 - 1) > 0$, i.e. the complete model (1) has three equilibrium points, then it holds that*

$$h(\beta_2) < 0,$$

where β_2 is the β-coordinate of the equilibrium point E_2 for the complete system (1).

Theorem II.7 *If*

$$a_4|_{\beta=0} < \frac{a_3^2-4a_1a_5}{a_1^2}|_{\beta=0} < (a_2^2-4a_4)|_{\beta=0}$$

and $\Delta = r_a^2 + 4r_b(p_0/a_0 - 1) > 0$, there exists $\beta = \beta^* \in (0, \beta_2)$, at which the Hopf bifurcation occurs.

Proof. This is a direct result by intermediate value theorem from the two proceding lemmas and our Hopf theorem.

5 Insulin sensitivity

Then insulin sensitivity is considered as a measure of how sensitive the glucose concentration reacts to the secretion of insulin. It measures the ability of endogenous insulin to take down glucose in extracellular fluids by stimulating the peripheral consumption of glucose and inhibiting glucose release from the liver. The glucose-clamp technique is used to measure insulin sensitivity in practice. Quantitatively, the insulin dependent glucose uptake term in first equation of model (1) is used to define such parameter.

The function $f_4(I_i)$ is of Mechaelis Menten form. Previous works present the insulin dependent glucose uptake as a linear term S_iGI, where S_i is referred as the insulin sensitivity. In model (1), the corresponding term is $f_3(G)f_4(I_i) = c_1Gf_4(I_i)$. So we propose that insulin sensitivity can be examined by the value c_1 multiplied by the tangent of the turning point of function $f_4(I_i)$, according to the linear form definition. The following computation suggests the actual form of the insulin sensitivity.

$$\begin{aligned}
\frac{\partial}{\partial I_i} f_4(I_i) &= \frac{\partial}{\partial I_i}[\frac{r_3 I_i^{n_2}}{k_3^{n_2} + I_i^{n_2}} + c_2] \\
&= r_3 \frac{\partial}{\partial I_i} \frac{I_i^{n_2}}{k_3^{n_2} + I_i^{n_2}} \\
&= r_3 \frac{\partial}{\partial I_i} (1 - \frac{k_3^{n_2}}{k_3^{n_2} + I_i^{n_2}}) \\
&= -r_3 k_3^{n_2} \frac{\partial}{\partial I_i} (k_3^{n_2} + I_i^{n_2})^{-1} \\
&= r_3 k_3^{n_2} (k_3^{n_2} + I_i^{n_2})^{-2} (n_2 I_i^{n_2 - 1}) \\
&= r_3 n_2 k_3^{n_2} I_i^{n_2 - 1} (k_3^{n_2} + I_i^{n_2})^{-2}
\end{aligned}$$

$$\begin{aligned}
\frac{\partial^2}{\partial I_i^2} f_4(I_i) &= \frac{\partial}{\partial I_i}[r_3 n_2 k_3^{n_2} I_i^{n_2 - 1} (k_3^{n_2} + I_i^{n_2})^{-2}] \\
&= r_3 n_2 k_3^{n_2} [(n_2 - 1) I_i^{n_2 - 2} (k_3^{n_2} + I_i^{n_2})^{-2} + I_i^{n_2 - 1} (-2)(k_3^{n_2} + I_i^{n_2})^{-3} (n_2 I_i^{n_2 - 1})] \\
&= r_3 n_2 k_3^{n_2} I_i^{n_2 - 2} (k_3^{n_2} + I_i^{n_2})^{-3} [(n_2 - 1)(k_3^{n_2} + I_i^{n_2}) - 2 n_2 I_i^{n}{}_2]
\end{aligned}$$

To find the turning point, we let $\frac{\partial^2}{\partial I_i^2} f_4(I_i) = 0$ and thus have

$$
\begin{aligned}
&(n_2 - 1)(k_3^{n_2} + I_i^{n_2}) - 2n_2 I_i^{n_2} = 0 \\
&(n_2 - 1)(k_3^{n_2} + I_i^{n_2}) = 2n_2 I_i^{n_2} \\
&(n_2 - 1)k_3^{n_2} + (n_2 - 1)I_i^{n_2} = 2n_2 I_i^{n_2} \\
&(n_2 - 1)k_3^{n_2} = (n_2 + 1)I_i^{n_2} \\
&I_i^{n_2} = \frac{n_2 - 1}{n_2 + 1} k_3^{n_2} \\
&I_i = (\frac{n_2 - 1}{n_2 + 1})^{\frac{1}{n_2}} k_3
\end{aligned}
$$

Then it is substituted into the expression of first derivative of $f_4(I_i)$, resulting in

$$
\begin{aligned}
S_i : &= c_1 \cdot r_3 n_2 k_3^{n_2} [(\frac{n_2 - 1}{n_2 + 1})^{\frac{1}{n_2}} k_3]^{n_2 - 1} (k_3^{n_2} + [(\frac{n_2 - 1}{n_2 + 1})^{\frac{1}{n_2}} k_3]^{n_2})^{-2} \\
&= c_1 r_3 n_2 k_3^{n_2} (\frac{n_2 - 1}{n_2 + 1})^{\frac{n_2 - 1}{n_2}} k_3^{n_2 - 1} (k_3^{n_2} + \frac{n_2 - 1}{n_2 + 1} k_3^{n_2})^{-2} \\
&= c_1 r_3 n_2 k_3^{2n_2 - 1} (\frac{n_2 - 1}{n_2 + 1})^{\frac{n_2 - 1}{n_2}} [k_3^{n_2} (1 + \frac{n_2 - 1}{n_2 + 1})]^{-2} \\
&= c_1 r_3 n_2 k_3^{2n_2 - 1} k_3^{-2n_2} (\frac{n_2 - 1}{n_2 + 1})^{\frac{n_2 - 1}{n_2}} (1 + \frac{n_2 - 1}{n_2 + 1})^{-2} \\
&= \frac{c_1 r_3 n_2}{k_3} \frac{(\frac{n_2 - 1}{n_2 + 1})^{\frac{n_2 - 1}{n_2}}}{(1 + \frac{n_2 - 1}{n_2 + 1})^2}
\end{aligned}
$$

Therefore, we formally propose that the insulin sensitivity to be examined by the following value

$$
S_i := \frac{c_1 r_3 n_2}{k_3} \frac{(\frac{n_2 - 1}{n_2 + 1})^{\frac{n_2 - 1}{n_2}}}{(1 + \frac{n_2 - 1}{n_2 + 1})^2} \tag{23}
$$

Remark. This calculation of insulin sensitivity is in fact based on the linearization of the Mechaelis Menten function. It is evaluated as the slope of the tangent line at the turning point because it captures the geometric features of the old definition. However, this new evaluation uses four parameters instead of only one in old definition to be more acurate. c_1 and r_3 are the parameters relating to

maximum insulin-dependent glucose uptake rate. k_3 is the half saturation insulin level for insulin-dependent glucose uptake. n_2 is the order parameter in this term and $n_2\frac{(\frac{n_2-1}{n_2+1})^{\frac{n_2-1}{n_2}}}{(1+\frac{n_2-1}{n_2+1})^2}$ is an adjustment in the evaluation of insulin sensitivity.

6 Some useful mathematical results

For the sake of exploring the long term changes of body conditions, we are curious about the long term trajectory behavior and have the following lemma.

Lemma II.5 *If* $\lim_{t\to\infty}\beta(t)=0$*, then the trajectory is attracted to* E_0*.*

Proof. We begin by adding up the second and third equations of model (1).

$$\begin{aligned}(I_p+I_i)' &= \beta f_1(G)-\frac{I_p}{t_p}-\frac{I_i}{t_i}\\ &< \beta f_1(G)-\frac{I_p}{t_{pi}}-\frac{I_i}{t_{pi}}\\ &= \beta f_1(G)-\frac{I_p+I_i}{t_{pi}},\end{aligned}$$

where $t_{pi}=\max\{t_p,t_i\}$.

Let $I=I_p+I_i$, then we have a new differential inequality

$$I'(t)<\beta(t)f_1(G)-\frac{I}{t_{pi}} \tag{24}$$

Moreover, we have $f_1(G)=\frac{r_1G^{n_1}}{k_1^{n_1}+G^{n_1}}<r_1$, and thus

$$I'(t)<r_1\beta(t)-\frac{I}{t_{pi}}. \tag{25}$$

The differential equation

$$J'(t)=r_1\beta(t)-\frac{J(t)}{t_{pi}},\ J(0)=J_0 \tag{26}$$

can be solved in this way:

$$
\begin{aligned}
J'(t) + \frac{J(t)}{t_{pi}} &= r_1\beta(t), \\
e^{t/t_{pi}}(J'(t) + \frac{J(t)}{t_{pi}}) &= e^{t/t_{pi}} r_1\beta(t), \\
\mathrm{e}^{t/t_{pi}} J(t)' &= r_1 e^{t/t_{pi}}\beta(t), \\
e^{t/t_{pi}} J(t) - e^{0/t_{pi}} J(0) &= r_1 \int_0^t e^{t/t_{pi}}\beta(t)dt, \\
e^{t/t_{pi}} J(t) &= r_1 \int_0^t e^{t/t_{pi}}\beta(t)dt + J_0, \\
J(t) &= r_1 e^{-t/t_{pi}}[\int_0^t e^{t/t_{pi}}\beta(t)dt + J_0].
\end{aligned}
$$

By comparison theorem, $I'(t) < J'(t)$ leads to

$$
I(t) < J(t) = r_1 e^{-t/t_{pi}}[\int_0^t e^{t/t_{pi}}\beta(t)dt + J_0]. \tag{27}
$$

Therefore, if $\lim_{t\to\infty}\beta(t) = 0$, then there exists $\delta > 0$ such that $\beta(t) < \delta$ provided $t > M$, for some large enough $M > 0$. Then we have

$$
\begin{aligned}
I(t) &\leq r_1 e^{-t/t_{pi}}[\int_0^t e^{t/t_{pi}}\delta dt + J_0], \\
&= r_1 e^{-t/t_{pi}}[\delta t_{pi}(e^{t/t_{pi}} - 1) + J_0], \\
&= r_1 e^{-t/t_{pi}}[\delta t_{pi} e^{t/t_{pi}} + (J_0 - \delta t_{pi})], \\
&= r_1\delta t_{pi} + e^{-t/t_{pi}}(J_0 - \delta t_{pi}), \\
&< r_1 t_{pi}\delta + J_0\delta = (r_1 t_{pi} + J_0)\delta,
\end{aligned}
$$

for $t > M$, i.e. $\lim_{t\to\infty} I(t) = 0$.

Then $\lim_{t\to\infty} I_p(t) = 0$ and $\lim_{t\to\infty} I_i(t) = 0$. This is to say the trajectory is attracted to E_0.

Proof is done.

Remark. This theorem suggests that if the beta-cell mass diminshes gradually to zero, then the body develops the pathological state with almost zero insulin and

extremely high glucose level. Further suppose $G(t)$ and $I(t)$ are periodic, or alternatively undergoing the ultradian oscillation. Then the trajectory must not be attracted to E_0. Therefore, it implies that $\lim_{t\to\infty}\beta(t) \neq 0$. That said, the glucose/insulin level oscillation keeps the beta-cell mass from dying out.

Next, we want to check the boundedness of all the solutions. The well-known Fluctuation Lemma [33] will be of great help.

Lemma II.6 ***(Fluctuation)*** *Let f be a differentiable function. If*

$$l = \liminf_{t\to\infty} f(t) < \limsup_{t\to\infty} f(t) = L,$$

then there are sequences $\{t_k\} \uparrow \infty$ and $\{s_k\} \uparrow \infty$ such that, for all k

$$f'(t_k) = f'(s_k) = 0,\ \lim_{k\to\infty} f(t_k) = L \quad \textit{and} \quad \lim_{k\to\infty} f(s_k) = l.$$

Moreover, the following differential inequality will also be applied several times in the proof of boundedness.

Lemma II.7 *If $h'(t) \leq p - qh(t)$, or $h'(t) \geq p - qh(t)$, on the interval (T_1, T_2), where $p, q > 0$, then*

$$h(t) \leq \frac{p}{q} + \Big(h(T_1) - \frac{p}{q}\Big)e^{q(T_1 - t)},$$

or

$$h(t) \geq \frac{p}{q} + \Big(h(T_1) - \frac{p}{q}\Big)e^{q(T_1 - t)},$$

for all $t \in (T_1, T_2)$.

Proof. We make transformations on the differential inequality in this way: on the interval (T_1, T_2), we have

$$
\begin{aligned}
h'(t) &\leq p - qh(t) \\
h'(t) + qh(t) &\leq p \\
(h'(t) + qh(t))e^{qt} &\leq pe^{qt} \\
(h(t)e^{qt})' &\leq pe^{qt} \\
h(t)e^{qt}|_{T_1}^{t} &\leq p\int_{T_1}^{t} e^{qt}dt, \text{ integrate both sides} \\
h(t)e^{qt} - h(T_1)e^{qT_1} &\leq \frac{p}{q}e^{qt}|_{T_1}^{t} \\
h(t)e^{qt} - h(T_1)e^{qT_1} &\leq \frac{p}{q}(e^{qt} - e^{qT_1}) \\
h(t)e^{qt} &\leq \frac{p}{q}e^{qt} + h(T_1)e^{qT_1} - \frac{p}{q}e^{qT_1}, \text{ multiply both sides by } e^{-qt} \\
h(t) &\leq \frac{p}{q} + (h(T_1) - \frac{p}{q})e^{q(T_1 - t)}
\end{aligned}
$$

When the inequality sign is reversed, the above transformations are exactly the same. Thus the proof is done.

Theorem II.8 *$G(t)$ is uniformly bounded above and below away from 0.*

Proof. Let us examine the expressions of functions in model (1) again.

$$
\begin{aligned}
f_1(G) &= \frac{r_1 G^{n_1}}{k_1^{n_1} + G^{n_1}}, \\
f_2(G) &= \frac{r_2 G}{k_2 + G}, \\
f_3(G) &= c_1 G, \\
f_4(I_i) &= \frac{r_3 I_i^{n_2}}{k_3^{n_2} + I_i^{n_2}} + c_2, \\
f_5(x_3) &= \frac{r_4 k_4^{n_3}}{k_4^{n_3} + x_3^{n_3}}, \\
p(I_p) &= \frac{p_0 I_p}{r_0 + I_p^2},
\end{aligned}
$$

$$a(G, I_p) = \frac{a_0 I_p}{r_0 + I_p^2}(1 - r_a G + r_b G^2).$$

Notice that if $G(t) = 0$, for some $t \geq 0$, then $G'(t) = G_{in} - f_2(0) - f_3(0)f_4(I_i) + f_5(x_3) = G_{in} + f_5(x_3) \geq G_{in} > 0$. Thus $G(t) \geq 0$ for all $t \geq 0$. By Lemma II.6, there is a sequence $\{s_k\} \uparrow \infty$ such that,

$$G'(s_k) = 0, \text{ and } \lim_{k\to\infty} G(s_k) = \underline{G}.$$

Thus by the first equation of model (1),

$$0 = G'(s_k) = G_{in} - f_2(G(s_k)) - f_3(G(s_k))f_4(I_i(s_k)) + f_5(x_3(s_k)), \text{ for all } k.$$

For any $\eta > 0$, there exists s_{k_0}, such that,

$$G(s_{k_0}) < \underline{G} + \eta.$$

Since f_2, f_3, f_4 are increasing functions and f_5 is a decreasing function,

$$\begin{aligned} 0 &= G'(s_{k_0}) = G_{in} - f_2(G(s_k)) - f_3(G(s_k))f_4(I_i(s_k)) + f_5(x_3(s_k)) \\ &\geq G_{in} - f_2(\underline{G} + \eta) - f_3(\underline{G} + \eta)f_4(r_3 + c_2) \\ & f_2(\underline{G} + \eta) + f_3(\underline{G} + \eta)f_4(r_3 + c_2) \geq G_{in} \end{aligned}$$

Letting $\eta \to 0$, we obtain

$$f_2(\underline{G}) + f_3(\underline{G})f_4(r_3 + c_2) \geq G_{in}.$$

Suppose $\underline{G} = 0$, this equation implies that $f_2(0) + f_3(0)f_4(r_3 + c_2) = 0 \geq G_{in}$. A contradiction occurs, as $G_{in} > 0$ by our model assumption. Thus $\underline{G} > 0$, or there exists $\delta > 0$ such that $\underline{G} = \delta$.

Next we have

$$\begin{aligned} G' &= G_{in} - f_2(G) - f_3(G)f_4(I_i) + f_5(x_3) \\ &\leq G_{in} - c_1 G c_2 + r_4 \\ &= (G_{in} + r_4) - c_1 c_2 G \end{aligned}$$

By Lemma II.7, $G(t) \leq \frac{G_{in}+r_4}{c_1c_2} + (G(0) - \frac{G_{in}+r_4}{c_1c_2})e^{-c_1c_2t}$ for all $t \in (0, \infty)$. Thus

$$G(t) \leq \frac{G_{in} + r_4}{c_1c_2} + G(0)e^{-c_1c_2t} \leq \frac{G_{in} + r_4}{c_1c_2} + G(0), \tag{28}$$

for all $t \in (0, \infty)$. The proof is done.

Remark. Our intensive numerical simulations demonstrate that the solutions of the system are also bounded above. So we conjecture that the system is permanent.

3 Numerical simulation

In this section, numerical simulations will be conducted by Matlab to validate some findings of analytical results.

1 Phase space analysis

We analyzed the model numerically with parameters determined by experiment data and literatures, and estimates as well.

The table given below includes important parameters used.

TABLE 1

Parameters in model - [92] Table 1, unit conversion applied

Parameter	Value	Unit	Interpretation
G_{in}	2.16	mg$\cdot$ dl^{-1} min^{-1}	glucose infusion rate
t_p	6	min	delay time parameter
t_i	100	min	delay time parameter
t_d	36	min	delay time parameter
E	0.067	min^{-1}	transfer rate of insulin between plasma and intercellular space
r_1	0.08	μ U ml^{-1} min^{-1}	maximal secretion rate of insulin stimulated by glucose
k_1	203.3	mg$\cdot$ dl^{-1}	half saturation glucose concentration
r_2	0.8	mg$\cdot$ dl^{-1} min^{-1}	maximal insulin-independent glucose consumption rate
k_2	9.7	mg$\cdot$ dl^{-1}	half saturation glucose concentration

Using our model with the above carefully selected parameter values, we simulated the dynamics of the glucose and insulin concentration along with the beta-cell mass over a long time peroid.

First we analyze the case when taking β as a bifurcation parameter. Notice that β is also the slow variable changing throughout time. Thus the type of equilibrium of sub-system (4) may change as time passes.

Based on the above theorem, we can prove there exists a value for parameter β, denoted by β^*, where the sub-system (4) undergoes a Hopf bifurcation.

The following Fig. 4 is the bifurcation diagram for β, which is produced by numerical simulation of fast sub-system dynamic.

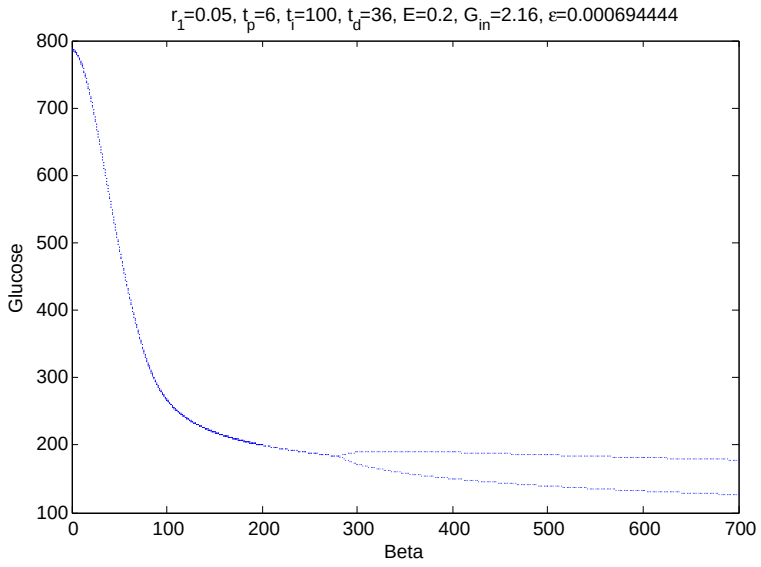

Figure 4. Bifurcation diagram for β

When the value of β is small, the fast sub-system has a unique stable equilibrium point. As β increases and reaches the Hopf bifurcation value, the unique equilibrium point becomes unstable and a limit cycle bifurcates out. Further, the amplitude grows as β increases.

Then numerical simulation of the complete system was carried out.

When the initial β_0 chosen is small, the Routh-Hurwitz criteria is satisfied. Under such case, the fast sub-system equilibrium is locally stable. When viewing the dynamics of the complete system, the trajectory will go to the critical manifold through fast dynamics, and then be attracted to E_0, the trivial equilibrium of the system, through slow dynamics. Fig. 5 and Fig. 6 present the phase space trajectory and the solution curves, respectively.

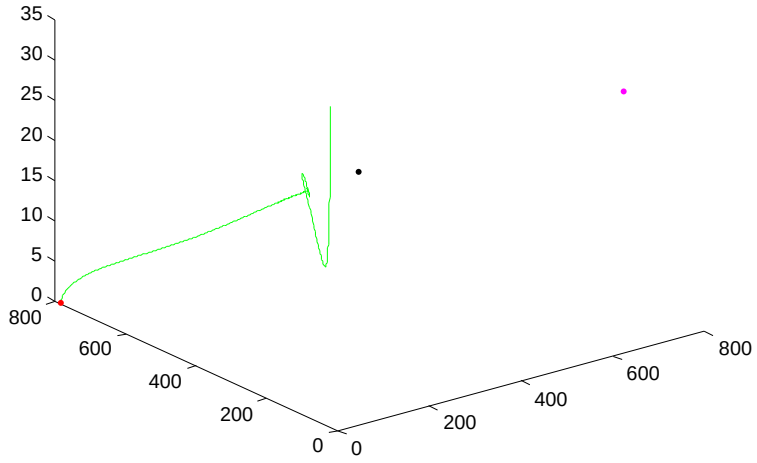

Figure 5. Phase space trajectory

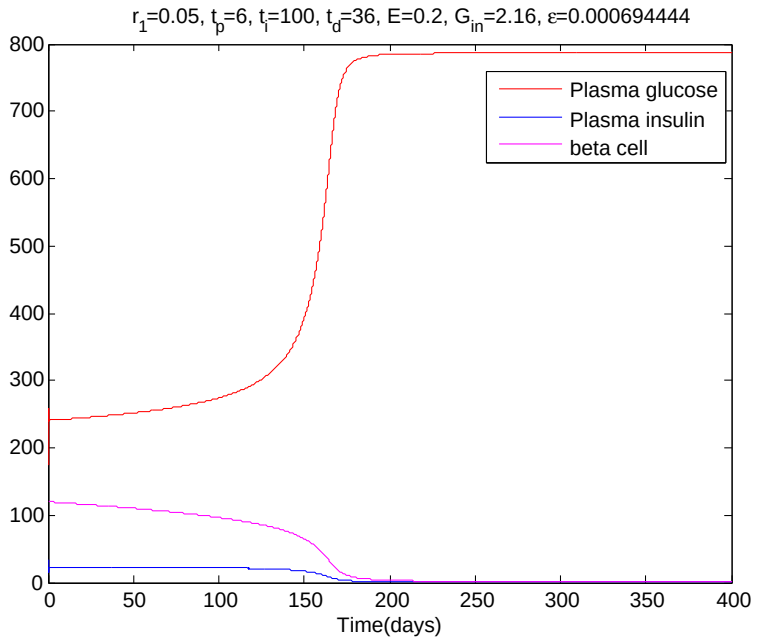

Figure 6. Solution curves

This simulation result may indicate that if the beta-cell mass has not been

formed sufficiently during embryonic and postnatal development, it might diminish gradually and eventually die out over years. Under such circumstance, the body will not produce any insulin, which is the typical symptom of T1DM.

Then the Pima indians T2DM development data is used to fit this dynamics.

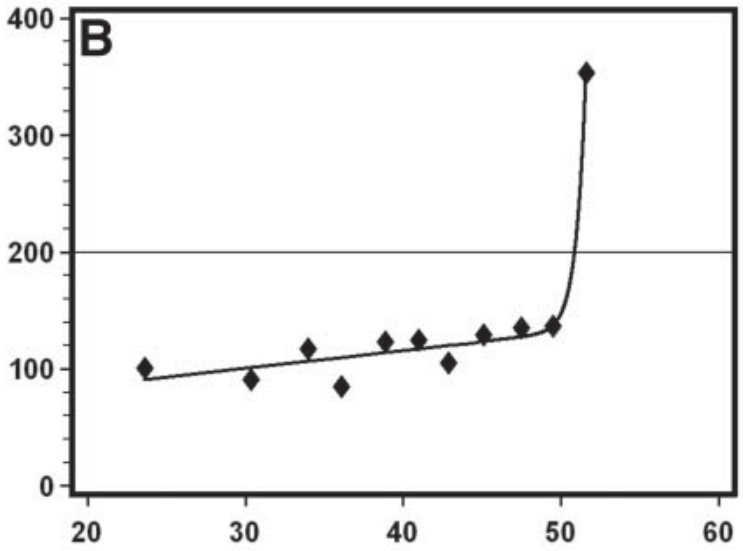

Figure 7. Data from Pima Indian: glucose level versus age

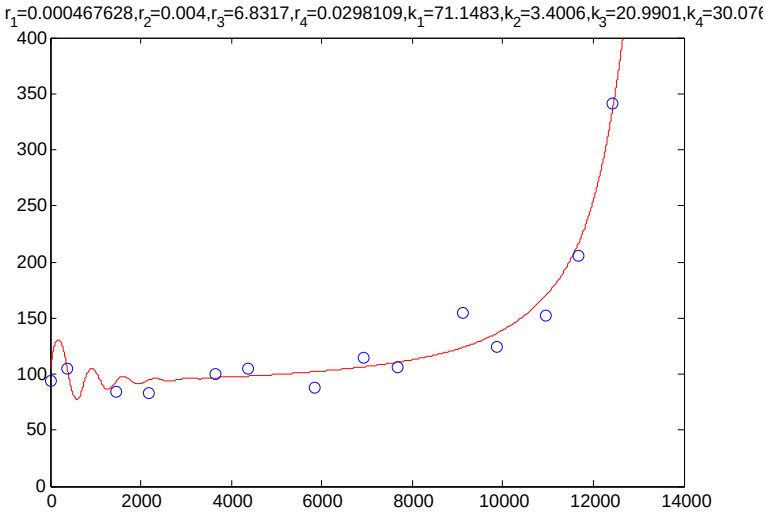

Figure 8. Model fitted

When β_0 chosen is larger than β^*, the stability of the equilibrium point of (4) changes. A limit cycle will be bifurcated out in the fast sub-system. The bigger β, the larger amplitude of the limit cycle, which is observed in the bifurcation diagram, Fig. 4. However, in the full system dynamics, this limit cycle breaks, since β changes slowly over time. The following figure illustrates two trajectories starting from two different initial conditions with only differences in β_0.

This simulation finding has a similar dynamic to that of the ultradian oscillation of insulin secretion discussed in [92]. As suggested in previous literatures ([57],[92]), such oscillation may be the result of the Hopf bifurcation in the insulin-glucose negative feedback mechanism. The profile shows a clear self-sustained oscillation if we do not take into account the change in β over time.

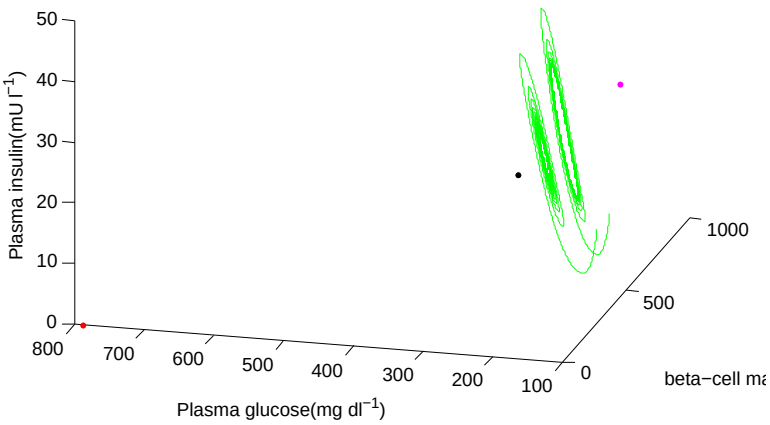

Figure 9. Trajectories starting from various initial conditions

The zoom-in trajectory is illustrated in the next figure, Fig. 10, together with the corresponding solution curves, Fig. 11. The limit cycle predicted by the bifurcation diagram for fast sub-system is 'broken' in the β direction in the phase space.

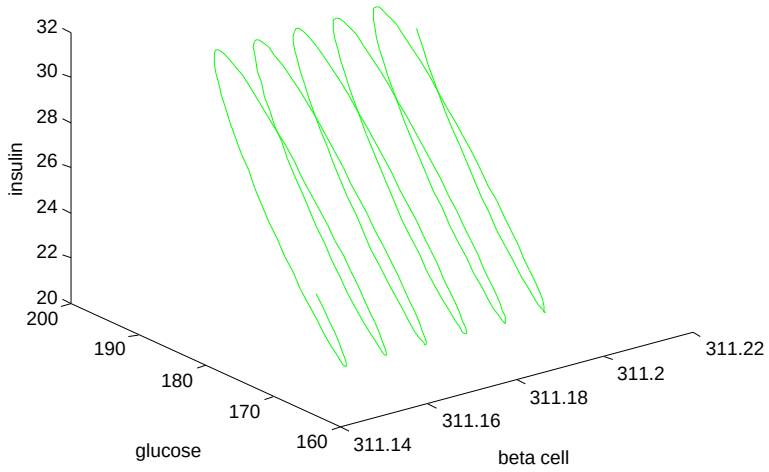

Figure 10. Zoom-in Trajectory - phase space

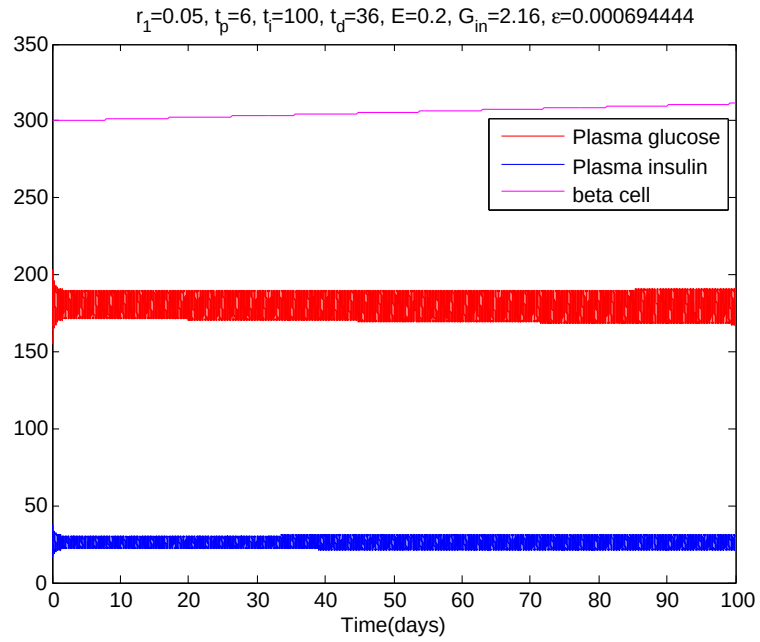

Figure 11. Zoom-in Trajectory - solution curves

Interestingly, we have also found the possibility of the existence of a global

limit cycle for the full problem. As illustrated in the following figures, Fig. 12, trajectories starting from different initial conditions show the trend approaching a certain 'limit cycle'. The left panel presents a trajectory that going spirally with the β value increasing, while the right panel presents another trajectory that going spirally with the β value decreasing. It is logically natural to speculate that there exists a limit cycle of the full system between these two trajectories. That is, we conjecture that the omega-limit set is a limit cycle of the full system.

In fact, the middle panel shows a simulation which appears to be a limit cycle of the full system, even though numerical simulations cannot ensure it is one indeed.

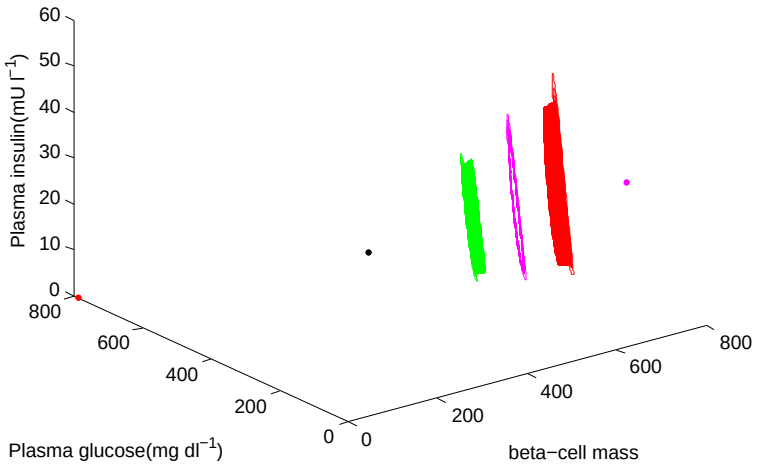

Figure 12. Trajectories approaching a limit cycle(purple) for the full system

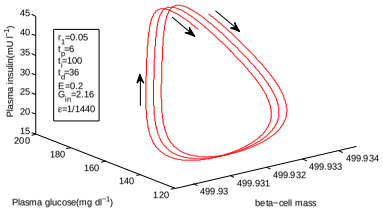

Figure 15. Trajectory - beta decreases

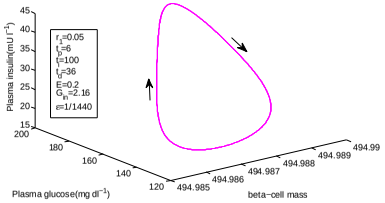

Figure 14. Limit cycle

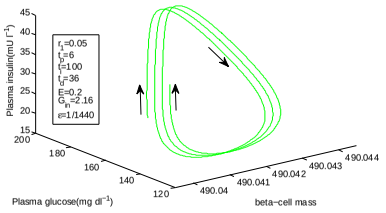

Figure 13. Trajectory - beta increases

2 Insulin sensitivity analysis

The insulin sensitivity is a significant factor in development of diabetes. The insulin sensitivity declining usually associates with the diabetes development. For the insulin sensitivity index change over time, the following simulation results were produced.

Sensitivity index S_i is assumed to change over time in an exponentially decreasing manner, i.e. $S_i = e^{-at}$, which satisfies the equation $\frac{dS_i}{dt} = -aS_i$. Fig. 16 presents this setting.

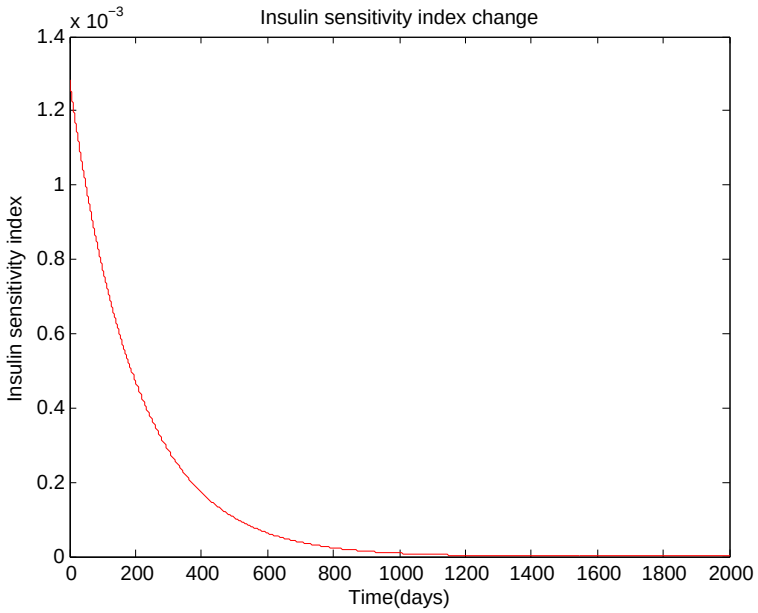

Figure 16. S_i development over time

Next, we carried out simulations for the system dynamics assuming that sensitivity index S_i behaves with a curve shown in Fig. 16. The glucose, insulin concentrations and beta-cell mass are graphed against the sensitivity index S_i, we have the following output. Higher S_i corresponds to lower equilibrium glucose level, indicating that sensitivity index plays crucial role in determining the blood glucose level. As is clearly shown Fig. 17 below, low S_i may reflect the hyperglycemia. As Fig.

18 illustrates, equilibrium insulin level is also reversely related to sensitivity index. When the insulin sensitivity is low, high insulin level is present. This figure can be explained by the compensatory insulin secretion to offset the low sensitivity index. The beta-cell figure demonstrates similar profile. Beta-cell compensation is resulted from low insulin sensitivity index or high insulin resistance. This series of simulation results is a significant observation since both high glucose level and high insulin level occur in typical T2DM diagnoses.

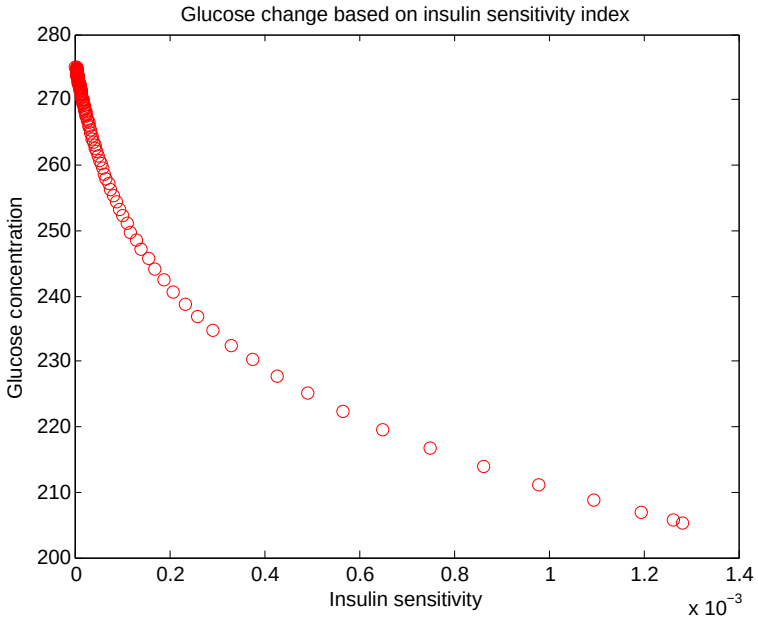

Figure 17. Glucose concentration changes against sensitivity index

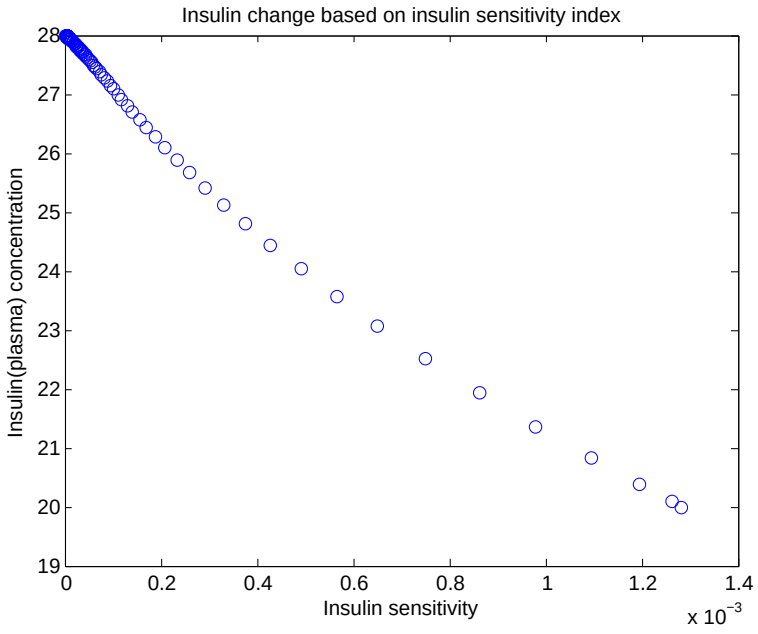

Figure 18. Insulin concentration changes against sensitivity index

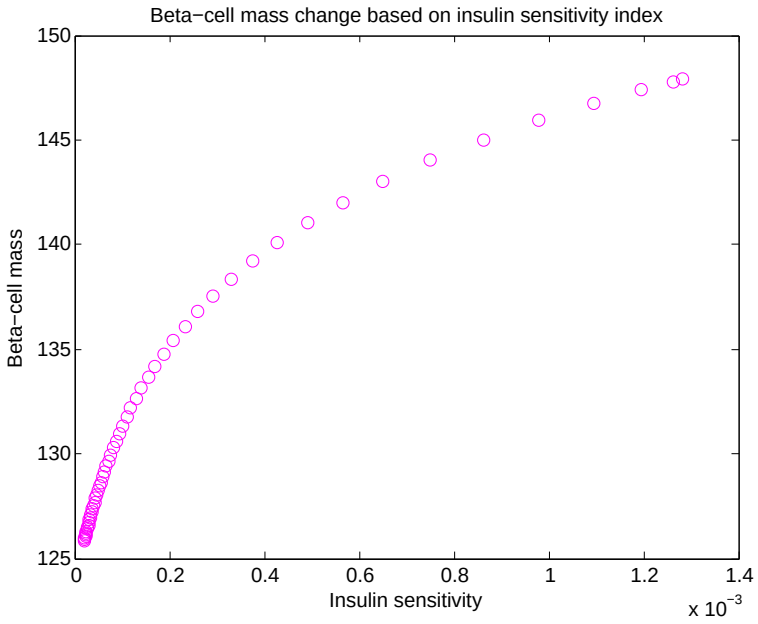

Figure 19. Beta-cell mass changes against sensitivity index

3 Bifurcation analysis for parameters w and E

Recall the complete model (1), where p_0 is the proliferation parameter and a_0 the apoptosis parameter. Recall that $w = p_0/a_0$ has been defined as the 'relative strength of beta-cell functionality'. And we do bifurcation analysis on this new parameter w. Simulation about different w is carried out to investigate its effect on the whole system.

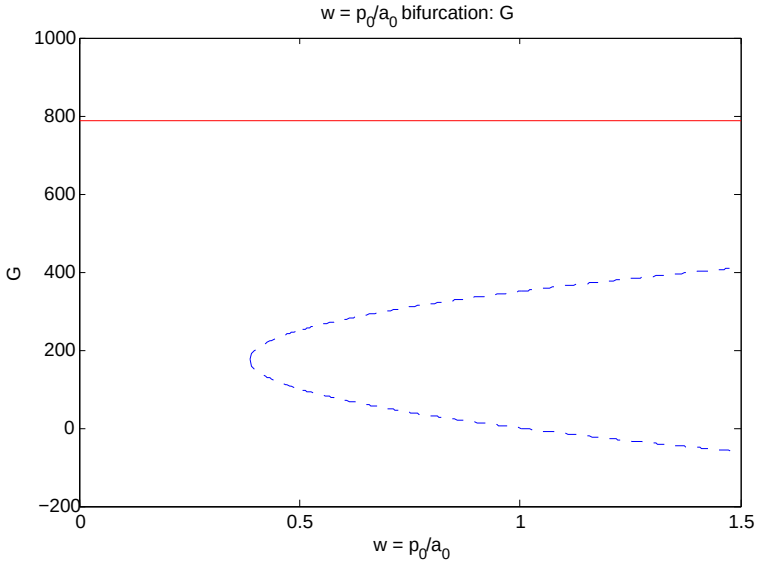

Figure 20. w bifurcation diagram against glucose

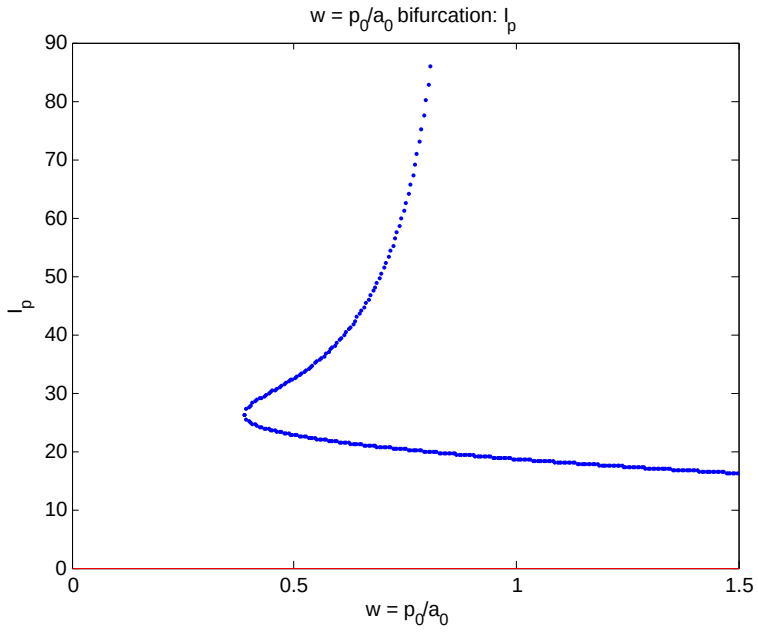

Figure 21. w bifurcation diagram against insulin

By Theorem II.3, if $w < 1 - \frac{4r_b}{r_a^2}$, the system has only one trivial equilibrium point. In such case, it is locally stable. If $w = 1 - \frac{4r_b}{r_a^2}$, there is one additional equilibrium point. If $1 - \frac{4r_b}{r_a^2} < w < 1$, there are total three equilibrium points. If $w \geq 1$, however, the quadratic equation (11) has one nonpositive root, which is physiologically meaningless. In this case, the nonpositive root is trimmed out. In Fig. 20, and Fig. 21, the trivial equilibrium point branch is drawn in as a red solid line.

The w bifurcation diagram may be easily interpreted in physiological context. When the relative strength of beta-cell functionality is weak, the body will eventually develop the theoretically pathological status, that is characterized by extreme hyperglycemia, zero insulin secretion and no beta-cell mass.

Now we consider the exchange rate E as a bifurcation parameter. With w assumed to be fixed at different values, let parameter E vary. The following results show the bifurcation analysis of parameter E based on $w = 0.3$, $w = 0.4$, $w = 1.2$,

respectively.

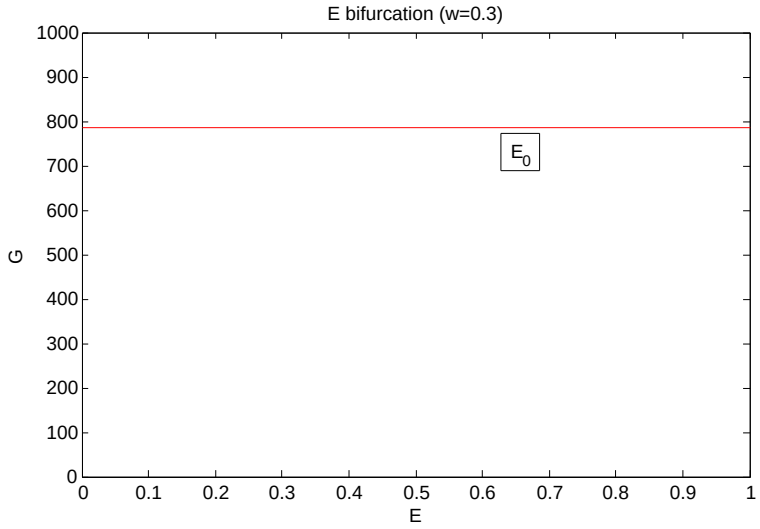

Figure 22. E bifurcation diagram against glucose at w=0.3

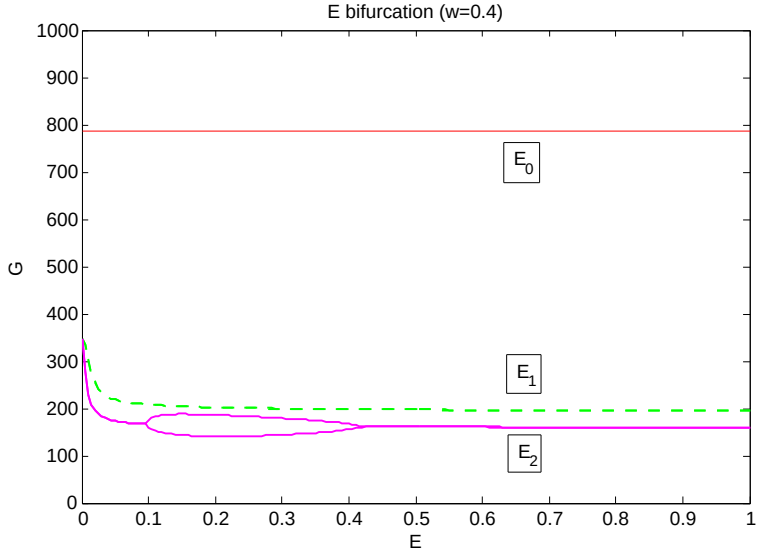

Figure 23. E bifurcation diagram against glucose at w=0.4

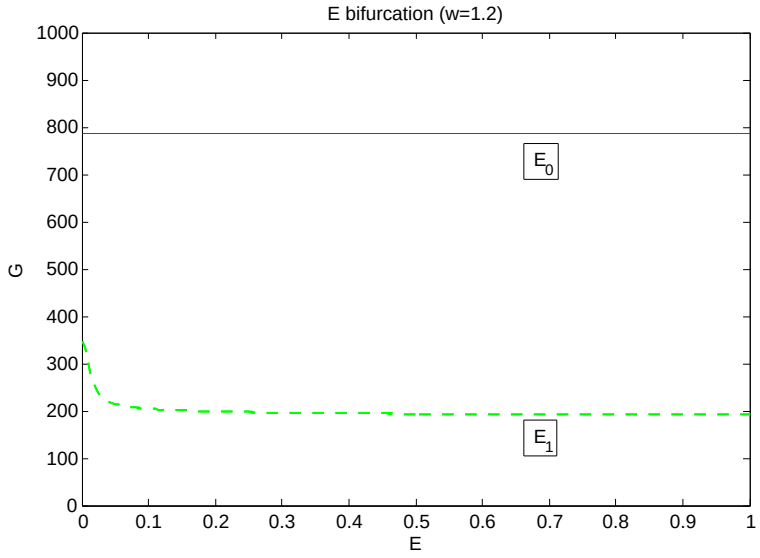

Figure 24. E bifurcation diagram against glucose at w=1.2

When $w = 0.3$, as illustrated in Fig. 22, there exists only one trivial equilibrium point and the value of parameter E has no impact on the equilibrium glucose level. When $w = 0.4$, in the simulation Fig. 23, the system has three equilibrium points. The transfer rate parameter E influences the equilibrium glucose level for equilibrium points E_1 and E_2. Particularly, when E is between the range 0.1 to 0.42, the glucose concentration oscillation is present around equilibrium point E_2. This might indicate that an appropriate transfer rate between plasma and interstitial compartments is needed to ensure the glucose/insulin oscillatory behavior. When $w = 1.2$, the simulation illustrated in Fig. 24 shows only two equilibrium points, trimming out the nonpositive one, as we mentioned above.

4 Discussion

The mathematical and numerical analysis in the preceding sections provide us with sufficient information in the attempt to explain and predict the observations in diabetes. The above results have the following physiological interpretations.

- Theorem II.6 shows that initial beta-cell mass may play a crucial part in maintaining glucose homeostasis and preventing diabetes. If beta-cell mass formed in embryo is not sufficient, the subject may experience hyperglycemia and develop diabetes in later life stage. If beta-cell mass is big enough initially, the oscillatory insulin secretion may be maintained and the subject will likely be in healthy status.

- Our simulation results have also suggested that the insulin sensitivity is a crucial indicator of the possible diabetic status. As is seen in diabetic subjects, low insulin sensitivity is associated with hyperglycemia and hyperinsulinemia. Subjects with low sensitivity, also referred to as insulin resistance, will require a larger amount of insulin in the body either from endocrine pancreatic secretion or exogenous injection in order to maintain the blood glucose level in normal range. Having insulin resistance is a sign that the body has difficulty of metabolising glucose.

- Another important factor to consider is the relative strength of beta-cell functionality. This parameter is defined as the ratio of beta-cell proliferation parameter to apoptosis parameter. According to our numerical simulation, as shown in Fig. 20 and Fig. 21, it must be above a threshold value to maintain the secretory ultradian oscillations. If this parameter is too low, which indicates poor beta-cell functionality, then the body may develop diabetes in the long run.

  A higher beta-cell functionality may be interpreted as that beta-cell proliferation is faster than or of the same speed as its apoptosis. This could be well justified not only in common sense, but also by our bifurcation analysis. However, if the apoptosis rate is relatively high, then the beta-cell mass might not maintain its proper level and would die out eventually, which is depicted as that trajectory could only be attracted to the trivial equilibrium point.

- It is also noted that an appropriate transfer rate between plasma and interstitial compartments is necessary to ensure the ultradian oscillations to occur. We can refer to our simulation result Fig. 23, the value should lie in the range of 0.1 to 0.42. This implies that if the transfer rate is too low or too high, the secretory oscillation may not sustain and do no good to the body.

  The transfer rate parameter is an indicator of the effectiveness of the insulin transport between plasma and interstitial space. If its value is either too high or too low, it may indicate malfunction of the transport process, which in turn would affect the behavior of the ultradian oscillatory secretion. But the actual mechanism should be further investigated by physiological experiments, rather than relying solely on mathematical modeling.

To sum up, our model studies both in analytical part and numerical part have suggested that there are several crucial factors that affect the development of diabetes in a prolonged period. Those are initial beta-cell mass formed in embryonic and postnatal development, insulin sensitivity, relative strength of beta-cell functionality, and transfer rate between plasma and interstitial space. The findings in this chapter could help us better understand the mechanism of the glucose-insulin endocrine regulatory system and the possible causes of diabetes. They may as well provide certain guideline to help develop more reasonable, effective, efficient and economic clinical treatment after necessary experiments. We also hope these mathematical studies could be utilized to facilitate the physiological researches on diabetes related topics in the future.

CHAPTER III

THE GLOBAL STABILITY OF THE EQUILIBRIUM OF A TIME DELAY IVGTT MODEL

In this chapter, we dedicate the effort to studying an IVGTT model, trying to help diagnose diabetes in clinical studies and research. The main work is published in

J Li, M Wang, A De Gaetano, P Palumbo, S Panunzi, *The range of time delay and the global stability of the equilibrium for an IVGTT model*, Math. Biosci. (2011), doi:10.1016/j.mbs.2011.11.005

Diagnostic protocol for onset of diabetes mellitus is the initial step in the treatments. The intravenous glucose tolerance test (IVGTT) has been considered as the most accurate method to determine the insulin sensitivity and glucose effectiveness. However, the range of the length of the delay in the existing IVGTT models are not fully discussed and thus in many cases the time delay may be assigned to a value out of its reasonable range. Several attempts had been made to determine when the unique equilibrium point is globally asymptotically stable. In addition, all these conditions are delay-independent. In this chapter, we discuss the range of the time delay and provide easy-to-check delay-dependent conditions for the global asymptotic stability of the equilibrium point for a recent IVGTT model through Liapunov function approach. Estimates of the upper bound of the delay for global stability are given in corollaries. In addition, the numerical simulation in this chapter is fully incorporated with functional initial conditions, which is natural and more appropriate in delay differential equation systems.

1 Introduction

Human bodies need to maintain a glucose concentration level in a narrow range (70-109 ml/dl or 3.9-6.04 mmol/l). If one's glucose concentration level is significantly out of the normal range (70-110 ml/dl), this person is considered to have a plasma glucose problem: hyperglycemia or hypoglycemia. Diabetes mellitus, or simply, diabetes, is characterized by high blood glucose levels resulted from defects in the glucose-insulin endocrine metabolic regulatory system, in which either the pancreas does not release insulin, or the cells do not properly use insulin to uptake glucose.

Diabetes mellitus has become an epidemic disease in the sense of life style. To diagnose whether or not an individual subject is already a diabetic or has the potential to develop such disease, the so-called metabolic portrait, including the insulin sensitivity index and glucose effectiveness, of the subject needs to be sketched. To this end, several glucose tolerance tests have been developed and applied in clinics and experiments ([58], [72], [89] and [10]). The fundamental idea of such tests is to examine the response of insulin, called insulin sensitivity, after a large amount of glucose is infused in to one's body. A commonly used protocol is the intravenous glucose tolerance test (IVGTT). In the procedure of IVGTT, the subject to be tested needs to fast 8-10 hours and is then given a bolus of glucose infusion, for example, 0.33 g/kg body weight ([102]) or 0.5 g/kg body weight of a 50% solution, and is administered into an antecubital vein in approximately 2 minutes. To observe the metabolic regulation between the glucose and insulin, within the next 180 minutes, the plasma glucose and serum insulin of the subject are sampled frequently at the time marks 2', 4', 6', 8', 10', 12', 14', 18', 21', 24', 30', 35', 40', 45', 50', 60', 70', 80', 90', 100', 120', 140', 160' and 180'. According to the rich information constituted in the sampled data, appropriate analysis can reveal the metabolic portrait.

One popular approach of the analysis is as follows: 1) formulate or choose a well-formulated kinetic model based on physiology; 2) estimate the parameters of the IVGTT model with experimental data, and then 3) the parameter values are used to

obtain physiological information, for example, the insulin sensitivity.

Several IVGTT models have been proposed and some are widely used ([7], [15], [55], [70], [75], [74], [91]). All these models incorporate the insulin secretion delay implicitly or explicitly. However, none of above work has discussed the reasonable range for the time delay and how to estimate the reasonable value of the delay according to the sampled data. Instead, the length of delay is often set to be larger than 20 minutes, which is in contrast to that the delay is between 5 and 15 minutes for normal subjects in normal environment ([79], [57], [89]). Intuitively, the length of the delay in the glucose tolerance test should not be longer than that in normal environment. In addition, several attempts have been made to obtain the conditions for the global stability of the equilibrium point of the models ([29], [55], [75] and [74]). Unfortunately all the conditions are delay-independent. For the information about the delay $\tau > 0$, it is only known that there exists a $\tau_0 > 0$ such that the equilibrium point is locally stable if $\tau < \tau_0$; and unstable otherwise (thus a periodic solution is bifurcated out). To reveal the insight regarding the time delay, it would be very helpful to know an estimate of the upper bound $\bar{\tau}$ so that the equilibrium point is globally stable when $\tau \leq \bar{\tau}$. Applying the Liapunov function approach, we obtain delay dependent conditions for the global stability of the most recent delay differential equation (DDE) model of IVGTT. Estimated upper bounds can be derived from these conditions explicitly or implicitly. We also improve the numerical studies by using functional initial conditions in the delay differential equation model, which lacks in all existing work ([15], [29], [55], [70], [75], [74]). To simulate the bolus glucose infusion and the abrupt insulin secretion, adjustments of the initial conditions of glucose and insulin concentrations at time $t = 0$ have to be made in all current work. This is neither natural to the design of the test, nor correct for a functional differential equation system. In this chapter, we will shift the starting time of glucose infusion to -2' and use a non-constant function as the initial value in $[-\tau, 0]$. The simulations fit the sampled data better and thus give more accurate estimations of

the parameters.

We organize this chapter as follows. We will first discuss the range of the length of delay, and preliminarily demonstrate how to estimate the delay for each subject according to the sampled data, secondly obtain delay-dependent conditions for the global stability of the equilibrium point, from which estimated upper bounds of τ_0 are given in corollaries, and lastly show the correct way in numerical simulations for DDE IVGTT models. We first in Section 3 introduce the IVGTT models proposed and studied in [29], [75] and [74], followed by the analysis of the models, in which delay dependent conditions of global stability of the unique equilibrium are given by utilizing Liapunov function in Section 4. In Section 5 we perform numerical simulations and we end this chapter with discussions in Section 6.

2 Range of the time delay of insulin secretion

All discrete and distributed delay differential equation models for IVGTT involve the time delay explicitly. Thus, it is intuitive to ask questions: What is the definition of the time delay? How long is the delay? De Gaetano and Arino [15] considered the length of delay as the the average of delays of all subjects. All IVGTT models in [29], [55], [70], [75] and [74] follow the same definition. However, the delay in existing models is assumed to be around 20 minutes without explanation in details ([29], [55], [70], [75] and [74]).

The events of the insulin secretion from pancreatic β-cells can be summarized as follows according to [57] and the references therein. As the plasma glucose concentration is elevated, the insulin secretion from β-cells takes several cascading complex electric processes inside islet. These processes can be described in the following steps: glucose transporter GLUT2 transports glucose molecules into islet, the ratio of ATP over ADP is increased, the K^+ channels are closed and consequently the Ca^{2+} channels open, and then the influx of Ca^{2+} ions triggers the insulin exocytosis from β-cell granules. Obviously such a chain of events causes a time delay for insulin to release in

responding to the elevated glucose concentration. Insulin release has effects on both hepatic glucose production and insulin-dependent glucose utilization [13]. It takes certain time for the newly synthesized insulin to cross the endothelial barrier and eventually become the so-called 'remote insulin', then help to uptake glucose. This total delay time is approximately in the range of 5-15 min ([13], [89], [92]).

Bolus glucose infusion causes abrupt increase in plasma glucose concentration. Such an abrupt glucose increase stimulates bi-phasic insulin secretions, a rapid and approximately linear but short first phase release, followed by a slower and longer second phasic secretion. According to Overgaard et al.[73] and the references therein, such secretions relate to multiple aspects including the impact of glucose on β-cells, insulin synthesis, movements of insulin in β-cells, and eventually insulin release from granules. As the glucose is infused in intravenous, the metabolic system responds quickly. The rate of the proinsulin synthesis is approximately linearly increased in translation of proinsulin mRNA. The proinsulin is split into insulin and C-peptide and stored in granules. A fractional such granules are docked to the surface of the plasma while others stay in the intracellular space with the ability of free movement. The group of granules docked on the surface of the plasma is called readily-releasable pool (RRP), the insulin in which is released at the quick infusion of the glucose and forms the first phase of secretion. This release is instantaneous or almost instantaneous since it takes almost no time for the glucose infuse in intravenous to transport to pancreas and the insulin in the ready releasable pool. This instantaneous insulin release is followed by the following actions: grandules in intracellular space are becoming in PPR and then the insulin is released. This release forms the second phase of secretion. As in the normal environment, the series of chemical and electrical events cause that a time lag exists in the release after the observation of the increased glucose concentration. This time lag can be a few minutes [73].

Apparently, the second phase secretion in IVGTT is not significantly distinguishable from the secretion under normal environment. Therefore time delay should

exist and the range of the delay should not be longer than that in normal status. According to physiology cited in their work, Li et al.[57] defined the delay as the length of the delay τ as "from the time that the glucose concentration level is elevated to the moment that the insulin has been transported to interstitial space and becomes remote insulin", and determined that the possible value of the delay falls in the biological range of 5 minutes to 15 minutes [79]. Therefore we suspect that for most subjects, the length of the delay is shorter than 15 minutes in IVGTT. In most of the previous work, the time delay was chosen between 18 minute and 24 minutes. The mean value, according to [75] and [74], is 19.271 minutes. This is possibly due to the observation of the time that the peak of the second physical insulin secretion is achieved. However, the effect of stimulation by glucose starts at the valley before the peak of the second phasic release. So intuitively the delay should be approximately at the time such valley is reached, if the valley exists.

It is well known that a large delay can destabilize a system [44]. An accurate estimation of such delay can play a critical role to estimate the parameters and thus the insulin sensitivity index.

3 Single delay models for intravenous glucose tolerance test

1 The models

The Minimal Model, proposed by Bergman and his colleague in 1979 [7] and 1980 [91], is believed to be the first IVGTT model that is the most accepted and the most widely used [61]. The Minimal Model is in fact a combination or unity of two separate ordinary differential equation (ODE) models, one is for glucose kinetics and one is for insulin kinetics. The time delay in the glucose-insulin regulatory system was simulated by the chain trick trough an auxiliary variable [85]. However, certain mathematical defects exist in this unity, for example, there does not exist any equilibrium point. In 2000, De Gaetano and Arino [15] pointed out these issues and

proposed the first and novel delay differential equation (DDE) model, called *dynamic model*. This novel DDE model is not only well-posed in mathematics, but also more physiologically appealing as the time delay is contained in the model explicitly. The dynamic model was then generalized by Li et al.[55] in 2001, which takes even a later proposed model in 2004 by Mukhopadhyay et al.[70] as a subfamily. De Gaetano and his colleagues proposed a slightly different general model [75], and focused on a special case of the model in their application work [74]. According to the authors of [74], such a simplified model is close enough to model the tolerance test.

This simplified model [74] is given.

$$\begin{cases} G'(t) = b - eG(t) - aG(t)I(t) \\ \\ I'(t) = df(G(t-\tau)) - cI(t) \end{cases} \tag{29}$$

where $G(t) > 0$ (mg/dl) and $I(t) > 0$ (μU/ml) are the plasma concentrations of glucose and insulin at time $t \leq 0$, respectively; $b > 0$ (mg/dl/min) is the constant glucose input; $e \leq 0$ (1/min) is the insulin independent glucose utilization by, e.g., brain cells; $a > 0$ (ml/μU/min) is the insulin dependent glucose utilization; $c > 0$ (1/min) is the insulin degradation; and the term $df(G(t-\tau))$ is the insulin secretion responded to the glucose stimulation with time delay $\tau \geq 0$

$$f(x) = \frac{x^\gamma}{\alpha^\gamma + x^\gamma} \tag{30}$$

with $d > 0$ (μU/mg/min) as the maximum secretion, $\alpha > 0$ as the half-saturation and $\gamma > 0$. If $\gamma \leq 1$, $f(x)$ is in the shape of Mechaelis-Menton kinetics; if $\gamma > 1$, $f(x)$ is in sigmoidal shape. We would like to point out that this simplified model is a special case of the model proposed by Li et al. in [55] as well, therefore all the analytical results obtained in [55] apply.

Notice that for simplicity we use different notations of the parameters in model (29) and the function (30) from that in [29], [75] and [74]. The relations are as follow: $a = K_{xgi}$, $b = T_{gh}/V_G$, $c = K_{xi}$, $d = T_{iG_{max}}/V_I$, and $e = K_{xg}$.

According to Minimal Model ([7], [91]) and the model (29) [74], the parameter a is called the insulin sensitivity index, and the parameter e is called the glucose effectiveness.

IVGTT has relatively short dynamics that has a duration of about two hours after the injection of bolus glucose. In the short dynamics, the insulin independent glucose utilization might be relatively small and thus was assumed negligible ([29], [75] and [74]), i.e., $e = 0$, or the removal rate is relatively a constant and the parameter b is considered as the net input of glucose, which results in $e = 0$ as well [74]. Therefore model (29) is further simplified to following model [74]

$$\begin{cases} G'(t) = b - aG(t)I(t) \\ \\ I'(t) = df(G(t-\tau)) - cI(t) \end{cases} \tag{31}$$

However, impaired insulin-dependent glucose disposal is one of the reasons of insulin resistance that is typical in type 2 diabetes. Decreased insulin-dependent glucose transport by GLUT4, which is associated with type 2 diabetes, and occurs, for example, in chronic alcohol users [82]. Low insulin sensitivity in type 1 diabetes could be caused by impaired GLUT4 translocation. GLUT4 contents in muscle are similar in both normal subjects and type 1 diabetics. In addition, the function of insulin to trigger GLUT4 translocation into the myocyte plasma membrane is erratic in type 1 diabetics [18]. This indicates that GLUT1 may be dominant in translocation of glucose molecules [18]. Therefore, in modeling, we should not ignore the parameter e, although it could be small, and furthermore we cannot simply conclude that e must be smaller than the parameter a as well.

2 Existing analytical results and numerical observations

While analysis of the original Minimal Model focused on numerical simulations ([7] and [91]), a number of analytical studies for subsequent IVGTT models are carried out ([15], [29], [55], [70], [75]). Typically, the authors studied the local stability of the

unique steady state and then numerically demonstrated that larger delay would not destabilize the steady state as numerically determined Hopf bifurcation point is far beyond meaningful physiological range. Some analytical delay-independent conditions for global stability of the steady state were obtained for the models proposed by [29], [55], and [75]. Particularly, a set of sufficient and necessary conditions is given for the model (29) [75]. However, physiology ([53], [57], [61], [79], [84], [89], [92]) and all the clinical data ([29], [75], [74]) show the existence of the time delay of the glucose stimulated insulin secretion. The existing delay dependent condition ([29], Theorem 3) on the global stability is not satisfied with clinical data ([75], Remark 11), although the conditions hold with some critical modification, for example, the time delay has to be smaller ([29], Remark 9).

Studies and applications of these models are extended by Panunzi et al.[74] and Giang at al.[29]. For more details for the formulation and applications of model (29) and model (31), interested readers can refer to [29], [75], and [74].

Let $(G(t), I(t))$ be a solution of (29) or model (31). Throughout this chapter, we define

$$\overline{G} = \limsup_{t\to\infty} G(t), \qquad \underline{G} = \liminf_{t\to\infty} G(t) \qquad \overline{I} = \limsup_{t\to\infty} I(t), \qquad \underline{I} = \liminf_{t\to\infty} I(t).$$

We summarize in following the analytical results obtained in above references:

(A1) Model (29) and model (31) are persistent ([75], Theorem 2). Thus, the limits defined above are finite.

(A2) Following inequalities hold ([75], Remark 5).

$$\begin{aligned} df(\underline{G}) \le c\underline{I} \le c\overline{I} \le df(\overline{G}) \\ (e + a\underline{I})\overline{G} \le b \le (e + a\overline{I})\underline{G} \end{aligned} \tag{32}$$

(A3) The necessary and sufficient conditions for delay independent global stability of model (29) and model (31) is ([75], Theorem 4 and Theorem 6.)

$$\frac{\gamma a I_b}{1 + \left(\frac{G_b}{\alpha}\right)^\gamma} \le e + aI_b. \tag{33}$$

(A4) If the inequality in (2) does not hold, then there is a $\tau_0 > 0$ such that (i) when $\tau < \tau_0$, the equilibrium (G_b, I_b) is locally stable; (ii) when $\tau \geq \tau_0$, the equilibrium is unstable. In other words, the model (29) and the model (31) undergo a Hopf bifurcation at $\tau = \tau_0$ when τ increases from $\tau = 0$. ([75], Theorem 4 and Theorem 6.)

(A5) In the model (29), the equilibrium is a global attractor if

$$\frac{adG_b}{ce}\sqrt{\sup_{[0,G_b]} f'(G) \sup_{[G_b,\infty)} f'(G)} < 1.$$

([29], Theorem 2.)

(A6) Every fastly oscillated solution of the model (31) converges to the positive equilibrium if

$$(1 - e^{-2c\tau})\frac{adG_b}{ceI_b}\sqrt{G_b M_* \sup_{[0,G_b]} f'(G) \sup_{[G_b,\infty)} f'(G)} < 1,$$

where M_* satisfies $m_* f(M_*) = M_* f(m_*) = G_b f(G_b)$ for $m_* < G_b < M_*$. A fastly oscillated solution is defined as a solution $(G(t), I(t))$ that oscillates around the equilibrium (G_b, I_b) and within two consecutive zeros $t_0 < t_1$ of $I(t) - I_b$, $I(t)$ attains its maximum or minimum at $t_* < t_0 + 2\tau$. ([29], Definition 6 and Theorem 3.)

Both conditions in (A3) and in (A5) are delay independent globally asymptotical stability of the equilibrium. But (A3) is a necessary and sufficient condition, so the result in (A5) shall be either a weaker condition or equivalent to (A3). Nevertheless, according to [75], only 3% of clinical data satisfy the condition in (A3). So to ensure the global attractive behavior of the tolerance test, analysis on delay dependent global stability is necessary. Notice that the insulin dynamics in IVGTT may often reach its basal level without oscillation ([75], [74]) as defined in [29], the application of the result in (A6) is limited. In addition, (A6) requires τ to be small

enough so that the parameters fitted from the clinical data satisfy the condition ([29], Remark 9.)

4 Global stability of the equilibrium

Clearly, as discussed in [75], the model 29 has a unique equilibrium at baseline (G_b, I_b) provided that the parameters satisfy

$$b = G_b(e + aI_b)$$

and

$$d = cI_b(1 + (\alpha/G_b)^\gamma).$$

This results in that the number of parameters to be estimated is six (including the delay parameter τ), as G_b and I_b are known.

We state the following well known fact without proof, which is useful in estimating the bounds of a solution $(G(t), I(t))$ of the model (29).

Lemma III.1 *If $h'(t) \leq p - qh(t)$, or $h'(t) \geq p - qh(t)$, where $p, q > 0$, then*

$$h(t) \leq \frac{p}{q} + \Big(h(0) - \frac{p}{q}\Big)e^{-qt},$$

or

$$h(t) \geq \frac{p}{q} + \Big(h(0) - \frac{p}{q}\Big)e^{-qt},$$

for all $t \geq 0$.

A direct application of Lemma III.1 is to estimate the bounds of a solution $(G(t), I(t))$. We have the following result.

Lemma III.2 *If $(G(t), I(t))$ is a solution of the model (29), then*

$$m_I \doteq \min\Big\{I(0), \frac{k_2}{c}\Big\} \leq I(t) \leq M_G \doteq \max\Big\{I(0), \frac{d}{c}\Big\}$$

and

$$m_G \doteq \min\Big\{G(0), \frac{b}{k_1}\Big\} \le G(t) \le M_G \doteq \max\Big\{G(0), \frac{b}{k_3}\Big\}.$$

where $k_1 = e + aM_I$, $k_2 = df(m_G)$ *and* $k_3 = e + am_I$.

The proof is straightforward.

Remark The bounds given by Lemma III.2 are more accurate than the consequence in A2 of [75], which would result in

$$\frac{bc}{ec + ad} \le \underline{G} \le \overline{G} \le \frac{bc}{ec + adf(\frac{bc}{ec+ad})}.$$

However the upper bound M_G of $G(t)$ for $t > 0$ rather than the bound at limiting status of $G(t)$ plays an important role when applying the theorem III.1 to determine the global stability of the equilibrium. Notice that M_G is dependent of the initial values $G(0)$ and $I(0)$ of the solution $(G(t), I(t))$ only.

For the sake of convenience, we denote

$$L = d\frac{(\gamma+1)^2}{4\gamma\alpha}\Big(\frac{\gamma-1}{\gamma+1}\Big)^{\frac{\gamma-1}{\gamma}}, \tag{34}$$

which is the maximum value of the derivative of $df(G)$ for $G > 0$, and

$$R = e + aI_b, \qquad \text{and} \qquad K = aM_G. \tag{35}$$

By Lemma III.2, L, R and K are independent of τ. When consider the model (31), $R = aI_b$.

When $\tau = 0$, model (29) and (31) become a two-dimensional ordinary differential equation system. It is easy to show that the unique equilibrium (G_b, I_b) is globally asymptotically stable by Poincare-Bendixson Theorem. When $\tau > 0$, the models are functional differential equations. The Poincare-Bendixson Theorem does not apply. To establish a criterion of delay dependent global stability, we build a Liapunov function and prove that the solutions of model (29) or model (31) are attracted to the equilibrium (G_b, I_b).

Theorem III.1 *If there exist positive constants $u > 0$ such that*

$$\tau \ < \min\Big\{\frac{2u}{L}, \frac{2c}{L(R+2K)}\Big\}, \tag{36}$$

and

$$\Delta \doteq M_u^2 - 4R\Big(u - \frac{\tau}{2}L\Big)\Big(c - \frac{\tau}{2}L(R+2K)\Big) < 0, \tag{37}$$

where $M_u = \max\{L, Ku\}$, then the equilibrium (G_b, I_b) of model (29) is globally and asymptotically stable.

Proof. Let

$$W(G(t), I(t)) = \frac{1}{2}u(G(t) - G_b)^2 + \frac{1}{2}(I(t) - I_b)^2, \tag{38}$$

$$U(G(t), I(t)) = C\int_{t-\tau}^{t}\int_{z}^{t}(G(s) - G_b)^2 dsdz + D\int_{t-\tau}^{t}\int_{z}^{t}(I(s) - I_b)^2 dsdz. \tag{39}$$

where $C = \frac{1}{2}RL$ and $D = \frac{1}{2}KL$.

Let

$$V(G(t), I(t)) = W(G(t), I(t)) + U(G(t), I(t)),$$

then, clearly, V is a Liapunov function.

By the Mean Value Theorem, we have

$$\begin{aligned} d(f(G(t-\tau)) - f(G_b)) &= df'(\xi)(G(t-\tau) - G_b) \\ &= df'(\xi)\Big((G(t-\tau) - G(t)) + (G(t) - G_b)\Big) \end{aligned}$$

where ξ is between $G(t-\tau)$ and $G(t)$. Also, since $uv \le \frac{1}{2}(u^2 + v^2)$ for all $u, v \ge 0$, we have

$$(I(t) - I_b)(G(t) - G(t-\tau)) = (I(t) - I_b)\int_{t-\tau}^{t} G'(s)ds$$

$$
\begin{aligned}
&= \int_{t-\tau}^{t} \Big(b - eG(s) - aG(s)I(s)\Big)\Big(I(t) - I_b\Big)ds \\
&= \int_{t-\tau}^{t} \Big(e(G(s) - G_b)(I(t) - I_b) + aG(s)(I(s) - I_b)(I(t) - I_b) \\
&\qquad +aI_b(G(s) - G_b)(I(t) - I_b)\Big)ds \\
&= \int_{t-\tau}^{t} \Big((e + aI_b)(G(s) - G_b)(I(t) - I_b) + aG(s)(I(s) - I_b)(I(t) - I_b)\Big)ds \\
&\leq \frac{1}{2}\Big[(e + aI_b)\Big(\int_{t-\tau}^{t}(G(s) - G_b)^2 ds + \tau(I(t) - I_b)^2\Big) \\
&\qquad +aG_M\Big(\int_{t-\tau}^{t}(I(s) - I_b)^2 ds + \tau(I(t) - I_b)^2\Big)\Big] \\
&\leq \frac{1}{2}\Big[R\int_{t-\tau}^{t}(G(s) - G_b)^2 ds + K\int_{t-\tau}^{t}(I(s) - I_b)^2 ds \\
&\qquad +\tau(R + K)(I(t) - I_b)^2\Big].
\end{aligned}
$$

Then

$$
\begin{aligned}
\frac{d}{dt}W &= u(G(t) - G_b)\Big[- e(G(t) - G_b) - a(G(t)(I(t) - I_b) + I_b(G(t) - G_b))\Big] \\
&\quad +(I(t) - I_b)\Big[d(f(G(t - \tau)) - f(G_b)) - c(I(t) - I_b)\Big] \\
&= -ue(G - G_b)^2 - uaG(G - G_b)(I - I_b) - uaI_b(G - G_b)^2 \\
&\quad +d(I - I_b)\Big[f(G(t - \tau)) - f(G_b)\Big] - c(I - I_b)^2 \\
&= -(ue + uaI_b)(G - G_b)^2 - AaG(G - G_b)(I - I_b) - c(I - I_b)^2 \\
&\quad +d(I - I_b)\Big[f(G(t - \tau)) - f(G_b)\Big] \\
&= -u(e + aI_b)(G - G_b)^2 - uaG(G - G_b)(I - I_b) - c(I - I_b)^2 \\
&\quad +df'(\xi)(I - I_b)\Big[(G(t - \tau) - G(t)) + (G(t) - G_b)\Big] \\
&= -u(e + aI_b)(G - G_b)^2 + (df'(\xi) - uaG)(G - G_b)(I - I_b) - c(I - I_b)^2 \\
&\quad +df'(\xi)(I - I_b)(G(t - \tau) - G(t)) \\
&\leq -u(e + aI_b)(G - G_b)^2 + |df'(\xi) - uaG||G - G_b||I - I_b| - c(I - I_b)^2 \\
&\quad +L|(I - I_b)(G(t - \tau) - G(t))| \\
&\leq -uR(G - G_b)^2 + |df'(\xi) - uaG||G - G_b||I - I_b| - c(I - I_b)^2 \\
&\quad +\frac{1}{2}L\Big[R\int_{t-\tau}^{t}(G(s) - G_b)^2 ds + K\int_{t-\tau}^{t}(I(s) - I_b)^2 ds
\end{aligned}
$$

$$
\begin{aligned}
&+\tau(R+K)(I(t)-I_b)^2\Big].\\
=\ & -uR(G-G_b)^2+|df'(\xi)-uaG||G-G_b||I-I_b|\\
&-\Big(c-\frac{\tau}{2}BL(R+K)\Big)(I-I_b)^2\\
&+C\int_{t-\tau}^{t}(G(s)-G_b)^2ds+D\int_{t-\tau}^{t}(I(s)-I_b)^2ds
\end{aligned}
$$

Furthermore,

$$
\begin{aligned}
\frac{dU}{dt} &= -C\Big[\int_{t-\tau}^{t}(G(s)-G_b)^2ds+\int_{t-\tau}^{t}(G(t)-G_b)^2dz\Big]\\
&\quad -D\Big[\int_{t-\tau}^{t}(I(s)-I_b)^2ds+\int_{t-\tau}^{t}(I(t)-I_b)^2dz\Big]\\
&= -C\int_{t-\tau}^{t}(G(s)-G_b)^2ds+C\tau(G(t)-G_b)^2\\
&\quad -D\int_{t-\tau}^{t}(I(s)-I_b)^2ds+D\tau(I(t)-I_b)^2
\end{aligned}
$$

So, along the solution $(G(t),I(t))$ of model (29), we have

$$
\begin{aligned}
\frac{dV}{dt} &\le -uR(G-G_b)^2+|df'(\xi)-uaG||G-G_b||I-I_b|\\
&\quad -\Big(c-\frac{\tau}{2}L(R+K)\Big)(I-I_b)^2\\
&\quad +C\int_{t-\tau}^{t}(G(s)-G_b)^2ds+D\int_{t-\tau}^{t}(I(s)-I_b)^2ds\\
&\quad -C\int_{t-\tau}^{t}(G(s)-G_b)^2ds+C\tau(G(t)-G_b)^2\\
&\quad -D\int_{t-\tau}^{t}(I(s)-I_b)^2ds+D\tau(I(t)-I_b)^2\\
&= -(uR-C\tau)(G-G_b)^2+|df'(\xi)-uaG||G-G_b||I-I_b|\\
&\quad -\Big(c-\tau\Big(\frac{1}{2}L(R+K)+D\Big)\Big)(I-I_b)^2\\
&= -\Big(uR-\frac{\tau}{2}LR\Big)(G-G_b)^2+|df'(\xi)-uaG||G-G_b||I-I_b|\\
&\quad -\Big(c-\tau\Big(\frac{1}{2}L(R+K)+\frac{1}{2}LK\Big)\Big)(I-I_b)^2\\
&= -R\Big(u-\frac{\tau}{2}L\gamma\Big)(G-G_b)^2+|df'(\xi)-uaG||G-G_b||I-I_b|\\
&\quad -\Big(c-\frac{\tau}{2}L(R+2K)\Big)(I-I_b)^2\\
&\le -R\Big(u-\frac{\tau}{2}L\gamma\Big)(G-G_b)^2+M_u|G-G_b||I-I_b|
\end{aligned}
$$

$$
\begin{aligned}
& -\Big(c - \frac{\tau}{2}L(R+2K)\Big)(I - I_b)^2 \\
< \;& 0
\end{aligned}
$$

in observing that the conditions (a) and (b) hold.

Remark. Since M_u is dependent of $G(0)$ and $I(0)$, the global stability is not uniform.

We derive two corollaries from the above theorem, which give the estimates of the bounds for the delay τ, which ensures the equilibrium is globally stable. Denote

$$
p_1 = \frac{cK + L(R+2K)}{KL(R+2K)}, \qquad q_1 = \frac{4Rc - KL}{KRL(R+2K)}
$$

and

$$
\tilde{\tau} = \min\Big\{\frac{2}{K}, \frac{2c}{L(R+2K)}\Big\}.
$$

Then we have the following result.

Corollary III.1 *The unique equilibrium of the model (29) is globally asymptomatically stable, if the delay τ satisfies either of the following conditions:*

$$
\begin{aligned}
&(i) \quad \tau < \tilde{\tau}, \ \text{if } p_1^2 - q_1 < 0; \\
&(ii) \quad \tau < \min\{\tilde{\tau}, p_1 - \sqrt{p_1^2 - q_1}\}, \ \text{if } p_1^2 - q_1 > 0 \text{ and } q_1 > 0; \\
&(iii) \quad \tau \in (p_1 + \sqrt{p_1^2 - q_1}, \tilde{\tau}), \ \text{if } p_1^2 - q_1 > 0 \text{ and } p_1 + \sqrt{p_1^2 - q_1} < \tilde{\tau}; \\
&(iv) \quad \tau < \tilde{\tau} \text{ and } \tau \neq p_1, \ \text{if } p_1^2 - q_1 = 0;
\end{aligned} \tag{40}
$$

Proof. Notice that $M_u = \max\{L, Ku\}$ in Theorem III.1. If $M_u = L$, $u \leq L/K$. In observing (37), we can choose $u = L/K$. Therefore (36) becomes $\tau < \tilde{\tau}$, and (37) holds if and only if

$$
\begin{aligned}
& M_u^2 - 4R\Big(u - \frac{\tau}{2}L\Big)\Big(c - \frac{\tau}{2}L(R+2K)\Big) \\
= \;& L^2 - 4R\Big(\frac{L}{K} - \frac{\tau}{2}L\Big)\Big(c - \frac{\tau}{2}L(R+2K)\Big)
\end{aligned}
$$

$$
\begin{aligned}
&= L\Big[L - 4R\Big(\frac{1}{K} - \frac{\tau}{2}\Big)\Big(c - \frac{\tau}{2}L(R+2K)\Big)\Big] \\
&= L\Big[L - 4R\Big(\frac{c}{K} - \frac{\tau}{2}c - \frac{\tau}{2}\frac{L(R+2K)}{K} + \frac{\tau^2}{4}L(R+2K)\Big)\Big] \\
&= L\Big[L - \frac{4Rc}{K} + 2\tau R\Big(c + \frac{L(R+2K)}{K}\Big) - \tau^2 RL(R+2K)\Big] \\
&= -L^2R(R+2K)\Big[\frac{-L + \frac{4Rc}{K}}{RL(R+2L)} - \frac{2R(c + \frac{L(R+2K)}{K})}{RL(R+2K)}\tau + \tau^2\Big] \\
&= -L^2R(R+2K)\Big[\frac{4Rc - KL}{KRL(R+2K)} - \frac{2(cK + L(R+2K))}{KL(R+2K)}\tau + \tau^2\Big] \\
&= -L^2R(R+2K)(q_1 - 2p_1\tau + \tau^2) \\
&< 0.
\end{aligned}
$$

Then it is straight forward to obtain the conclusion.

Denote

$$
H = c - \frac{\tau}{2}L(R+2K) \qquad \text{and} \qquad \bar{\tau} = \frac{2Rc}{L(R+K)^2}.
$$

If $\tau < \bar{\tau}$, then

$$
\begin{aligned}
2RH - K^2L\tau &= 2RH - K^2L\tau \\
&= 2R\Big(c - \frac{\tau}{2}L(R+2K)\Big) - K^2L\tau \\
&= 2Rc - (RL(R+2K) + K^2L)\tau \\
&= 2Rc - L(R(R+2K) + K^2)\tau \\
&= 2Rc - L(R^2 + 2RK + K^2)\tau \\
&= 2Rc - L(R+K)^2\tau \\
&> 0.
\end{aligned}
$$

Thus

$$
u_0 = \frac{4RH + \sqrt{8RH(2RH - K^2L\tau)}}{2K^2} > 0.
$$

Therefore, we have the following result.

Corollary III.2 *The unique equilibrium of the model (29) is globally asymptomatically stable if*

$$\tau < \min\Big\{\frac{2u_0}{L}, \bar{\tau}\Big\}, \qquad and \qquad u_0 > \frac{L}{K}. \tag{41}$$

Proof. We choose an appropriate $u > 0$ so that the inequality (37) holds. Let $u > L/K$. Then $M_u = Ku$ in Theorem III.1 and thus (37) holds if and only if

$$K^2u^2 - 4R(u - \frac{\tau}{2}L)H = K^2u^2 - 4RHu + 2RLH\tau < 0.$$

So the existence of such $u > 0$ is equivalent to

$$(4RH)^2 - 4K^2 \cdot 2RLH\tau = 8RH(2RH - K^2L\tau) > 0,$$

and the larger root u_0 of $P(u) = K^2u^2 - 4RHu + 2RKH\tau = 0$ is greater than L/K. Notice (41). We choose any $u \in (L/K, u_0)$ so that both conditions in the Theorem III.1 are satisfied.

Remark. The inequality of (i), (ii) and (iv) in corollary III.1 provide estimated upper bounds of the time delay of insulin secretion stimulated by glucose. Since H in (41) is dependent of τ, one can estimate an upper bound of τ implicitly.

We will apply Corollary III.1 and Corollary III.2 in next section with experimental data obtained from [15] and [74].

5 Parameter estimate and numerical simulations

We use Matlab delay differential equation solver dde23 [83] and the weighted least square method to estimate parameters of the model (29). We obtained three set of experimental data from [15] listed in Table 2, and two set from [74] listed in Table 3. It has been assuming that the time mark 0' is the starting time of the bolus glucose infusion is started, and the time mark 2' is the first blood sampling time. We make a -2' shift of the time marks in observing that indeed the bolus glucose infusion belongs to the initial condition of the delay differential equation model (29).

The initial condition for a delay differential equation with maximum delay τ is a function defined in the interval $[-\tau, 0]$. Therefore we use a piece-wise liner function

$$\phi(t) = \begin{cases} G_b, & \text{for } t \in [-\tau, -2] \\ \\ G_0 + \dfrac{G_0 - G_b}{2}t, & \text{for } t \in (-2, 0]; \end{cases} \tag{42}$$

while $I(0) = I_0$. Here G_b and I_b are taken from the first row at time mark $-2'$ in the data tables and G_0 and I_0 are taken from the second row at time mark $0'$ from the data tables. Assume that $\phi(G) = G_b$ on $[-\tau, -2]$ to reflect that the subject has been in fast state and has maintained the glucose level at baseline. Assuming that $\phi(t)$ is linearly increasing from G_b to G_0 in $(-2, 0]$ is in observation that the glucose infusion finishes in 2 minutes and the measurement starts. By comparison with the simulations of these subjects, such an initial condition setup is not only correct in mathematics, but it also produces more reasonable profiles (refer to Fig. 25 - Fig. 29, Fig. 1 - Fig. 3 in [15], and Fig. 3 and Fig. 4 in [74]). The first valleys in subject 6, 7, 13 and 27 are clearly seen.

The optimization is performed on minimizing the following function in estimating the parameters:

$$z = \sum_{k=1}^{n} \Big\{ \frac{(G_k - \hat{G}_k)^2}{G_0^2} + \frac{(I_k - \hat{I}_k)^2}{I_0^2} \Big\} \tag{43}$$

where $\{G_k\}$ and $\{I_k\}$ are the numerical solution values, and $\{\bar{G}_k\}$ and $\{\bar{I}_k\}$ are the experimental data, $k = 1, 2, 3, ..., N$ with N is the total number of samples. Since function (43) is nonlinear, there could exist multiple local minimum points. With a set of fixed parameters as a seed, we generate random values of the parameters with a 300% range to perform optimization multiple times. Our simulations clearly show that at least local minimum points are reached in relatively large scopes for each subjects.

In applying the corollaries to these subjects after parameters are estimated, we found that the parameters for subject 6 and 8 satisfy both Corollary III.1 and

TABLE 2

Experimental data published in [15]. The first column is the time in minute to sample the blood with a two-minute shift. The second and third columns are the data for subject 6. The first valley is at about 8' mark. The fourth and fifth columns are the data from for the subject 7 and its first valley is at about 12' mark. The sixth and seventh columns are the data for subject 8 and there is no clear valley.

min	**G(mg/dl)**	**I(μU/l)**	**G(mg/dl)**	**I(μU/l)**	**G(mg/dl)**	**I(μU/l)**
-2	87.7358	67.9245	87.2117	38.5744	77.9874	57.9000
0	225.4717	413.2075	299.3711	179.4549	226.4151	1031.4000
1	214.1509	410.3774	259.9581	103.9832	228.9308	915.7000
4	203.7736	305.6604	253.2495	99.7904	203.7736	759.7000
6	200.0000	286.7925	244.0252	93.9203	201.2579	772.3000
8	195.2830	234.9057	225.5765	104.8218	196.2264	646.5000
10	192.4528	317.9245	223.8994	77.1488	183.6478	669.2000
13	174.5283	278.3019	203.7736	88.8889	173.5849	513.2000
18	158.4906	238.6792	188.6792	95.5975	148.4277	508.2000
23	150.0000	250.0000	170.2306	79.6646	123.2704	440.3000
28	131.1321	233.9623	150.9434	97.2746	115.7233	327.0000
33	118.8679	203.7736	134.1719	86.3732	100.6289	286.8000
38	115.0943	153.7736	119.9161	108.1761	95.5975	226.4000
48	106.6038	169.8113	101.4675	44.4444	85.5346	166.0000
58	93.3962	115.0943	89.7275	24.3187	75.4717	148.4000
78	82.0755	111.3208	85.5346	33.5430	72.9560	118.2000
98	77.3585	53.7736	85.5346	29.3501		
118	83.0189	46.2264	88.0503	37.7358	77.9874	67.9000
138	83.0189	58.4906	87.2117	31.0273	80.5031	42.8000
158	82.0755	64.1509	86.3732	33.5430	77.9874	60.4000
178	85.8491	55.6604	87.2117	46.9602	80.5031	57.9000

TABLE 3

Experimental data published in [74]. The first column is the time in minute to sample the blood with a two-minute shift. The second and third columns are the data for subject 13. The first valley is at 18' mark. The fifth and sixth columns are the data for subject 27. The first valley is at about 12' mark.

min	**G(mg/dl)**	**I(μU/l)**	**min**	**G(mg/dl)**	**I(μU/l)**
-2	74.20	24.0	-2	86.47	44.00
0	183.40	231.0	0	345.90	1036.00
2	171.90	127.5	2	275.64	1067.00
4	164.80	124.5	4	263.03	914.00
6	164.10	146.0	6	241.41	415.00
8	150.10	102.5	8	228.80	455.00
10	140.00	129.0	10	227.90	404.00
13	135.10	92.0	12	218.89	216.00
18	136.20	88.5	16	208.98	344.00
23	127.00	113.5	19	199.97	282.00
28	118.90	179.5	22	192.77	232.00
38	100.90	126.5	28	175.65	294.00
48	90.10	91.5	33	163.94	193.00
58	83.40	64.0	38	157.64	227.00
68	79.10	34.0	43	149.53	210.00
78	76.40	30.0	48	147.73	188.00
118	73.30	28.0	58	132.41	116.00
138	77.30	27.0	68	108.99	194.00
158	76.40	33.5	78	97.28	154.00
178	73.00	23.5	88	93.68	95.00
			98	89.18	72.00
			118	84.67	50.00
			138	79.27	38.00
			158	72.06	36.00
			178	72.06	33.00

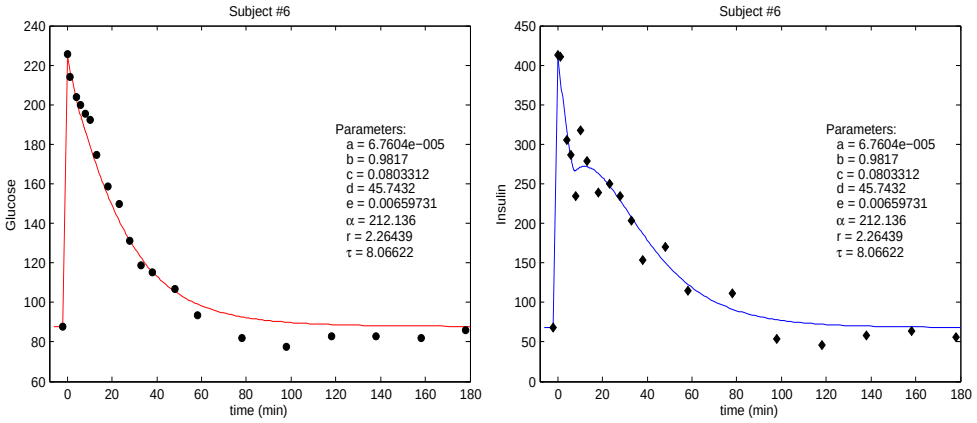

Figure 25. Profiles of subject 6 in [15] produced by the model (29). The estimated parameters satisfy the condition (40) in Corollary III.1, and both condition (41) in Corollary III.2. The upper bound estimated by Corollary III.1 is 8.35226; while the bound estimated by Corollary III.2 is 17.2249.

Corollary III.2. Numerically we determined that an upper bound for the delay for subject 6 is 8.35226 minutes, and 8.06007 minute for subject 8. However, the estimated parameters of subject 7, 13 and 27 do not satisfy either of the corollaries, although numerically the global stability of the equilibrium is obvious. We noticed in simulations that conditions of the corollaries are not satisfied due to the rough estimate of the upper bound M_G in Lemma III.2. We suspect that better estimate of M_G would improve the scope of applications of Corollary III.1 and Corollary III.2.

It is worthy to note that since the initial condition for $G(t)$ in $[-\tau, 0)$ is set differently from that in [15], [75] and [74], the estimated parameter values are not the same (Table 4). A significant difference is the values of the delay parameter τ. According to the profiles in this chapter and other references, the values taken in this chapter seems more reasonable. Another difference is the parameter value e. In [75] and [74], the parameter insulin-independent glucose elimination rate e is set to be zero according to Akaike information Criterion (AIC) in model selection by comparing the model (29), the model (31), and two other candidate models. However, difference of the AIC values between these two models is only 0.73% $(= (386.71 - 383.90)/383.90)$ and insignificant. Furthermore, the physiologically insulin-independent glucose elimi-

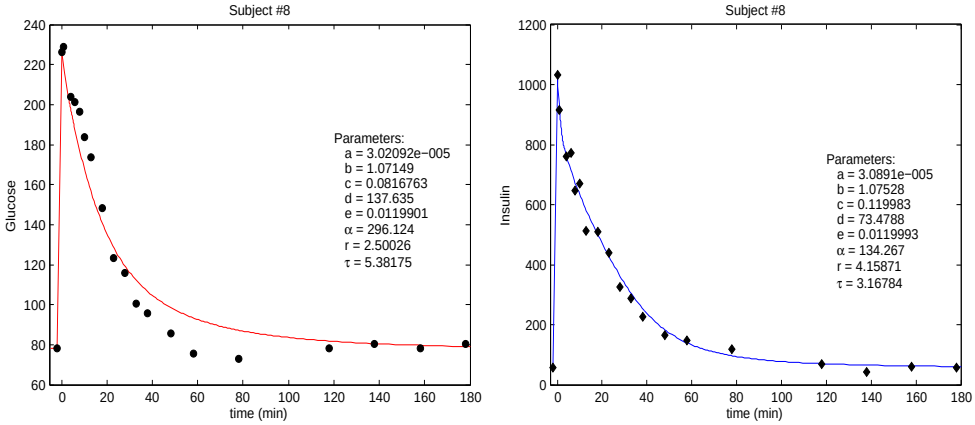

Figure 26. Profiles of subject 8 in [15] produced by the model (29). The estimated parameters satisfy the condition (40) in Corollary III.1, and both condition (41) in Corollary III.2. The upper bound estimated by Corollary III.1 is 8.06007; while the bound estimated by Corollary III.2 is 15.474.

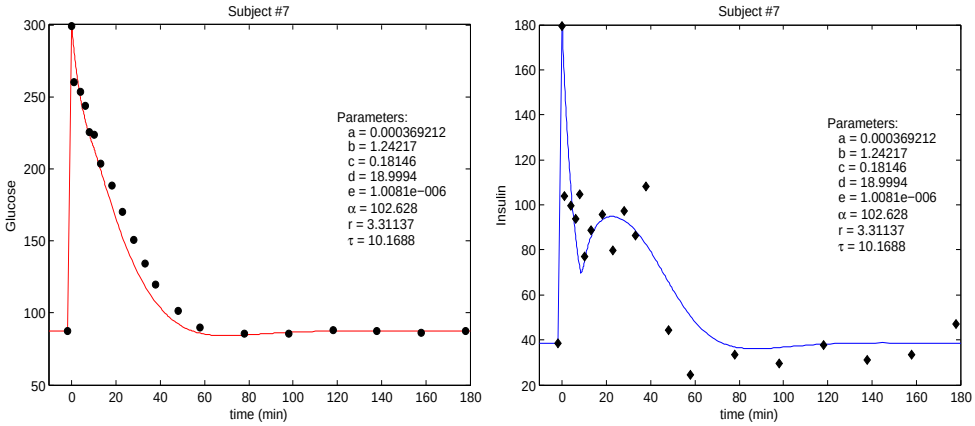

Figure 27. Profiles of subject 8 in [15] produced by the model (29). The estimated delay parameter τ is out of the upper bounds estimated by Corollary III.1 and Corollary III.2.

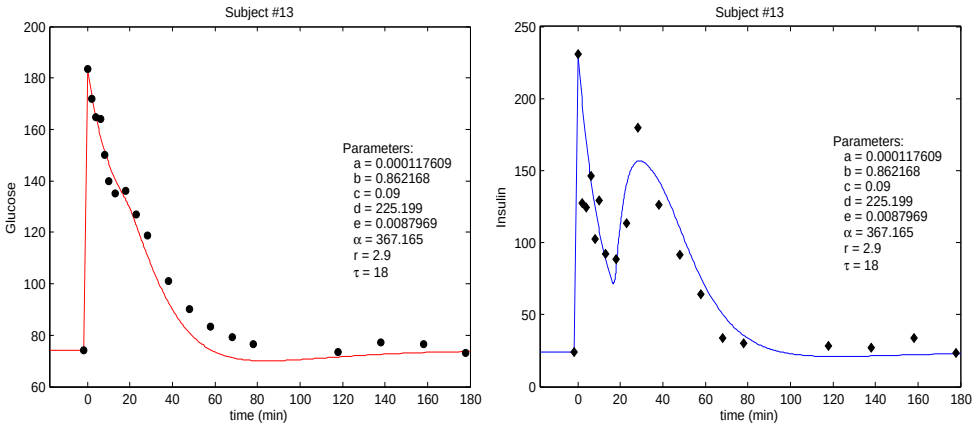

Figure 28. Profiles of subject 13 in [74] produced by the model (29). The estimated delay parameter τ is out of the upper bounds estimated by Corollary III.1 and Corollary III.2.

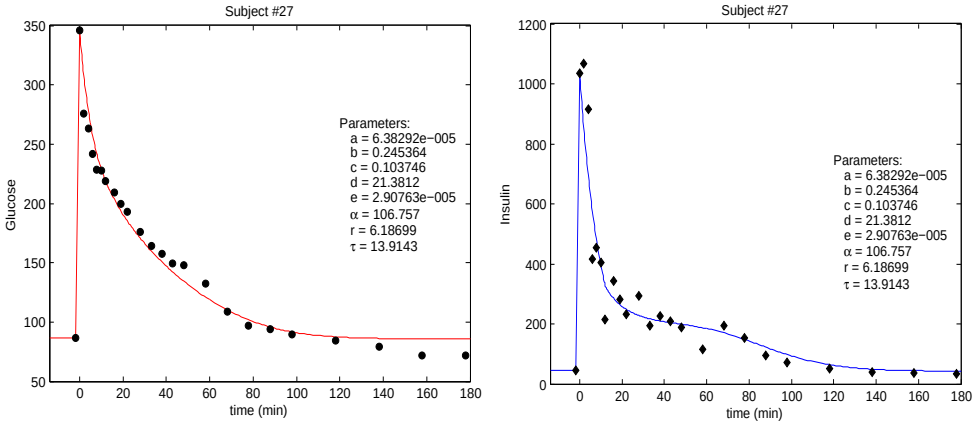

Figure 29. Profiles of subject 27 in [74] produced by the model (29). The estimated delay parameter τ is out of the upper bounds estimated by Corollary III.1 and Corollary III.2.

TABLE 4
Parameters fitted by experimental data ([75], [29]).

	τ	**a**	**b**	**c**	**d**	**e**	**References**
1	23.5	4.4300e-005	0.0122	0.1130	54.7372	0	Remark 11 in [75]
2	23.5	5.3000e-005	0.0145	0.0590	26.1868	0	Remark 9 in [75]
3	18	5.3000e-005	0.0145	1.0000e-003	0.4438	0	Remark 9 in [29]

nation rate could be not only greater than zero, but also larger than insulin-dependent glucose elimination rate ([18], [82]). So the term for insulin-independent glucose elimination rate should not be simply ignored.

6 Discussions

The length of delay in a delay differential equation model often plays a critical role in that a large delay can destabilize the system. Determining the length of delay based on physiology is appropriate in theoretical study and clinical data. In this chapter, we suggest that the value of the delay parameter should be set at the time mark of the first clear valley in insulin data. This would remove confusions in determining such value in applications.

In addition, in performing numerical studies for delay differential equations, functional initial condition is essential. In this chapter, we demonstrated that the profiles produced by using functional initial conditions are better than that by using constant values. This produces more accurate and convincible numerical results in clinical applications.

It is important to find out delay dependent condition on the global stability for the model (29), under which the clinical data satisfy the conditions. According to Theorem III.1 and its corollaries, adding a term of insulin-independent glucose uptake, although small, would help to ensure the global stability of the equilibrium. This has been recognized by the authors of [29], [75] and [74] in their numerical studies, even

though AIC does not support this addition from a mere statistical viewpoint, and even though the physiological significance of this term is debatable. Indeed, setting $e = 0$ or $e > 0$ small might not affect the remainder parameter point estimates to substantial degree. Since a small value of insulin-independent glucose tissue uptake cannot be excluded physiologically according to [18] and [82], we add it to the model in order to exploit the mathematical advantage, which offers in satisfying the conditions of both corollaries.

CHAPTER IV

LOCAL INSULIN MODEL TO STUDY SIGNALING EFFECT IN A PANCREATIC ISLET

In this chapter, we restrict our view to a single islet of Langerhans in pancreas. By understanding the dynamics in the micro-organ, we might be able to aquire in-depth knowledge about insulin signaling and beta-cell survival. The main work is published in

M Wang, J Li, GE Lim, JD Johnson, *Is dynamic autocrine insulin signaling possible? A mathematical model predicts picomolar concentrations of extracellular monomeric insulin within human pancreatic islets*, PLoS ONE 8(6) (2013).

Insulin signaling is essential for beta-cell survival and proliferation *in vivo*. Insulin also has potent mitogenic and anti-apoptotic actions on cultured beta-cells, with maximum effect in the high picomolar range and diminishing effect at high nanomolar doses. In order to understand whether these effects of insulin are constitutive or can be subjected to physiological modulation, it is essential to estimate the extracellular concentration of monomeric insulin within an intact islet. Unfortunately, the *in vivo* concentration of insulin monomers within the islet cannot be measured directly with current technology. Here, we present the first mathematical model designed to estimate the levels of monomeric insulin within the islet extracellular space. Insulin is released as insoluble crystals that exhibit a delayed dissociation into hexamers, dimers, and eventually monomers, which only then can act as signaling ligands. The rates at which different forms of insulin dissolve *in vivo* have been estimated from studies of peripheral insulin injection sites. We used this and other information to

formulate a mathematical model to estimate the local insulin concentration within a single islet as a function of glucose. Model parameters were estimated from existing literature. Components of the model were validated using experimental data, if available. Model analysis predicted that the majority of monomeric insulin in the islet is that which has been returned from the periphery, and the concentration of intra-islet monomeric insulin varies from 50C300 pM when glucose is in the physiological range. Thus, our results suggest that the local concentration of monomeric insulin within the islet is in the picomolar 'sweet spot' range of insulin doses that activate the insulin receptor and have the most potent effects on beta-cells *in vitro*. Together with experimental data, these estimations support the concept that autocrine/paracrine insulin signalling within the islet is dynamic, rather than constitutive and saturated.

1 Introduction

There is increasing evidence that insulin has critical autocrine or paracrine feedback actions within pancreatic islets [39], [49]. There are also data that suggests that human islets may undergo insulin resistance in type 2 diabetes [32], potentially unifying the etiology of type 2 diabetes. Two lines of evidence have been presented that suggest that β-cell insulin signaling is physiologically relevant. First, *in vivo* loss-of-function studies demonstrate that β-cell insulin signaling plays an important role in the control of β-cell apoptosis, proliferation and mass. For example, Kulkarni's group has shown that knockout of the β-cell insulin receptor reduced functional β-cell mass and increased apoptosis [46],[47],[95],[96]. Moreover, the same group has demonstrated that β-cell proliferation in response to both genetic and diet-induced insulin resistance was absent in mice lacking β-cell insulin receptors [72]. Our observation that physiological hyperinsulinemia is required for the high fat diet-induced increase in β-cells implies sensitivity to dynamic changes in insulin [64]. Complementing these *in vivo* loss-of-function studies, we and others have shown that exogenous insulin protects primary human and mouse islet cells from serum-withdrawal-induced apoptosis,

via NAADP-dependent Ca^{2+} release, a signalling hub involving 14-3-3ζ, RAF1, MEK, ERK, and BAD, as well as master transcription factors such as PDX1 and FOXO1 [58],[41],[4],[3],[59]. We also showed that insulin, but not glucose, directly increases proliferation of primary mouse dispersed islet β-cells [5]. These observations complement the work of multiple groups that suggest that insulin promotes β-cell survival. Whether insulin can affect β-cell secretory function or protein synthesis acutely is more controversial [10] and may depend on the dose, duration and context of the insulin signal [60].

Perhaps the most unexpected observation of our previous studies was that the dose-response relationships between insulin and apoptosis or proliferation did not follow a typical dose-response relationship [39]. We have consistently observed that lower doses of insulin, typically 200 pM, were more effective than higher doses in the nanomolar range [58],[41],[4],[3],[40]. However, the *in vivo* relevance of signaling events activated by picomolar insulin doses has been questioned due to the speculative assumption that β-cells are exposed to extremely high levels of insulin within the islet. Although it may seem intuitive to some that local insulin levels would be high near the β-cell, there is no direct evidence for this. The insulin concentration in the native β-cell microenvironment has never been measured experimentally. The physically closest insulin measurements to the islet *in vivo* are those of the portal vein (400-1200 pM depending on the glucose concentration)[88], but this represents the net insulin release from 1 million islets dispersed throughout the pancreatic parenchyma (40 cm3)[81] concentrated into the relatively small volume of a single vein. Moreover, there are two important clues that support the possibility that β-cells may be exposed to insulin concentrations less than that of the portal circulation. First, some β-cells must be exposed first, before other cells, within the complex microvasculature of the islet [58],[71], and would therefore be exposed to insulin levels identical to non-endothelial cells bathed by the peripheral circulating insulin, which is 40-100 pM at rest and 400 pM after a meal [88]. Second, it is known that insulin is stored

and secreted as an insoluble microcrystal, dissolving only when exposed to the pH of blood [66]. This means that the amount of local monomeric insulin capable of binding to β-cell receptors depends on both the secretion rate and the rate at which insulin crystals dissolve into active monomers. There is also the argument that β-cells would be optimally tuned to the range of insulin they see *in vivo*, and we have shown they are most responsive at 200 pM [58],[41],[4],[3],[40]. Insulin binding assays have shown that the IC50 of the ligand for the insulin receptor is in the picomolar range (88 pM) [102]. Given the current hurdles to experimentally measure the intra-islet insulin concentration, a powerful alternate approach is to undertake quantitative estimates using mathematical modeling [52]. We expect that the technology to measure insulin monomer levels *in vivo* will eventually be developed and permit our predictions to be tested experimentally.

An accurate model to distinguish the contribution of peripheral insulin and newly secreted insulin on β-cell dynamics requires detailed knowledge of a number of key parameters, including the rate of insulin secretion and the rate by which insulin crystals convert to monomers. In this work, local insulin refers to the newly synthesized and released insulin while peripheral insulin refers to insulin in blood entering islets. The insulin surrounding the β-cell is therefore a blend of these two concentrations. After synthesis, insulin is packaged in dense-core secretory granules as an insoluble zinc-associated crystal and is released following Ca^{2+}-dependent exocytosis in response to glucose [66],[68]. At high concentrations, such as those contained in therapeutic insulin formulations, insulin is primarily aggregated into hexamers as the default state [87]. Two sequential steps are required for the dissolution of the released insulin crystal into monomers, which interact with their cognate receptors. Each insulin hexamer must first dissolve into three dimers, followed by the breakdown into six insulin monomers [87],[54],[69]. With these delays, a fraction of insulin crystals may flow and/or diffuse away from the immediate vicinity of the β-cells. Therefore, the concentration of the local monomeric insulin that contributes to active signaling

could be lower than the total insulin released. Mathematical modeling becomes an important in silico tool for biologists to better understand the properties and actions of insulin *in vivo* in sites where it cannot be measured directly. Here, we report the outputs from the first such model, which illustrates the possible kinetics of the endogenous local insulin near β-cells. This work provides new insight into whether signaling events activated by high picomolar insulin might be relevant *in vivo*.

2 Results

1 Model formulation and logical considerations

The islets of Langerhans are clusters of 50-1000 endocrine cells. They are dispersed throughout the pancreas and represent 1-2% of the total pancreatic volume. Pancreatic islets are highly vascularized micro-organs, with a central core of β-cells surrounded by other endocrine cells, although this organization is less strict in adult human islets [71] or >1 year-old adult mouse islets [38]. Insulin secreting β-cells comprise the majority (50-70%) of islet endocrine cell types, although this can depend on the islet and on the individual [11]. A pancreatic islet is composed of 65% endocrine cells and 35% extracellular space and vasculature [76].

The present model is built on the logical assumption that the kinetics by which insulin crystals dissolve plays a critical role in the local islet insulin concentration. The release of intact insulin crystals from single β-cells has been demonstrated by multiple groups (e.g. Fig. 3I, in reference [66]), and it follows that it must take some time for these crystals to dissipate after exocytosis (Fig. 4F in reference [66]). The rate at which insulin hexamers dissolve into dimers and then monomers after subcutaneous injection at a point source has previously been addressed by our group and others (Fig. 1 in Li and Kuang [54]) and it happens on a time-scale of hours [87],[94]. The *in vivo* half-life of insulin is known to be 5-6 minutes [63], which means virtually all of the body's insulin must be replaced by the 1 million islets in 10 minutes. The baseline

peripheral insulin concentration in the whole body circulation is 50-80 pM. While we are not aware of studies that have directly measured insulin levels in arteries flowing into the pancreas, one would assume that non-degraded peripheral insulin returns to the pancreas at concentrations similar to any other organ. In addition to the prominent insulin degradation in the periphery, we also expect significant insulin re-uptake and degradation in islets, since β-cells are highly enriched with insulin receptors [4] and the endocytosis of insulin: insulin receptor complexes leads to their degradation in lysosomes (T. Albrecht, J.D. Johnson, unpublished data).

We initially considered whether the rate of blood flow in the pancreas might also be an important component of the model. Arterial blood flows into the pancreas through an artery connected to the aorta and flows out of the pancreas via the portal vein after passing through a network of fine capillaries. Although it was originally though that islet blood flow always proceeded from the inside out, recent *in vivo* imaging of intra-islet blood flow in mice has revealed multiple patterns of local islet blood flow (Fig. 5 in Meier et al. [71],[65]). There is also evidence that blood can fill some whole islets evenly without a flow direction (Fig. 4 of Nyman et al. [71]). Regardless of the direction, each case will have some 'prime' or 'upstream' β-cells exposed to fresh arterial blood with other cells subsequently exposed to locally released insulin. The percentage of cells exposed to fresh arterial blood is related to the width of an islet, which is relatively uniform and conserved throughout evolution. For simplicity, we will assume that, on average, the blood flow in the islet is irregular relative to the location of a given β-cell. Islet capillaries have been shown by electron microscopy to possess very thin endothelial cells, which are highly fenestrated and permeable [48], suggesting that the local barriers to the movement of insulin crystals, hexamers or dimers are negligible. For the sake of simplicity, this initial model will not consider physical barriers between the β-cell and the circulation. Newly released insulin flows out of the pancreas and into the liver through the hepatic portal vein within a few seconds. The mean portal vein blood flow rate has been measured

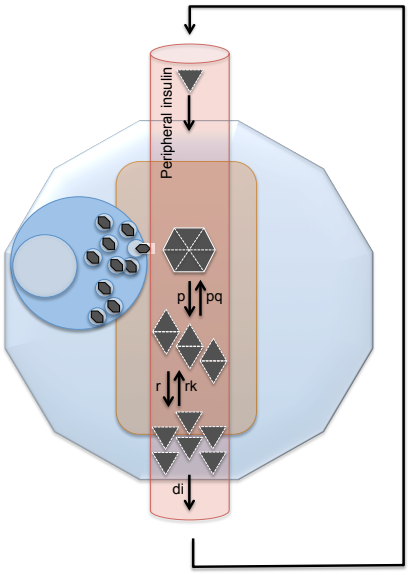

between 0.8 and 1.1 L/min, and no changes are observed between the basal state and a hyperglycemic clamp [88]. The total rate of pancreatic blood flow through the entire pancreas has been estimated using computed tomography to be 1.5 ml/min per ml of pancreas tissue [67]. Since we only consider a single prototypical islet as the point source in this model, and blood flow does not need to be considered, as its rate is relatively constant in and out of the islet. In other words, the dilution of 'islet blood' with re-circulating insulin in peripheral blood cancels out the addition of new insulin to the blood downstream of the islet.

All of the above considerations are summarized in the single islet model diagram (Fig. 1). These can also be summarized in the following word equation system for this model that considers a single islet and follows the law of mass action and the law of conservation. The rate of change of the concentration of insulin in any form can be expressed as the

$$\text{Rate of Change} = \text{Input Rate - Output Rate.}$$

We denote the concentration of insulin hexamers by H (in pM), dimers by D

(in pM), monomers by M (in pM), and peripheral insulin monomers returned to the islet by I (in pM). The transfer of peripheral insulin monomers should be same as the monomeric insulin concentration that remains in the circulation. We therefore obtain the following model for relative concentrations of local free insulin hexamers, dimers and monomers, and peripheral insulin:

$$\begin{cases} H' = f(G_0)/6 - p(H - qD^3) \\ D' = p(H - qD^3) - r(D - kM^2) \\ M' = r(D - kM^2) - d_i M \\ I' = \alpha M - d_i I \end{cases} \tag{44}$$

with the initial condition $H(0) = H_0 \geq 0$, $D(0) = D_0 \geq 0$, $M(0) = M_0 \geq 0$, $I(0) = I_0 \geq 0$. The transport from newly secreted insulin to peripheral insulin is assumed to be proportional to the level of monomers, $g(M) = \alpha M$, $\alpha > 0$, and the secretion of insulin hexamers is stimulated by glucose, which follows the dynamics of Hill function $f(G) = \frac{\sigma G^n}{a^n + G^n}$, which has been employed in other models [54],[75],[74],[56],[57],[89]. The division of $f(G_0)$ by 6 is due to the secretion of insulin from the β-cells as insulin hexamers. All parameters have the following meanings.

p (min^{-1}) the dissolution rate from hexamer to dimer.

q (L^2/pmol^2) the coefficient of the aggregation from dimer to hexamer.

r (min^{-1}) the dissolution rate from dimer to monomer. It is faster for a dimer to dissolve into two monomers than for a hexamer to dissolve into three dimers. Hence $r > p$.

k (L/pmol) the coefficient of the aggregation from monomer to dimer.

G_0 (mM) the clamped glucose concentration (normal *in vivo* range is 3.9 6.1 mM)

d_i (min^{-1}) the degradation rate of insulin (both local free and peripheral).

σ (pM/min/mM) maximum secretion rate of insulin stimulated by glucose.

α (min^{-1}) the transfer rate of newly secreted insulin to peripheral insulin.

a (mM) half-saturation point in Hill function $f(G)$.

2 Model analysis

Next, we studied the qualitative behaviors of the model (44). The model has a unique equilibrium $E^* = (H^*, D^*, M^*, I^*)$, given by

$$M^* = \frac{c}{d_i},\ I^* = \frac{\alpha M^*}{d_i},\ D^* = \frac{c}{r} + kM^{*2},\ H^* = \frac{c}{p} + qD^{*3}, \tag{45}$$

where $c = f(G_0)/6$. Since the system (44) is cooperative, it is intuitive that the unique equilibrium is globally stable. To this end, we first obtain the following:

Theorem IV.1 *Any solution of the model 44 with initial condition,* $H_0 \geq 0$, $D_0 \geq 0$, $M_0 \geq 0$, $I_0 \geq 0$, *is positive and bounded.*

The proof of this analytical result can be found below and in Figure 5. Then, with direct application of Theorem IV.1, and Theorem 2.3.1 (in Smith, HL, page 8 of reference [86]), we obtain the following theorem that ensures that our model is quantitatively reliable, and in next section we demonstrate that our numerical analysis is qualitatively reasonable.

Theorem IV.2 *The unique equilibrium point* E^* *is globally asymptotically stable.*

It can be seen by (45) that, at equilibrium, the concentrations of local insulin M, peripheral insulin I, hexamers and dimers depend on G_0 in nonlinear relationships. However, the ratio of the newly synthesized insulin and the peripheral insulin at equilibrium can be expressed by

$$\frac{M^*}{I^*} = \frac{d_i}{\alpha}. \tag{46}$$

The equation (46) indicates that the ratio of the concentration of local free insulin and peripheral insulin is linearly dependent of insulin degradation d_i, and inversely proportional to the transfer rate α. On the other hand, insulin concentration of intra-islet can be estimated by

$$M^* = \frac{d_i I^*}{\alpha}. \tag{47}$$

3 Parameter estimation and numerical simulations

As detailed in the following section, model parameters were selected based on the existing literature, regression fitting of experimental data found in the literature, or with reasonable assumptions from known physiological principles. Using the resulting model, we then simulated insulin secretion dynamics under conditions of various clamped glucose inputs. We chose the initial condition of the model as $H(0) = 0$, $D(0) = 0$, $M(0) = 0$, and $I(0) = 0$ as Theorem IV.1 guarantees that the equilibrium is globally stable and thus the initial conditions do not affect the equilibrium.

The estimation of insulin secretion rate $f(G)$ was as follows. It is widely accepted that the insulin secretion response to glucose takes a sigmoid shape function, namely Hill's function $f(G) = \frac{\sigma G^2}{a^2+G^2}$. To estimate the parameters σ, a and n, we primarily used published data of *in vivo* insulin secretion rates at various glucose levels in human subjects [77],[42] as shown in following Table 1 by employing the Least Square Method. Additional points on the curve were estimated and added for fitting. The fitting results in $\sigma = 111.96$, $a = 9.34$ and $n = 3.15$. Fig. 2 illustrates the fitted curve. It is noteworthy that the estimated values are in agreement to those

estimated in IVGTT models [75],[74],[56]. As mentioned, this secretion rate should be divided by 6 to obtain the secreted concentration of insulin hexamers.

The estimation of p and q was as follows. We estimated the values of the parameters p and q for human insulin based on insulin analogues, with the assumption that the dissolution and aggregation rates of human insulin falls between the rates associated with fast insulin analogues and slow insulin analogues. According to Li and Kuang, 2009 [54]; Tarin 2005 [90] and Trajanoski 1993 [94], the value of the parameter p (min-1) remains the same for fast and slow insulin analogues. So we assume that $p = 0.5$ (min^{-1}) for human insulin as well. Table 2, adopted from Tarin 2005 [90], shows the values of the parameter q (L2/pM2) for various insulin analogues. Therefore, the parameter q for human insulin is estimated as the value for Semilente, i.e., $q = 7.6 \times 10^{-2}$ $\text{ml}^2/\text{U}^2 = 1.6 \times 10^{-15}$ L^2/pmol^2 after unit conversion by a factor 2.1×10^{-14}.

The estimation of r and k was as follows. It is intuitive that it is faster for a dimer to dissolve to two monomers than for a hexamer to dissolve to three dimers. So it is reasonable to assume $r = \frac{3}{2} \times p = 0.75$ min^{-1} and $k = \frac{2}{3} \times q = 1.0 \times 10^{-15}$.

The estimation of d_i was as follows. Values for the degradation rate d_i of insulin have been reported within a wide range between 0.03-0.2 [22]. To select a reasonable value for d_i, observing that in general a substrate decays exponentially, we considered the following ordinary differential equation,

$$I' = -d_i I,\ I(0) = I_0,$$

where the initial condition represents the case of no secretion. The solution of this differential equation $I = I_0 e^{-d_i t}$ represents the change of amount of insulin over time. Notice that the half life of insulin is approximately in a range of 4-6 minutes [63]. Assuming that the half-life of insulin is 6 min, when $t = 6$ min, $I = I_0/2$ and thus $I_0/2 = I_0 e^{-6d_i}$. Solving this equation for d_i yields $d_i = (\ln 2)/6 = 0.1$ min^{-1}.

The estimation of α was as follows. We estimated the parameter α(fraction coefficient of peripheral insulin) as follows. As expressed in equation (44), the rate of

change of the returned peripheral insulin concentration in an islet, I', is affected by its degradation d_i and the concentration of newly secreted insulin monomers, M. Assume that x units of insulin monomers are secreted by a single islet. Thus, a total of x million units of insulin will be released into the portal vein from the one million islets of the pancreas, after which it becomes peripheral insulin. It is established that 50% of secreted insulin is removed from the circulation by the liver on the first pass. We assume an insulin degradation rate of $d_i = 0.1$ min^{-1} according to the estimation of d_i given above. Since it takes about 25 seconds for a complete circulation of blood, newly released insulin must return to the pancreas in the same time, where it is assumed evenly distributed among the one million islets. So, approximately $0.5xe^{-d_iT} = 0.48x$ units of insulin return the same islet. Therefore, we estimate that $\alpha = 0.48$ min^{-1}.

Using our model with the above carefully selected parameter values, we simulated the dynamics of the various insulin concentrations at a range of clamped glucose concentrations. A stepwise increase in glucose from 0 mM to any value we tested resulted in an increase in peripheral insulin that reached a maximum in 30 minutes (Fig. 3). As expected, the aggregated forms reached their peak much faster. The concentration of monomeric insulin that has been newly release reaches only 100 pM after a jump to 15 mM glucose (a glucose concentration is much higher than what is seen in humans after a meal).

Importantly, we are able to use our model to estimate the total concentration of insulin monomers within the islet (i.e. newly made insulin + insulin returning from the periphery). By (46) and the parameter values we estimated above we can derive the total monomeric insulin present in the islet at any glucose concentration. Simple computation shows that 75% of local monomeric insulin is peripheral insulin while 25% is new monomeric insulin (Fig. 4). Our simulations clearly show that the majority of insulin in an islet is returned as monomeric peripheral insulin, whereas the newly secreted monomeric insulin from the islet provides a minor contribution in all cases tested. Therefore, our model predicts that the levels of insulin monomers in

the islet do not exceed the picomolar range, even in extreme clamp studies (Fig. 4). Physiological meal-induced glucose excursions rarely fall outside the 4 mM to 8 mM range in normal humans, and our model suggests that monomeric insulin is unlikely to exceed 300 pM in these conditions (Fig. 4).

3 Model validation

We validated the glucose-response component of our model by comparing the model-predicted values of glucose-stimulated insulin responses with the experimental data in [77]. The comparison is shown in Table 6.

It is well known that a swift increase of secretion occurs when glucose concentrations rise higher than fasting levels, but becomes saturated beyond the hyperglycemic range. No model can predict the true physiology perfectly, but we suggest that this verification is valid because the response function of insulin secretion rate is obtained statistically according to the experimental data. The model-predicted dose response is in approximate agreement with the observed dose response in the same experiment. Some aspects of the model simulations, namely the exact concentration of monomeric insulin in the immediate vicinity of intact human islets *in vivo* must await the technology to measure this directly.

1 Proof of Theorem IV.1

Notice that the first three equations of model (44) do not involve I, hence we first consider the sub-model

$$\begin{cases} H'(t) = c - p(H(t) - qD^3(t)) \\ D'(t) = p(H(t) - qD^3(t)) - r(D(t) - kM(t)^2) \\ M'(t) = r(D(t) - kM(t)^2) - d_i M(t) \end{cases} \tag{48}$$

and then the original model (44).

The first quadrant of phase space is invariant. In fact, on the coordinate plane $H = 0$, $H' = c + pqD^3 > 0$; on $D = 0$, $D' = pH + rkM^2 \geq 0$; on $M = 0$, $M' = rD \geq 0$. Therefore, trajectories starting from the first quadrant will not cross any of the coordinate plane to negative side. We next construct a bounded region Ω(see Fig. 30) in the first quadrant such that the trajectory $\gamma(E_0)$ starting from $E_0 = (H(0), D(0), M(0))$ will not cross the boundaries of Ω; that is, Ω is invariant, thus $\gamma(E_0)$ is bounded. We choose $a > max(H*, H(0))$ to be large. Let π_1 be the plane through the point $P_1(a, 0, 0)$ with the normal vector $(-1, 1, 1)$. Plane π_1 intersects the plane $D = D^*$ at the line P_2P_3, where P_2 is on the plane $M = 0$ and P_3 is on the plane $M = M^*$. Let P_6 be the intersection point of the plane π_1, $D = 0$ and $M = M^*$. Thus P_3P_6 is parallel to P_1P_2, whose direction vector is $(1, 1, 0)$. Let π_2 be the plane passing through the line P_2P_3 with the normal vector $(-1, -1, 1)$. Then π_2 intersects the plane $H = 0$ at the line P_4P_5, where P_4 is on the plane $M = 0$, P_5 is on the plane $M = M^*$, and a is large enough so that the point $(H(0), D(0), 0)$ is on the same side of the line P_2P_4 as the origin in the plane $M = 0$. Clearly the line P_3P_5 is in the plane $M = M^*$. Let π_3 be the plane passing through the line P_3P_5 with the normal vector $(-1, -1, -1)$, where we require that a was chosen large enough so that the point $(H(0), D(0), M(0))$ is on the same side of the plane π_3 as the origin. Let π_4 be the plane through the line P_3P_6 and perpendicular to the plane $M = M^*$. Since P_3P_6 is parallel to P_1P_2 and the direction vector of P_1P_2 is $(1, 1, 0)$, the inward normal vector of π_4 is $(-1, 1, 0)$. Therefore, the planes π_i, $i = 1, 2, 3, 4$ and the coordinate planes $H = 0$, $D = 0$, $M = 0$ form a closed region Ω(refer to Fig. 30), and $E_0 \in \Omega$.

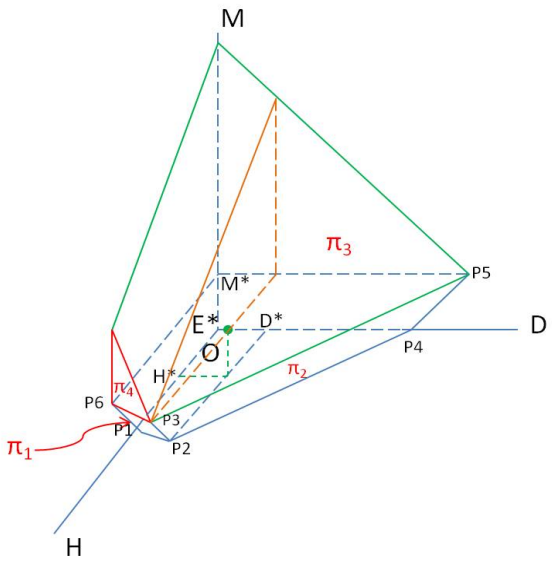

Figure 30. Bounded area Ω

Now we shall show that the bounded area Ω is invariant and thus $\gamma(E_0) \in \Omega$. To this end, we need only to show that the inner products of the inward normal vectors of the plane π_i, $i = 1, 2, 3, 4$, with the direction vector of trajectory starting from these planes are nonnegative.

On π_1, $M \leq M^*$, $D \leq D^*$ and $H \geq H^*$.

$$\begin{aligned}
& (H', D', M') \cdot (-1, 1, 1) = -H' + D' + M' \\
= \; & -c + p(H - qD^3) + p(H - qD^3) - r(D - kM^2) \\
& +r(D - kM^2) - d_i M \\
= \; & -c + 2p(H - qD^3) - d_i M \\
\geq \; & -c + 2p(H - qD^3) - d_i M^* \\
= \; & -2c + 2p(H - qD^3) \\
\geq \; & 2c + 2p(H^* - qD^{*3}) \\
= \; & 2(-c + p(H^* - qD^{*3})) = 0.
\end{aligned}$$

On π_2, $D \geq D^*$ and $M \leq M^*$, thus we have

$$\begin{aligned}
& (H', D', M') \cdot (-1, -1, 1) = -H' - D' + M' \\
= \; & -c + p(H - qD^3) - p(H - qD^3) + r(D - kM^2) \\
& + r(D - kM^2) - d_i M \\
= \; & -c + 2r(D - kM^2) - d_i M \\
\geq \; & -c + 2r(D - kM^{*2}) - d_i M^* \\
= \; & -2c + 2r(D - kM^{*2}) \\
\geq \; & -2c + 2r(D^* - kM^{*2}) \\
= \; & 2(-c + r(D^* - kM^{*2})) = 0.
\end{aligned}$$

On π_3, $M \geq M^*$, thus we have

$$\begin{aligned}
& (H', D', M') \cdot (-1, -1, -1) = -H' - D' - M' \\
= \; & -c + p(H - qD^3) - p(H - qD^3) + r(D - kM^2) \\
& - r(D - kM^2) + d_i M \\
= \; & -c + d_i M \geq -c + d_i M^* = 0.
\end{aligned}$$

On π_4, $M \geq M^*$, $D \leq D^*$ and $H \geq H^*$, thus we have

$$\begin{aligned}
& (H', D', M') \cdot (-1, 1, 0) = -H' + D' \\
= \; & -c + p(H - qD^3) + p(H - qD^3) - r(D - kM^2) \\
= \; & -c + 2p(H - qD^3) - r(D - kM^2) \\
\geq \; & -c + 2p(H^* - qD^{*3}) - r(D^* - kM^{*2}) \\
= \; & -c + 2c - c = 0.
\end{aligned}$$

Therefore these inner products are nonnegative, which implies the trajectory on boundaries π_i, $i = 1, 2, 3, 4$ goes inward of Ω. Moreover, we have proved the first quadrant is invariant. Therefore, we conclude that Ω is invariant.It is equivalent to

say the solution to the sub-model 48 is bounded.Now for the model (44), since M is bounded, thus clearly I is bounded. We complete the proof.

4 Discussion

The goal of the present work was to estimate the local insulin concentrations within a working human pancreatic islet. This estimation is essential for efforts to understand the physiological relevance and mode of islet paracrine insulin signaling. More specifically, it has the potential to elucidate if signaling is constitutive as a result of saturating local insulin levels or dynamic with monomeric insulin varying in a range that permits optimal activation of the insulin receptor. To the best of our knowledge, this is the first time any such estimation has been systematically generated. Our model suggests that locally produced insulin at steady state makes a relatively minor contribution to the local levels of monomeric insulin in an individual islet (estimated to be 25%). In contrast, the majority of locally available monomeric insulin within the islet derives from newly returned insulin from the peripheral circulation. Regardless, our model indicates that within an islet, the percentage of new insulin converted to monomers before being swept away by the blood flow is always less than the insulin returned from the peripheral circulation. Since the peripheral insulin concentration is well known, we can be confident that the total monomeric insulin concentration in the islet is not in orders of magnitude higher than it is in the periphery, as has been implied by some commentators. The model is dynamic, and our simulations show that the majority of the changes take place within 30 minutes, regardless of the glucose step. Since the initial conditions used in the simulations are somewhat arbitrary, one should not imply too much from the shape of these curves. Nevertheless, it is clear that the monomeric insulin concentration in the islet is relatively low in response to an increase in glucose at each time point before equilibrium is reached. It should also be noted that our model focuses primarily on glucose as the main stimulus for insulin release, and does not exclude modulatory contributions of incretin hormones

or neural inputs, which increase insulin levels.

Many studies have investigated the effects of insulin on pancreatic β-cells; however, the vast majority have employed insulin doses in the high nanomolar range. This, together with culture conditions that allow insulin to accumulate, may be one of the reasons that some investigators have failed to observe significant effects of insulin in their *in vitro* experiments. Our model suggests that such high doses are non-physiological and up to 1000 times higher than the locally present levels. Importantly, nanomolar doses of insulin would maximally stimulate IGF1 receptors [17], which do not play an essential role in islet survival and have only a minor role on beta-cell function [47],[45]. Our model also suggests that the concentration of free monomeric insulin in the islet may not exceed 300 pM while glucose is in the physiological range. Thus, local autocrine/paracrine insulin signaling is likely to be dynamic and physiologically relevant in the picomolar range. This also means the experimentally defined 'sweet spot' where β-cells respond *in vitro* optimally to picomolar insulin is likely to be well within the *in vivo* physiological range [39]. This might seem counterintuitive, but our model suggests that the slow kinetics by which insulin crystals dissolve keeps the local monomeric insulin levels surprisingly low. Although we have not considered the rate of islet blood flow in our model, it may nonetheless be important and should be considered in future models. Changes in islet vasculature and/or blood flow might therefore represent physiological and pathological modes of altering local insulin signaling.

One important assumption of our model is that the percentage of insulin released in its crystalized form is high. This generally appears to be well supported by the literature, but there are cases where it might not be as assumed here. Some species of rodents (e.g. porcupines) have insulin genes with alterations in amino acids known to be important in zinc binding and crystal formation [35]. In these examples, we might therefore expect an increased ratio of monomeric to hexameric local insulin and possibly a desensitization of islet insulin signaling, but this should be investi-

gated in future modeling studies. Similarly, a human mutation (AspB10) has been described that alters insulin binding to zinc and complex assembly, and we would predict that autocrine insulin signaling might be altered in such patients, in addition to multiple other defects [12]. It would also be interesting to determine if modifications in insulin packaging caused by recently described genetic polymorphisms in zinc transporters might affect the ratio of insulin released in a post-crystalized form under specific conditions [50]. In each of these cases, we expect insulin signaling pathways to compensate in the face of altered monomeric insulin levels [36].

We speculate that our findings also have implications for efforts to understand the evolution and function of the endocrine pancreas. Remarkably, the size of islets is relatively similar between mammals of different body sizes, with the total number of islets varying between small and large species. The islets of Langerhans are also somewhat unique as an endocrine organ in that they are spread throughout the large pancreas in a diffuse, but non-random manner. We speculate that this architecture evolved to prevent the accumulation of high levels of insulin in and around the islets. Insulin is a powerful mitogen [37] and we have shown it can stimulate primary islet cell proliferation [5]. We have recently shown that pancreatic insulin hypersecretion is required for the increase in islet size observed during high fat feeding [64]. Thus, the diffuse distribution of relative small islets might be evolutionarily conserved to prevent excessive local insulin concentrations that might increase the risk of pancreatic cancer. Indeed, significant molecular, clinical and epidemiological findings point to important links between hyperinsulinemia and pancreatic cancer [24],[31],[23],[14],[51].

This work is the first to model the intra-islet concentration of monomeric islet insulin. We conclude that the major contributor to the human islet insulin levels is peripheral insulin owing to the relatively slow dissolution of newly secreted insulin crystals. We find that the total concentration of free monomeric insulin, capable of activating the insulin receptor, remains in the picomolar range regardless of glucose stimulation. Together, these findings add novel insight into pancreatic islet biology

and provide context to the experimental studies focused on the effects of islet insulin signaling. Our work helps contextualize *in vivo* and *in vitro* studies on the autocrine effects of insulin and lay the groundwork for future mathematical and physiological studies.

TABLE 5

Insulin secretion data rate and multiple glucose concentrations.

Glucose level(mM)	Secretion rate(pM/min)	References and Notes
3	1	Data point estimated and added for fitting
4	10	Data point estimated and added for fitting
5	16	The case of overnight fast in [43]. Glucose level ranges between 4 and 6 mM after an overnight fast. We chose 5 mM.
7	33	The case of 24-h on mixed diet in [43]. We assume at 7 mM.
9	47	[44]
16.5	102	The case of hyperglycemic clamp at 16.5 mM in [43].
25	103	Data point estimated and added for fitting

TABLE 6

Values of parameter q for different insulin formulations.[1]

Units	Lispro	Actrapid	Semilente	NPH, Glargine
ml^2/U^2	4.8×10^{-4}	1.9×10^{-3}	7.6×10^{-2}	3.0
$L^2/pmol^2$	9.8×10^{-18}	3.9×10^{-17}	1.6×10^{-15}	6.3×10^{-14}

[1]This table is adopted from Table IV in Tarin et al [90].

CHAPTER V

A BRIEF SUMMARY

So far we have proposed three dynamical system models and studied them with both analytical and numerical sessions. These works have revealed interesting mathematical features and novel physiological insights. Let us reiterate them briefly.

The fast-slow model studies have suggested that several crucial factors contribute to the development of diabetes in a prolonged period. Among these factors, initial beta-cell mass formed in embryonic and postnatal development, insulin sensitivity, relative strength of beta-cell functionality, and transfer rate between plasma and interstitial space play significant roles. The local stability, Hopf bifurcation and persistence of solutions also depict the rich features possessed by this model. We have observed the existence of a limit cycle through intensive numerical simulations, while these simulations also enable us to successfully fit available longitudinal T2DM data of Pima Indian tribe as a validation of the model.

The IVGTT model with delay differential equations has deeply examined the length of delay which often plays a critical role in that large delay can destabilize the system. The value of the delay parameter is suggested to be set at the time mark of the first clear nadir in insulin data. In addition, in performing numerical studies for delay differential equations, the functional initial condition is essential to produce more accurate and convincible numerical results in clinical studies when determining insulin sensitivity and glucose effectiveness. A delay dependent condition on the global stability for the model, under which many cases of clinical data satisfy the conditions, has been given as well.

The analysis of the third kinetic model, formulated to study the insulin signal-

ing effect within a single islet, suggests that local autocrine/paracrine insulin signaling is likely to be dynamic and physiologically relevant in the picomolar range. The experimentally defined 'sweet spot' by biologists refers to that β-cells respond *in vitro* optimally to picomolar insulin. As our model analyses and simulations have demonstrated, the new concept 'sweet spot' is likely applicable to the *in vivo* physiological range. Furthermore, this work is the first to model the intra-islet concentration of monomeric islet insulin, which is not measurable under current technology.

The findings in this dissertation could help us better understand the mechanism of the glucose-insulin endocrine regulatory system, the possible causes of diabetes and pancreatic islet insulin scaling effect. They may as well provide certain guideline to assist in developing more reasonable, effective, efficient and economic clinical treatment after necessary experiments. We also hope these mathematical studies could be utilized to facilitate future mathematical and physiological researches on diabetes related topics and help contextualize *in vivo* and *in vitro* studies on the autocrine effects of insulin.

REFERENCES

[1] American Diabetes Association, www.diabetes.org

[2] Ahren, B., Taborsky Jr., G.J., *B-cell function and insulin secretion.* In: Porte, D., Sherwin, R.S., Baron, A. (Eds.), Ellenberg and Rifkins Diabetes Mellitus, sixth ed.(2002) McGraw-Hill Professional, New York,

[3] EU Alejandro, JD Johnson, *Inhibition of raf-1 alters multiple downstream pathways to induce pancreatic beta-cell apoptosis*, Journal of Biological Chemistry 283 (2008): 2407-2417.

[4] EU Alejandro, TB Kalynyak, F Taghizadeh, KS Gwiazda, EK Rawstron, et al., *Acute insulin signaling in pancreatic beta-cells is mediated by multiple Raf-1 dependent pathways*, Endocrinology 151 (2010): 502-512.

[5] JL Beith, EU Alejandro, JD Johnson, *Insulin stimulates primary beta-cell proliferation via Raf-1 kinase*, Endocrinology 149 (2008): 2251-2260.

[6] DL Bennette and SA Gourley, Global stability in a model of the glucoseCinsulin interaction with time delay, *Eur. J. Appl. Math.*, 15 (2004) 203.

[7] RN Bergman, YZ Ider, CR Bowden, C Cobelli, *Quantitative estimation of insulin sensitivity*, Am. J. Physiol., (1979), 236:E667-E677.

[8] RN Bergman, , *Pathogenesis and prediction of diabetes mellitus: lessons from integrative physiology*, Irving L. Schwartz Lecture, Mount Sinai J. Med. 60 (2002), 280C290.

[9] S Bonner-Weir and A Sharma, *Are there pancreatic progennitor cells from which new islets form after birth?*, Nature Clinical Practice, Endocrinology Metabolism, **2** (2006), 240C241.

[10] C Bouche, X Lopez, A Fleischman, AM Cypess, S O'Shea, et al., *Insulin enhances glucose-stimulated insulin secretion in healthy humans*, Proc Natl Acad Sci U S A 107 (2010): 4770-4775.

[11] O Cabrera, DM Berman, NS Kenyon, C Ricordi, PO Berggren, et al., *The unique cytoarchitecture of human pancreatic islets has implications for islet cell function*, Proceedings of the National Academy of Sciences of the United States of America 103 (2006): 2334-2339.

[12] RJ Carroll, RE Hammer, SJ Chan, HH Swift, AH Rubenstein, et al., *A mutant human proinsulin is secreted from islets of Langerhans in increased amounts via an unregulated pathway*, Proceedings of the National Academy of Sciences of the United States of America 85 (1988): 8943-8947.

[13] AD Cherrington, D Sindelar, D Edgerton,K Steiner, OP McGuinness, *Physiological consequences of phasic insulin release in the normal animal*. Diabetes 51 (2002) (Suppl. 1), S103–S108.

[14] CJ Currie, CD Poole, EA Gale, *The influence of glucose-lowering therapies on cancer risk in type 2 diabetes*, Diabetologia 52 (2009): 1766-1777.

[15] A De Gaetano and O Arino, *Mathematical modeling of the intravenous glucose tolerance test*, J. Math. Biol., **40** (2000), 136–168.

[16] M Derouich, A Boutayeb, *The effect of physical exercise on the dynamics of glucose and insulin*. J. Biomechanics 35 (2002) , 911C917.

[17] P De Meyts, J Whittaker, *Structural biology of insulin and IGF1 receptors: implications for drug design*, Nat Rev Drug Discov 1 (2002): 769-783.

[18] R Duhlmeier, A Hacker, A Widdel, W von Engelhardt, and H-P Sallmann, *Mechanisms of insulin dependent glucose transport into porcine and bovine skeletal muscle*, Am J. Physiol. Regul. Integr. Comp. Physiol., 289: R187–R197, 2005.

[19] WC Duckworth,RG Bennett,FG Hamel, *Insulin degradation: progress and potential*. Endocr. Rev. 19 (1998), 608C624.

[20] Efanova, IB, Zaitsev, SV, Zhivotovsky, B, Kohler, M, Efendis, S, Orrenius, SBerggren, P. O. *Glucose and tolbutamide induce apoptosis in pancreatic beta-cells*. J. Biol. Chem. **273**, (1998), 33501-33507.

[21] S Efrat, *Beta-cell expansion for therapeutic compensation of insulin resistance in type 2 diabetes*, Expertimental Diab. Res., **4** (2001), 1C5.

[22] K Engelborghs, V Lemaire, J Belair, D Roose, *Numerical bifurcation analysis of delay differential equations arising from physiological modeling*, Journal of Mathematical Biology 42 (2001): 361-385.

[23] M Evert, J Sun, S Pichler, N Slavova, R Schneider-Stock, et al., *Insulin receptor, insulin receptor substrate-1, Raf-1, and Mek-1 during hormonal hepatocarcinogenesis by intrahepatic pancreatic islet transplantation in diabetic rats*, Cancer Res 64 (2004): 8093-8100.

[24] WE Fisher, LG Boros, WJ Schirmer, *Insulin promotes pancreatic cancer: evidence for endocrine influence on exocrine pancreatic tumors*, J Surg Res 63 (1996): 310-313.

[25] N Fenichel, *Persistence and smoothness of invariant manifolds for flows*, Indiana Univ. Math. Journal, 21 (1971) 193-226.

[26] N Fenichel, *Asymptotic stability with rate conditions*, Indiana Univ. Math. Journal, 23 (1974) 1109-1137.

[27] N Fenichel, *Asymptotic stability with rate conditions II*, Indiana Univ. Math. Journal, 26 (1977) 81-93.

[28] N Fenichel, *Geometric singular perturbation theory for ordinary differential equations*, J. Diff. Eq. 31 (1979) 53-98.

[29] DV Giang, Y Lenbury, A De Gaetano and P Palumbo, *Delay Model of Glucose-Insulin Systems: Global Stability and Oscillated Solutions Conditional on Delays*, JMAA, **343**(2) (2008), 996–1006.

[30] TA Gresl, RJ Colman, TC Havighurst, LO Byerley, DB Allison, DA Schoeller, JW Kemnitz, *Insulin sensitivity and glucose effectiveness from three minimal models: effects of energy restriction and body fat in adult male rhesus monkeys*, Am J. Physiol. Regul. Integr. Comput. Physiol. 285 (2003) R1340.

[31] L Gullo, *Diabetes and the risk of pancreatic cancer*, Ann Oncol 10 Suppl 4 (1999): 79-81.

[32] JE Gunton, RN Kulkarni, S Yim, T Okada, WJ Hawthorne, et al., *Loss of ARNT/HIF1beta Mediates Altered Gene Expression and Pancreatic-Islet Dysfunction in Human Type 2 Diabetes*, Cell 122 (2005): 337-349.

[33] MW Hirsch, S Smale, RL Devaney, *Differential Equations, Dynamical Systems, and an Introduction to Chaos*, Academic Press, 2004.

[34] A Hoorens, M Van De Casteele, G Kloppel D Pipeleers,. *Glucose promotes survival of rat pancreatic b-cells by activating synthesis of proteins which suppress a constitutive apoptotic program.* J. Clin. Invest. **98** (1996), 1568-1574.

[35] R Horuk, TL Blundell, NR Lazarus, RW Neville, D Stone, et al., *A monomeric insulin from the porcupine (Hystrix cristata), an Old World hystricomorph*, Nature 286 (1980): 822-824.

[36] R Horuk, P Goodwin, K O'Connor, RW Neville, NR Lazarus, et al., *Evolutionary change in the insulin receptors of hystricomorph rodents*, Nature 279 (1979): 439-440.

[37] D Ish-Shalom, CT Christoffersen, P Vorwerk, N Sacerdoti-Sierra, RM Shymko, et al., *Mitogenic properties of insulin and insulin analogues mediated by the insulin receptor*, Diabetologia 40 Suppl 2 (1997): S25-31.

[38] JD Johnson, NT Ahmed, DS Luciani, Z Han, H Tran, et al., *Increased islet apoptosis in Pdx1+/- mice*, J Clin Invest 111 (2003): 1147-1160.

[39] JD Johnson, EU Alejandro, *Control of pancreatic beta-cell fate by insulin signaling: The sweet spot hypothesis*, Cell Cycle 7 (2008): 1343-1347.

[40] JD Johnson, EL Ford, E Bernal-Mizrachi, KL Kusser, DS Luciani, et al., *Suppressed insulin signaling and increased apoptosis in CD38-null islets*, Diabetes 55 (2006): 2737-2746.

[41] JD Johnson, S Misler, *Nicotinic acid-adenine dinucleotide phosphate-sensitive calcium stores initiate insulin signaling in human beta cells*, Proc Natl Acad Sci U S A 99 (2002): 14566-14571.

[42] CN Jones, D Pei, P Staris, KS Polonsky, YD Chen, et al., *Alterations in the glucose-stimulated insulin secretory dose-response curve and in insulin clearance in nondiabetic insulin-resistant individuals*, The Journal of clinical endocrinology and metabolism 82 (1997): 1834-1838.

[43] J Keener, J Sneyd. Mathematical Physiology.(1998) Springer, New York.

[44] Y Kuang, *Delay Differential Equations with Applications in Population Dynamics* **Vol. 191** in the series of Mathematics in Science and Engineering, Academic Press, Boston (1993).

[45] RN Kulkarni, *New insights into the roles of insulin/IGF-I in the development and maintenance of beta-cell mass*, Rev Endocr Metab Disord 6 (2005): 199-210.

[46] RN Kulkarni, JC Bruning, JN Winnay, C Postic, MA Magnuson, et al., *Tissue-specific knockout of the insulin receptor in pancreatic beta cells creates an insulin secretory defect similar to that in type 2 diabetes*, Cell 96 (1999): 329-339.

[47] RN Kulkarni, M Holzenberger, DQ Shih, U Ozcan, M Stoffel, et al., *Beta-cell-specific deletion of the Igf1 receptor leads to hyperinsulinemia and glucose intolerance but does not alter beta-cell mass*, Nat Genet 31 (2002): 111-115.

[48] E Lammert, G Gu, M McLaughlin, D Brown, R Brekken, et al., *Role of VEGF-A in vascularization of pancreatic islets*, Curr Biol 13 (2003): 1070-1074.

[49] IB Leibiger, B Leibiger, PO Berggren, *Insulin signaling in the pancreatic beta-cell*, Annu Rev Nutr 28 (2008): 233-251.

[50] K Lemaire, MA Ravier, A Schraenen, JW Creemers, R Van de Plas, et al., *Insulin crystallization depends on zinc transporter ZnT8 expression, but is not required for normal glucose homeostasis in mice*, Proceedings of the National Academy of Sciences of the United States of America 106 (2009): 14872-14877.

[51] D Li, SC Yeung, MM Hassan, M Konopleva, JL Abbruzzese, *Antidiabetic therapies affect risk of pancreatic cancer*, Gastroenterology 137 (2009): 482-488.

[52] J Li, JD Johnson, *Mathematical Models of Subcutaneous Injection of Insulin Analogues: A Mini-Review*, Discrete and Continuous Dynamical Systems-Series B 12 (2009): 401-414.

[53] J Li, Y Kuang, *Analysis of a glucose-insulin regulatory models with time delays*. SIAM J. Appl. Math., **67**(3) (2007), 757–776.

[54] J Li, Y Kuang, *Systemically modeling the dynamics of plasma insulin in subcutaneous injection of insulin analogues for type 1 diabetes*, Math Biosci Eng 6 (2009): 41-58.

[55] J Li, Y Kuang, and B Li, *Analysis of IVGTT glucose-insulin interaction models with time delay*. Discrete Contin. Dyn. Syst. Ser. B., **1** (2001), 103–124.

[56] J Li, M Wang, A De Gaetano, P Palumbo, S Panunzi, *The range of time delay and the global stability of the equilibrium for an IVGTT model*, Math Biosc 235 (2012): 128-137.

[57] J Li, Y Kuang, CC Mason, *Modeling the glucose-insulin regulatory system and ultradian insulin secretory oscillations with two explicit time delays*, Journal of Theoretical Biology 242 (2006): 722-735.

[58] X Li, L Zhang, S Meshinchi, C Dias-Leme, D Raffin, et al., *Islet microvasculature in islet hyperplasia and failure in a model of type 2 diabetes*, Diabetes 55 (2006): 2965-2973.

[59] GE Lim, M Piske, JD Johnson, *14-3-3 proteins are essential signalling hubs for beta cell survival*, Diabetologia (2013).

[60] DS Luciani, JD Johnson, *Acute effects of insulin on beta-cells from transplantable human islets*, Molecular and Cellular Endocrinology 241 (2005): 88-98.

[61] A Makroglou, J Li, and Y Kuang, *Mathematical models and software tools for the glucose-insulin regulatory system and diabetes: an overview*. Appl. Numerical Math., **56** (2006), 559–573.

[62] A Mari, *Mathematical modeling in glucose metabolism and insulin secretion*. Curr. Opin. Clin. Nutr. Metab. Care 5 (2002), 495C501.

[63] DR Matthews, AS Rudenski, MA Burnett, P Darling, RC Turner, *The half-life of endogenous insulin and C-peptide in man asseessed by somatostatin suppression*, Clinical Endocrinology 23 (1985): 71-79.

[64] AE Mehran, NM Templeman, GS Brigidi, GE Lim, KY Chu, et al., *Hyperinsulinemia drives diet-induced obesity independently of brain insulin production*, Cell Metabolism 16 (2012): 723-737.

[65] JJ Meier, AE Butler, Y Saisho, T Monchamp, R Galasso, et al., *Beta-cell replication is the primary mechanism subserving the postnatal expansion of beta-cell mass in humans*, Diabetes 57 (2008): 1584-1594.

[66] DJ Michael, RA Ritzel, L Haataja, RH Chow, *Pancreatic beta-cells secrete insulin in fast- and slow-release forms*, Diabetes 55 (2006): 600-607.

[67] KA Miles, MP Hayball, AK Dixon, *Measurement of human pancreatic perfusion using dynamic computed tomography with perfusion imaging*, The British journal of radiology 68 (1995): 471-475.

[68] S Misler, DW Barnett, KD Gillis, DM Pressel, *Electrophysiology of Stimulus-Secretion Coupling in Human Beta-Cells*, Diabetes Sturis (1992): 1221-1228.

[69] E Mosekilde, KS Jensen, C Binder, S Pramming, B Thorsteinsson, *Modeling absorption kinetics of subcutaneous injected soluble insulin*, J Pharmacokinet Biopharm 17 (1989): 67-87.

[70] A Mukhopadhyay, A De Gaetano, O Arino, *Modelling the intra-venous glucose tolerance test: a global study for a single distributed delay model*, Discr Cont Dyn Syst B, (2004), 407-417.

[71] LR Nyman, KS Wells, WS Head, M McCaughey, E Ford, et al., *Real-time, multidimensional in vivo imaging used to investigate blood flow in mouse pancreatic islets*, J Clin Invest (2008).

[72] T Okada, CW Liew, J Hu, C Hinault, MD Michael, et al., *Insulin receptors in beta-cells are critical for islet compensatory growth response to insulin resistance*, Proc Natl Acad Sci U S A 104 (2007): 8977-8982.

[73] RV Overgaard, JE Henriken, H Madsen, *Insights to the minimal model of insulin secretion through a mean-field beta cell model*, J. Theor. Biol., 237 (2005), 382-389.

[74] S Panunzi, P Palumbo, A De Gaetano, *A discrete Single Delay Model for the Intra-Venous Glucose Tolerance Test*, Theoretical Biology and Medical Modelling, 4:35 (2007), doi:10.1186/1742-4682-4-35.

[75] P Palumbo, S Panunzi, A De Gaetano, *Qualitative behavior of a family of delay-differential models of the glucose-insulin system*, Discrete and Continuous Dynamical Systems-Series B 7 (2007): 399-424.

[76] A Pisania, GC Weir, JJ O'Neil, A Omer, V Tchipashvili, et al., *Quantitative analysis of cell composition and purity of human pancreatic islet preparations*, Laboratory investigation; a journal of technical methods and pathology 90 (2010): 1661-1675.

[77] KS Polonsky, BD Given, L Hirsch, ET Shapiro, H Tillil, et al., *Quantitative Study of Insulin Secretion and Clearance in Normal and Obese Subjects*, Journal of Clinical Investigations 81 (1988): 435-441.

[78] KS Polonsky, BD Given, W Pugh, J Liciniopaixao, JE Thompson, T Karrison, AH Rubenstein, *Calculation of the systemic delivery rate of insulin in normal man.* J. Clin. Endocrinol. Metab. **63** (1986), 113-118.

[79] N. Porksen, M. Hollingdal, C. Juhl, P. Butler, J. D. Veldhuis, and O. Schmitz, *Pulsatile insulin secretion: detection, regulation, and role in diabetes*. Diabetes, **51** (2002), S245–S254.

[80] RA Rizza, LJ Mandarino, JE Gerich, *Dose-response characteristics for effects of insulin on production and utilization of glucose in man*. Am. J. Physiol.(1981) **240**, E630-E639.

[81] Y Saisho, AE Butler, JJ Meier, T Monchamp, M Allen-Auerbach, et al., *Pancreas volumes in humans from birth to age one hundred taking into account sex, obesity, and presence of type-2 diabetes*, Clin Anat 20 (2007): 933-942.

[82] BM Sebastian, LE Nagy, *Decreased insulin-dependent glucose transport by chronic ethanol feeding is associated with dysregulation of the Cbl/TC10 pathway in rat adipocytes*, Am J. Physiol Endocrinol Metab 289:1077-1084, 2005. First published Aug 16, 2005; doi:10.1152/ajpendo.00296.2005

[83] LF Shampine, S Thompson, *Solving DDEs in MATLAB*, Appl. Numer. Math., 37 (2001), 441-458.

[84] C Simon and G Brandenberger, *Ultradian oscillations of insulin secretion in humans, Diabetes*. **51** (2002), S258–S261.

[85] H Smith, *An Introduction to Delay Differential Equations with Applications to the Life Sciences*, Springer (2010).

[86] H Smith, *Monotone Dynamical Systems, an Introduction to the Theory of Competitive and Cooperative Systems.* (1995).

[87] T Soeborg, CH Rasmussen, E Mosekilde, M Colding-Jorgensen, *Absorption kinetics of insulin after subcutaneous administration*, Eur J Pharm Sci 36 (2009): 78-90.

[88] SH Song, SS McIntyre, H Shah, JD Veldhuis, PC Hayes, et al., *Direct measurement of pulsatile insulin secretion from the portal vein in human subjects*, J Clin Endocrinol Metab 85 (2000): 4491-4499.

[89] J Sturis, KS Polonsky, E Mosekilde, E Van Cauter, *Computer model for mechanisms underlying ultradian oscillations of insulin and glucose*. Am. J. Physiol., **260** (1991), E801–E809.

[90] C Tarin, E Teufel, J Pico, J Bondia, HJ Pfleiderer, *Comprehensive pharmacokinetic model of insulin Glargine and other insulin formulations*, IEEE Trans Biomed Eng 52 (2005): 1994-2005.

[91] G Toffolo, RN Bergman, DT Finegood, CR Bowden, C Cobelli, *Quantitative estimation of beta cell sensitivity to glucose in the intact organism: a minimal model of insulin kinetics in the dog*, Diabetes (1980), 29:979-990.

[92] IM Tolic, E Mosekilde, J Sturis, *Modeling the insulin-glucose feedback system: The significance of pulsatile insulin secretion*. J.Theor.Biol., **207** (2000), 361-375.

[93] B Topp, K Promislow, G De Vries, RM Miura, DT Finegood, *A Model of β-cell mass, insulin, and glucose kinetics: pathways to diabetes*, J.Theor.Biol., **206** (2000), 605-619.

[94] Z Trajanoski, P Wach, P Kotanko, A Ott, F Skraba, *Pharmacokinetic model for the absorption of subcutaneously injected soluble insulin and monomeric insulin analogues*, Biomed Tech (Berl) 38 (1993): 224-231.

[95] K Ueki, T Okada, J Hu, CW Liew, A Assmann, et al., *Total insulin and IGF-I resistance in pancreatic beta cells causes overt diabetes*, Nat Genet 38 (2006): 583-588.

[96] K Ueki, T Okada, U Ozcan, R Kulkarni, *Endogenous insulin-mediated signaling protects apoptosis induced by glucose in pancreatic beta-cells*, Diabetes 52 (2003): A42-A42.

[97] CA Verdonk, RA Rizza, JE Gerich, *Effects of plasma glucose concentration on glucose utilization and glucose clearance in normal man.* Diabetes 30 (1981), 535-537.

[98] Wikipedia: Diabetes mellitus

[99] H Wang, J Li, Y Kuang, *Enhanced modeling of the glucose-insulin system and its applications in insulin therapies*, J. Biological Dynamics, 3 (2009), 22-38.

[100] H Wang, J Li, Y Kuang, *Mathematical modeling and qualitative analysis of insulin therapies*, Math. Biosci., **210** (2007), 17–33.

[101] M Wang, J Li, GE Lim, JD Johnson, *Is dynamic autocrine insulin signaling possible? A mathematical model predicts picomolar concentrations of extracellular monomeric insulin within human pancreatic islets*, PLoS ONE 8(6) (2013).

[102] L Whittaker, C Hao, W Fu, J Whittaker, *High-affinity insulin binding: insulin interacts with two receptor ligand binding sites*, Biochemistry 47 (2008): 12900-12909.

CURRICULUM VITAE

NAME: Minghu Wang

ADDRESS: Department of Mathematics
University of Louisville
Louisville, KY 40292

EDUCATION: M.A. Mathematics
University of Louisville 2011

PREVIOUS: B.S. Mathematics, B.E. Finance
Sichuan University 2008

RESEARCH: Mathematical Modeling
Differential Equations
Dynamical Systems

TEACHING: Contemporary Mathematics
Finite Mathematics
College Algebra
Elements of Calculus– GTA

AWARDS: